Development of polymeric membranes for the separation of water-alcohol mixtures for bioethanol purification in industry


SAPIENTIA
AEDIFICAVIT
SIBI DOMVM

Abstract

The increasing demand for sustainable energy solutions has intensified the focus on bioethanol production as a renewable fuel alternative. However, the energy-intensive distillation process for water-alcohol separation remains a significant challenge in bioethanol purification. This study explores the development and characterization of thin-film composite membranes (TFCMs) for efficient water-alcohol separation, aiming to provide a more energy-efficient alternative to traditional methods.

The membranes were evaluated under varying conditions of temperature (20°C, 30°C, 40°C, and 50°C) for their performance in separating water from methanol, ethanol, and isopropanol. Results demonstrated that the permeance of water remained dominant at higher temperatures (40°C and 50°C), highlighting the membranes' suitability for selective water removal in bioethanol purification processes. In contrast, alcohols such as methanol and ethanol exhibited higher permeance at lower temperatures (20°C and 30°C), indicating the membranes' tunable selectivity based on operating conditions.

The study further revealed the time-dependent behavior of permeance, with alcohols experiencing a rapid decline in transport efficiency before stabilizing, while water maintained consistent performance over extended periods. This dynamic underscore the membranes' potential for long-term industrial applications with appropriate optimization.

Overall, the developed membranes show promise for enhancing the efficiency of water-alcohol separation, contributing to the advancement of energy-efficient bioethanol production technologies. Future research is recommended to explore mixed water-alcohol systems and investigate membrane stability under real-world conditions.

Symbols

Symbols	Description	Units
αi,j	*Selectivity*	[-]
ε	*Porosity*	[%]
Δf	*Difference in transience across the membrane*	[bar]
ΔHcondensation	*Condensing heat*	[kJ/mol]
ΔHmixing	*Mixing Heat*	[kJ/mol]
ΔHs	*Heat of solution or sorption*	[kJ/mol]
λ	*Medium free path*	[nm]
μi	*Chemical potential*	[J/mol]
Am	*Effective membrane area*	[m^2]
cf,i	*Concentration of i in the feed*	[mol/m^3]
cp,i	*Concentration of i in the permeate*	[mol/m^3]
Di	*Diffusion coefficient*	[m^2/s]
Di/Dj	*Diffusivity selectivity*	[-]
dk	*Kinetic diameter*	[Å]
ED	*Diffusion activation energy*	[kJ/mol]
Ep	*Permeation activation energy*	[kJ/mol]
ff,i	*Fugacity in feeding*	[bar]
fp,i	*Fugacity in the permeate*	[bar]
Ji	*Gas flow*	[m^3(STP)/m^2h]

l	*Membrane thickness*	[m]
lp	*Pore length*	[m]
Li	*Permeance*	[m^3(STP)/m^2h bar]
Mw	*Molecular weight*	[g/mol]
P0, S0	*Pre-exponential factors*	[-]
pc	*Critical pressure*	[bar]
p0,i	*Pressure on the permeate side at the beginning of the measurement*	[bar]
pf,i	*Feed pressure*	[bar]
Pi	*Permeability coefficient*	[m^3(STP)/m^2h bar]
pp(t),i	*Pressure on the permeate side at the end of measurement*	[bar]
pp,i	*Permeate pressure*	[bar]
r	*Pore radius*	[nm]
R	*Ideal gas constant*	[m^3bar/kmol K]
Si/Sj	*Solubility coefficient*	[-]
T	*Temperature*	[°C, K]
Tc	*Critical temperature*	[K]
t	*Measuring time*	[h]
Vp	*Constant volume of permeate*	[m^3]
$\boldsymbol{\dot{V}_{p,i}}$	*Permeate volumetric flow rate*	[m^3(STP)/h]
Yi	*Concentration of i in the permeate*	[% en vol.]

Contents

1.-Introduction

We are currently living in strange times, world-wide instability, political tensions and a clear tendency towards the formation of a new multipolar global order. At the same time, we are experiencing big changes in our weather and climate, even with all our geopolitical or ideological differences, we all live in the same planet, so searching for sustainable solutions to transform our industry is still necessary to improve our environment and keep living in Earth, our home.

This new world needs circular economy and scientific solutions for our problems, not only for the obvious reasons related to climate change and the transformation of industry, but also from a strategic point of view. In this state of tension and insecurity, global trade routes security can not be taken for granted, so most, if not all governments, will look inside their own borders to ensure the autonomous production of strategically important resources.

This is the main focus of my master thesis, the production of industrial grade bioethanol for its use as biofuel or whatever industrial applications needed.[1–6]

Figure 1: Bioethanol production plant.

1.1.-Bioethanol

Bioethanol is an alcohol (specifically ethanol) produced from biomass, it is commonly used as a renewable energy source. Its primary and main component is ethanol (C_2H_5OH), a simple alcohol derived from the fermentation of carbohydrates in crops like sugarcane, corn, and wheat, or from cellulosic materials such as agricultural residues, wood chips, and grasses. The chemical process involves the conversion of sugars ($C_6H_{12}O_6$) by the fermentation done by certain microbes into ethanol and carbon dioxide (CO_2) in the presence of yeast or bacteria.

Figure 2: Commercial grade bioethanol for its consumer use as fuel.

Bioethanol production typically follows two main paths: first-generation and second-generation processes. First-generation bioethanol utilizes food crops rich in sugar or starch. The starch is then hydrolyzed to glucose using enzymes, which after that is fermented by microorganisms to produce ethanol. Second-generation bioethanol, on the other hand, is produced from lignocellulosic biomass. This involves the pre-treatment of the biomass to break down complex polymers like for example cellulose and hemicellulose into fermentable sugars, followed by microbial fermentation.

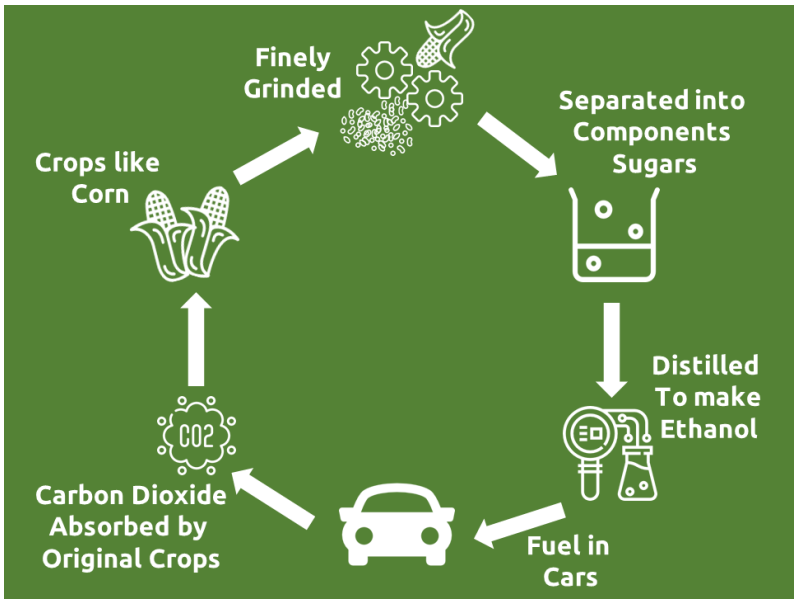

Figure 3: Circular model of bioethanol production and use.

The combustion of bioethanol for energy releases CO_2, which might seem contradictory as bioethanol is usually classified as a green source of energy. This can be explained because this CO_2 is offset by the carbon absorbed by plants during their growth, making it a more sustainable alternative to fossil fuels. Also, bioethanol combustion produces fewer particles and greenhouse gases compared to gasoline. However, the production and use of bioethanol also present challenges, including land use competition with food production in food-deprived regions, the energy-intensive nature of crop cultivation and processing, and the need for advanced technologies to efficiently convert the lignocellulosic biomass into bioethanol.[7–15]

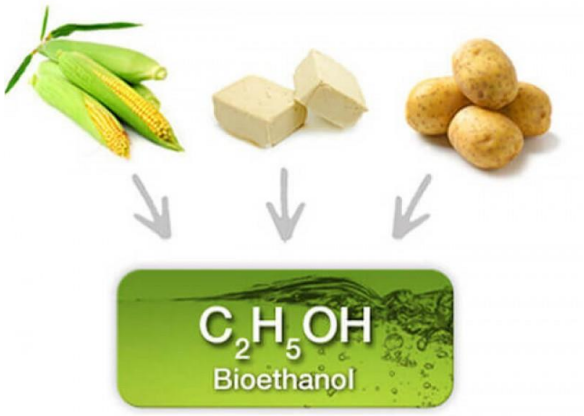

Figure 4: Some of the different resources used for bioethanol production.

In the context of biofuel applications, bioethanol is often blended with gasoline to form ethanol-gasoline mixtures, such as E10 (10% ethanol, 90% gasoline) and E85 (85% ethanol, 15% gasoline), enhancing the fuel's octane rating and reducing the gas vehicle emissions. Research in the field of bioethanol is ongoing, focusing on improving feedstock yield, fermentation efficiency, and developing robust microbial strains capable of processing a wide range of biomass types and resistant to inhibitory compounds formed during biomass pretreatment.

In this master thesis, we took a hands-on approach to the production and purification of this important biofuel, looking into the development of polymeric membranes that could achieve the separation of alcohol-water mixtures for the purification and use of bioethanol.

1.2.-Polymeric membranes for bioethanol production

In the realm of bioethanol production, the development of polymeric membranes marks a crucial leap forward, marrying cutting-edge materials science with renewable energy innovation. As bioethanol fuel continues to gain popularity as a sustainable alternative to fossil fuels, the efficiency and cost-effectiveness of its production processes are paramount. This is were polymeric membranes enter the scene, these are engineered barriers that can selectively separate components at the molecular level, completely revolutionizing the purification, dehydration and distillation stages of bioethanol production.

These advanced membranes, crafted from sophisticated polymers, offer us unparalleled performance in terms of selectivity, permeability, and durability. They enable more efficient ways of separation of water from ethanol, significantly reducing energy consumption compared to traditional distillation methods. The integration of polymeric membranes in bioethanol production plants would not only enhances the overall yield and purity of the biofuel but also drive down the operational costs and the environmental impact of this industry as a whole.

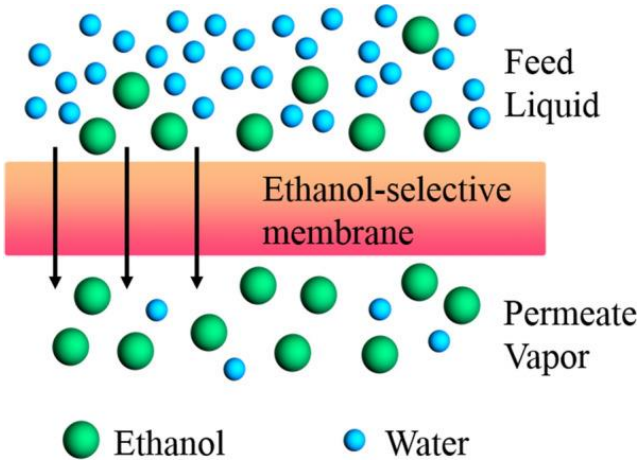

Figure 5: Schematic representation of an ethanol-selective membrane.

As we explore the state-of-the-art advancements in this field, we witness a confluence of interdisciplinary expertise, where chemistry, nanotechnology, and environmental science meet and converge. Some of the latest developments include the creation of hybrid membranes with nanoscale precision, bio-inspired materials that mimic natural separation processes, and smart membranes capable of adapting to varying process conditions. These innovations signal a new era in bioethanol production, positioning polymeric membranes at the forefront of sustainable energy technology and paving the way for a cleaner, greener future.[16–26]

1.3.-Objectives

The main objectives that we wanted to achieve were the following:

-To avoid the distillation phase in the production of bioethanol thanks to a membrane separation, this way, we could obtain the bioethanol cheaper and with a lower energy consumption.

- To obtain some structure-property relationships for the Water/Alcohol separation, especially for Water/Ethanol.

1.4.-Structure of this Master Thesis

In the first part of this Master Thesis, the intention is to give an introductory background of the current problems related with our study, as well as to give clear motivations and objectives for the research done.

Secondly, we will learn about the theoretical background that is needed to understand the main topics studied in this work, the state of the art of bioethanol production, the economic and environmental relevance of bioethanol in the whole world and an overlook of the way Thin Film Composite Membranes (TFCMs) work.

Thridly, we will take a look into the materials and experimental processes used to produce and characterize the films and membranes that were used for our experiments.

Lastly, we include the detailed presentation and discussion of all relevant results obtained during the experimental work, followed by an in-depth analysis of the experiments and the conclusions we arrived at.

2.-Bioethanol state of the art

2.1.-Production of bioethanol

In the year 2023 global bioethanol production was estimated to be around 110 billion liters, the main actors in world stage of bioethanol production would be the United States of America, with around 54% of global production and Brazil, controlling more than 30% of the global output. Other relevant productors would be the European Union, with Spain leading the production of bioethanol in Europe, and of course, the big asian giants, China and India.

The feedstocks used to produce bioethanol are mainly corn in the USA and Spain and sugarcane in Brazil, signaling the importance of self-grown national agriculture inside this industry.

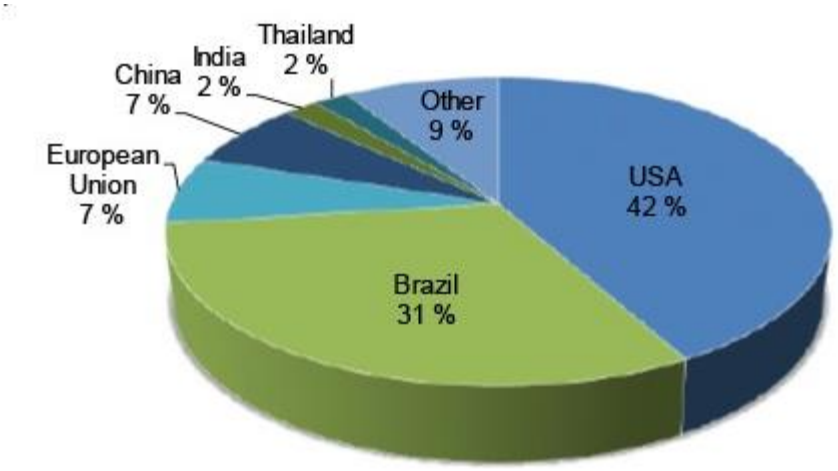

Figure 6: World production of bioethanol.

There have been some recent technological advancements, especially in enzyme technology and genetically modified yeasts, these advancements have improved the efficiency conversion of lignocellulosic biomass into bioethanol, in some cases achieving yields of up to 40%. It is also important to point out that modern bioethanol plants have drastically reduced its energy consumption, with the energy use per gallon of ethanol produced dropping by over 50% in the last 20 years.

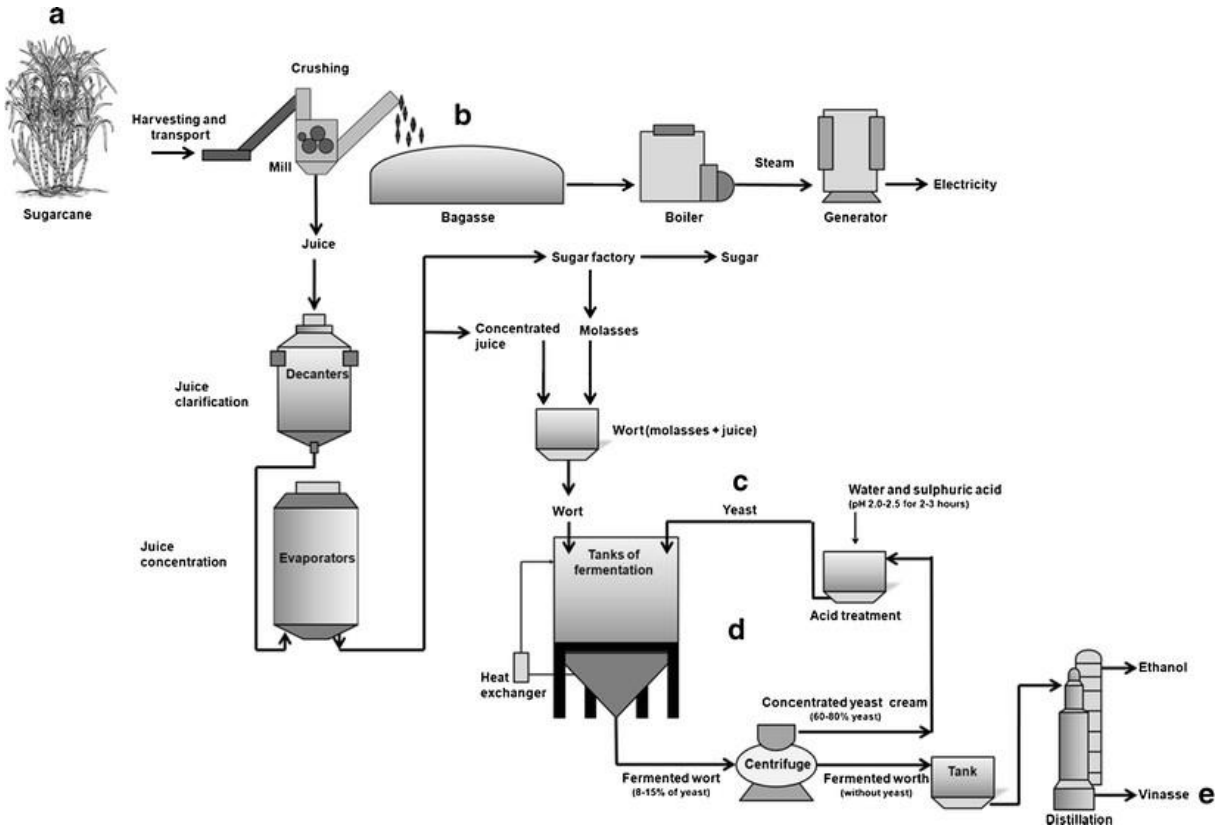

Figure 7: Schematic of the industrial production of bioethanol.

2.2.-Uses of bioethanol

As previously mentioned, the uses of bioethanol are diverse, but its most common use would be biofuel, blended with gasoline to achieve a reduction in greenhouse gas emissions, beyond its use as biofuel, its industrial applications are also relevant, for example in the production of industrial chemicals such as ethyl acetate, acetic acid or ethylene.

2.3.-Environmental and economic impact of bioethanol

One of the main advantages of the use of bioethanol is the up to 60% greenhouse gas emissions reduction when compared to conventional gasoline. Also, as bioethanol comes from plants (in the case of Spain mainly corn), it is considered a renewable energy source, helping to reduce the dependence on fossil fuels and ensuring energy security in the instable and chaotic world that we live in.

Another big important advantage of bioethanol in the matter of environmental impact would be the use of agricultural residues and waste products from the food industry, this way bioethanol production helps in waste management and reduces considerably landfill use for the disposal of this waste.

About the economic impact, we could talk about the creation of jobs. Currently, bioethanol industry supports hundreds of thousands of jobs in the whole world, from research, marketing and distribution to farming and in factory production. In the USA nowadays, the ethanol industry contributes around $40 billion annually, which constitutes around a 0,16% of its national GDP.[27–35]

2.4.-Bioethanol in Spain

The role of Spain in the production of bioethanol is key within the European conditions. Through the management of different strategic investments in the research for new technology, supportive policies and the leveraging of its own agricultural resources, Spain has managed to contribute significantly to the European Union's renewable energy objectives, while it has also fostered its own economic and environmental benefits.

The bioethanol production capacity of Spain is estimated to be around 500-600 million liters per year, with Abengoa Bioenergy being the largest player in the national market, with ownership of both "Biocarburantes de Castilla y Leon" (200 million liters/year) and "Ecocarburantes Españoles" (150 million liters/year).

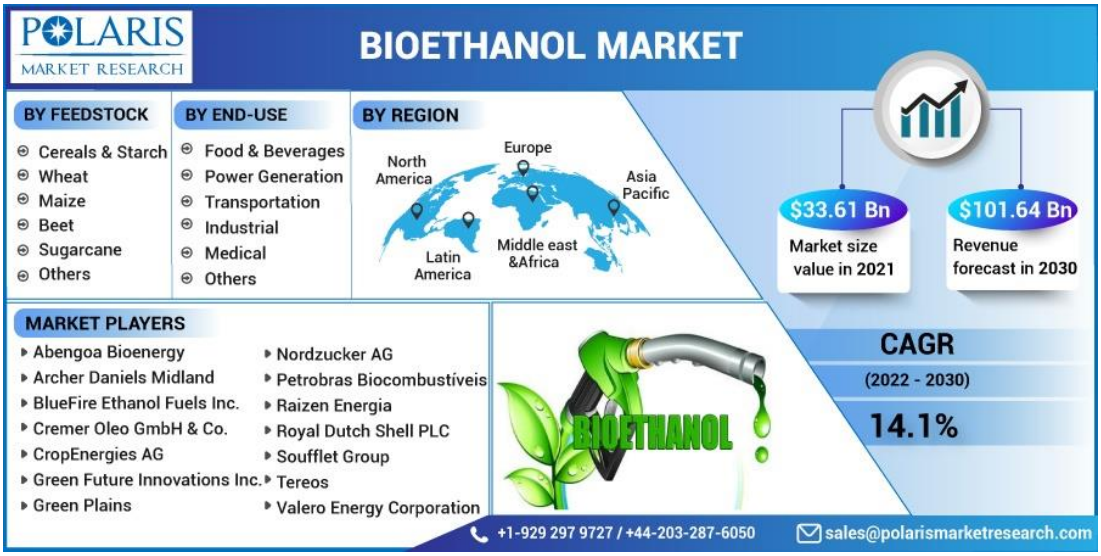

Figure 8: Overview of the bioethanol market.

Bioethanol production plants in Spain use both direct agricultural feedstocks and industrial by-products. These primary feedstocks used for bioethanol production in Spain would be cereals, representing approximately 60-70% of the industry (mainly corn with around a 50% of the total feedstock use and wheat, with 10-20%).

Another notable mention would be sugar beets, which represent between 15-20% of the total production, this is mainly because of Spain's historical and ongoing cultivation of sugar beets, this crop's high sugar content makes it a great feedstock for bioethanol production.

In the matter of policy and regulations, bioethanol production has been greatly favored, because as it was previously mentioned, it is a renewable energy source, there has been policies that encourage the production and use of bioethanol, as well as subsidies and tax incentives for its industry, this favourable situation has contributed to the development of the bioethanol industry inside Spain.

The main challenges bioethanol production faces currently are important nevertheless, such as for example, the need to ensure a sustainable and consistent supply of the feedstocks in a

country where agricultural production is in decline, economic viability is also important, as the direct competitors of bioethanol are fossil fuels, which offer a low-cost alternative.

Developing efficient technologies for second-generation bioethanol production is also one of the big challenges of industry.

Having already discussed the big feedstock availability in Spain, the benefits its use has for the environment and strategic relevance, as well as the economic viability, it is our job as chemists and researchers to look into developing new technologies and methods of making bioethanol production cheaper and more accessible.[36–42]

2.5.-Fermentation broth

During the first stages of this master thesis a big question arises in relation to the fermentation broth, as its components can be different depending on the feedstock used, in this chapter we will give a broad picture of the primary components of the fermentation broth.

The importance of the fermentation broth in bioethanol production is key because it directly affects the efficiency and yield of the process, as well as being a determining factor in the aging of whatever polymeric membrane we are trying to develop.

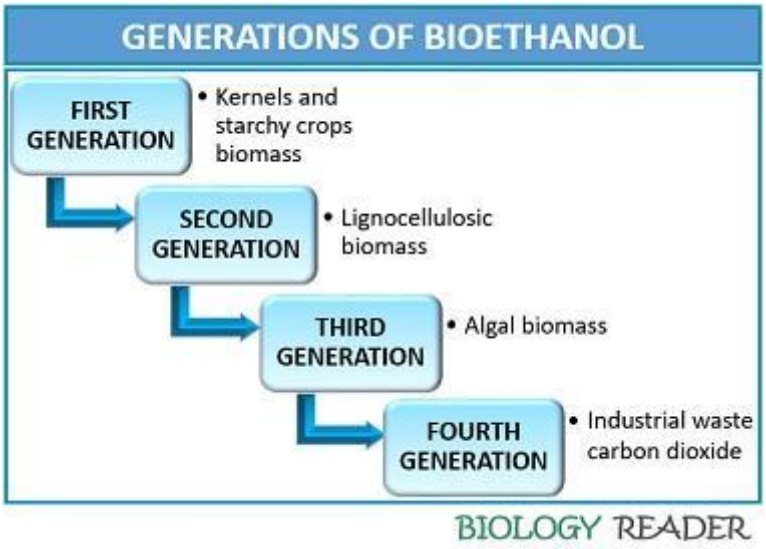

Figure 9: Schematic of the different generations of bioethanol.

The fermentation broth is a complex mixture with several different components that either facilitate or result from the fermentation of the sugars into ethanol, the primary components typically found in a fermentation broth would be the following:

-*Water:* This is of course the main solvent in the broth, it facilitates the dissolution and transport of substrates and nutrients.

-*Sugars*: Glucose, fructose and sucrose are the main fermentable sugars that come from the different feedstock that is used in each case, other monosaccharides such as xylose or arabinose can also be present depending on the feedstock (especially in the one that comes from lignocellulosic biomass)

-*Microorganisms:* Yeasts such as Saccharomyces cerevisiae are the primary fermenting agents that convert sugars into both ethanol and carbon dioxide. In some cases we can also find lactic acid bacteria or acetic acid bacteria, either as undesired contaminants or as part of a co-fermentation strategy in conjunction with the yeasts.

-*Ethanol*: Obviously this is the main product of the fermentation process, and can also appear in the fermentation broth coming from an early fermentation.

-*Carbon dioxide:* A by-product of fermentation, it is typically released as gas, as it has no further use in the industrial process that we are interested in.

-*Organic acids:* Different organic acids such as acetic acid, lactic acid and others can be by-products of the fermentation or a result from microbial contamination. It is also worth mentioning that formic acid and butyric acid can also be found depending on the feedstock origin and its contamination.

-*Protein and enzymes:* Yeast derived proteins that are released from yeast cells during fermentation and exogenous enzymes (cellulases and amylases for example) that are added with the goal of breaking down complex carbohydrates into fermentable sugars, especially used in lignocellulosic bioethanol production

-*Nutrients:* In the fermentation broth we can find nitrogen sources such as sulfate, urea and other nitrogenous compounds that help support yeast growth. There are also minerals such as magnesium, potassium, phosphorus and even trace elements like zinc and iron.

-*Metabolic by-products:* Glycerol, fusel alcohols and aldehydes and cetones my form in the fermentation broth in small quantities.

-*Feedstock residues*: Soluble fibers and non-fermentable sugars are some of the residual components of the feedstock that will not be converted into ethanol. In the case of lignocellulosic feedstocks, we can also find lignin present after the pre-treatment and the enzymatic hydrolysis steps.

-*pH adjusting agents*: Optimal pH for yeast activity is around pH 4-5 so different acids or bases can be added to maintain this pH levels.

-Antifoaming agents are also used to control the formation of foam during the fermentation process.

As we have seen, the fermentation broth used for bioethanol production is a dynamic and complex mixture, which has been actively designed to optimize the conversion of sugars into ethanol. The exact composition can vary depending on the feedstock, the fermentation

process and different specific production conditions. Nevertheless, this overview of the fermentation broth has to be taken into account when it is time to scale any innovation in polymeric membrane development into the industrial production level.[43–50]

3.-Polymeric membranes state of the art

Polymeric and Thin Film Composite Membranes (PM and TFCMs respectively) are gaining traction in crucial roles in the industry of bioethanol production, their lower energy requirements when compared to distillation make them great substitutes to distillation in the separation and purification stages of bioethanol. These advanced materials are designed and engineered to efficiently separate the bioethanol from the fermentation broth, this way the overall energy efficiency and sustainability for the bioethanol production process can be greatly improved and enhanced.

In the case of my master thesis, I focused on the study of specifically the TFCMs case, as in the Helmholtz Zentrum Hereon I had a great array of resources at my disposition that allowed me to create this new TFCMs from different polymeric materials.[51,52]

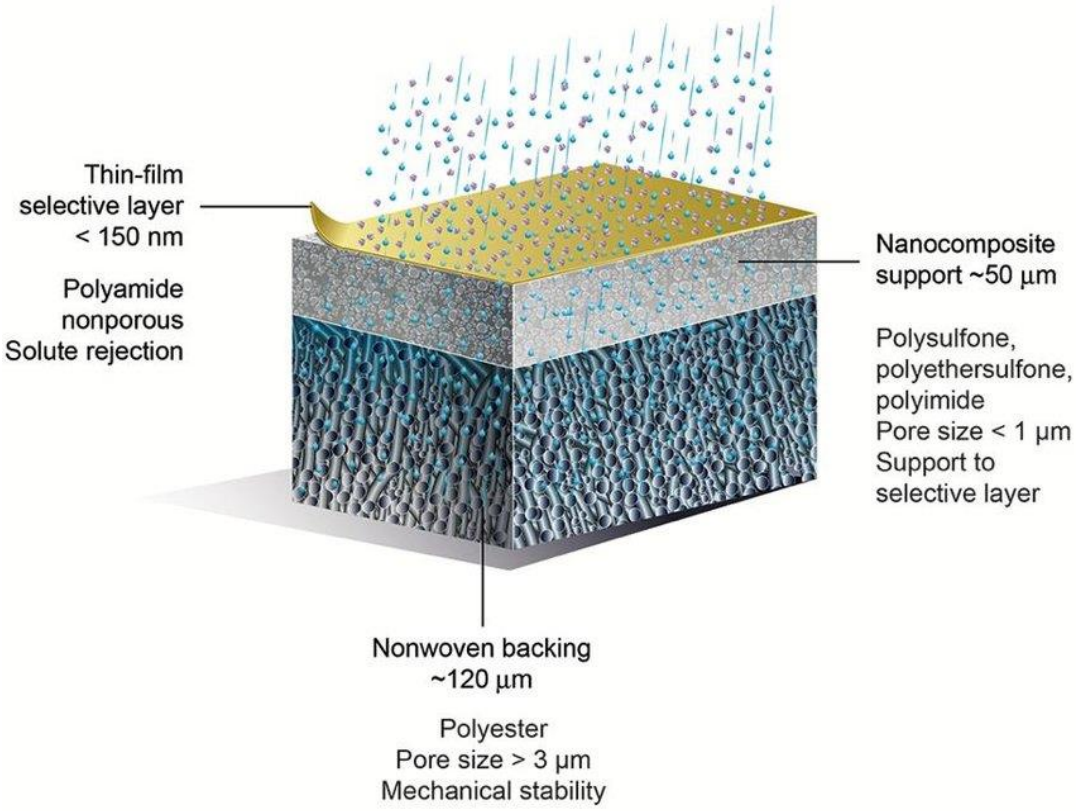

Figure 10: Thin Film Composite Membrane structure.

3.1.-Thin Film Composite Membranes

Thin Film Composite Membranes can be defined as specialized structures that are widely used in separation processes, mainly reverse osmosis and nanofiltration. These TFCMs are characterized by their multi-layered structure, designed to enhance the separation process performance while at the same time maintaining a high permeability and mechanical strength. In this section of the master thesis we will give a detailed explanation about the structure, action mechanism, advantages and of course, applications for this innovative new kind of membranes.[53,54]

3.1.1.-Structure

TFCMs are composed of three main layers:

-Support layer: This is typically made of a porous polymer such as polysulfone (PSU) or polyethersulfone (PES) and its main function is to provide a certain degree of mechanical strength and structural support to the membrane as a whole. Its porous nature ensures that it has minimal resistance to water flow while maintaining the structural integrity at the same time.

-Intermediate layer: It is often made from a microporous layer of either the same or a different polymer as the support layer previously mentioned. As for function, it helps in smoothing out the surface of the support layer, providing a better foundation for the thin film layer that comes next.

-Thin film layer: Its materials can vary greatly, but they are most commonly composed of a polyamide (PA) thin film. In our case we have used a few different polymers that will be detailed in another chapter of this master thesis. This thin film is the active layer that is responsible for the selective separation of the desired solutes, which in our case were alcohols (mainly ethanol) and water. This thin layer film is as its own name indicates, extremely thin, typically around the range of 100-200 nanometers, it is also dense, which allows it to selectively allow water molecules to pass through it while it rejects any other molecule or solute that we want to separate.[55–58]

3.1.2.-Mechanism of action

The active thin layer is selectively permeable, this way only specific molecules can pass through it based on size and chemical affinity, in this way TFCMs work as a kind of physicochemical filter.

TFCMs usually operate under a gradient of pressure, for example in reverse osmosis, where high pressure is applied to push water through the membrane, and in this way, leaving contaminants behind.

There is also an important solution-diffusion mechanism to take into account, molecules dissolve into the active layer and then they diffuse across it. As an example, in the process of desalinization, water molecules dissolve into the thin layer and then diffuse across to the permeate side, while salts are rejected because of their inability to dissolve and diffuse through the specific polymer matrix prepared for this purpose. Thanks to this characteristic, we can calculate a permeation rate, which is controlled by the solubilty of the different molecules in the material of the membrane and their diffusivity.

Following the example previously given, after the controlled filtering in the active thin polymeric layer, the purified water (or any molecule we desire) passes through the intermediate and support layer to exit the membrane, leaving any contaminant or other molecule of interest behind. In the case of our master thesis, the alcohol should stay behind, which would be then concentrated for further processing and achieving its use as biofuel.[59–63]

3.1.3.-Advantages of TFCMs

As we have already seen, TFCMs have a great variety of uses and applications, and its implementation in the world of industry can bring some great advantages, the TFCMs both high selectivity and permeability as well as its chemical resistance to a wide range of different chemical environments makes them great candidates for the optimization of processes in different industries.

Another important advantage is their customization, TFCMs properties can be tailored according to the needs of the industrial process where we want to use them. We can modify with relative ease the chemistry of the monomers or the interfacial polymerization conditions, allowing for a great variety of wide range of applications, from water desalinization to purification of bioethanol in our case.

In summary, TFCMs are highly engineered multi-layered structures that can leverage the benefits of a big spectrum of different materials to achieve efficient and selective seoaration in various applications. Their performance is primarily attributed to the different properties of the thin film layer depending on the polymer we are using.[64–67]

3.2.-PIMs

PIM is the abbreviation for Polymers of Intrinsic Microporosity. These polymers represent a new unique class of polymers defined by their rigid and knotted molecular structures, this characteristic prevents the efficient packing of the polymer molecules, this way creating an intrinsic microporosity inside its structure. This material possesses high specific surface areas, most of the time higher than 750 m2/g and of course a considerable free volume, which allows them to be considered as a highly effective polymer for applications such as gas storage, gas separation and membrane technology.

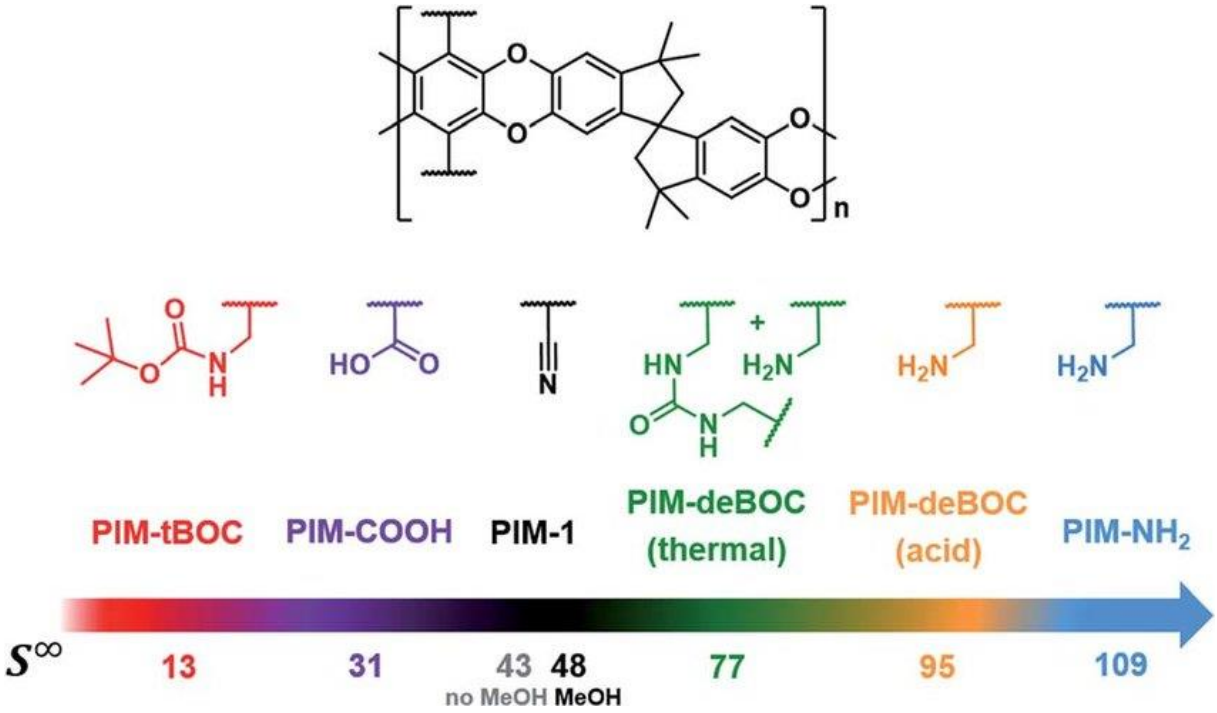

Figure 11: PIM-1 and some variations based on the functional groups of the polymer.

The intrinsic microporosity that PIMs have, comes from their specific molecular architecture, as they usually consist of bulky and rigid components that create a twisted and non-linear backbone. This structural characteristic is what avoids the packing of the chains in the solid state, which results in a highly porous material with voids interconnected with each other.

This voids are of molecular dimensions, usually less than 2 nm. The high surface area provided by its structure, as well as the free volume provided by the pores is what makes them a great candidate for the development of membranes that allow for the separation of the alcohol-water mixtures that we are studying in this master thesis.[68–72]

Maybe the most well-known PIM is PIM-1, which we used consistently during the duration of this master thesis. In the next chapter, we will give an in-depth explanation of its synthesis and use for membrane formation.

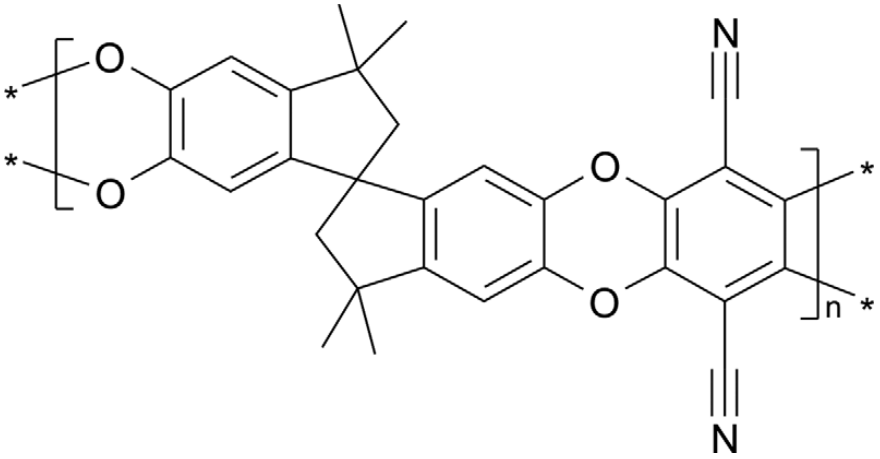

Figure 12: PIM-1 structure.

3.3.-Other relevant polymers

Two other relevant polymers that were consistently used during the duration of my master thesis were 6FDA-6FpDA and Matrimid. Both polymers are polyimides (polymers characterized by the presence of imide linkages in their core) and are classified as high-performance polymers, next, we will take a look into these polymers.

-6FDA-6FpDA: This polymer has certain characteristics such as its great thermal stability (more than 300C without almost any degradation), high mechanical strength and of course, gas separation properties. Its chemical structure is composed of 2 different components:

6FDA: This is a fluorinated dianhydride, which posess bulky and rigid structures and fluorine atoms integrated into the polymeric backbone. Its fluorine atoms content is what reduces the chain packing the chain packing of the polymer in solid state and helps enhance the free volume it has.

6FpDA: This is the diamine component of the final 6FDA-6FpDA polymer, it further adds to the free volume and rigidity thanks to the bulky trifluoromethyl groups in its structure.

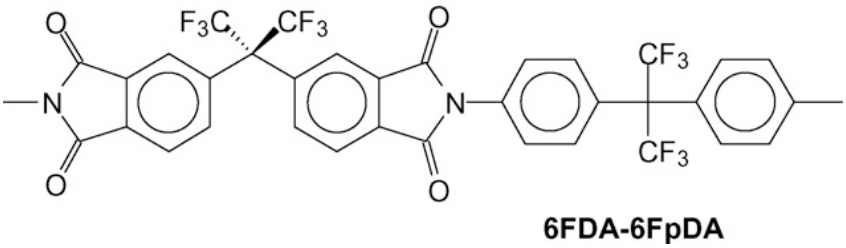

Figure 13: 6FDA-6FpDA structure.

-Matrimid: As previously mentioned, matrimid is a polyimide, the presence of both the imide links and aromatic rings gives this polymer the great characteristics it possess, including thermal stability, chemical resistance, mechanical strength and processability.[73–77]

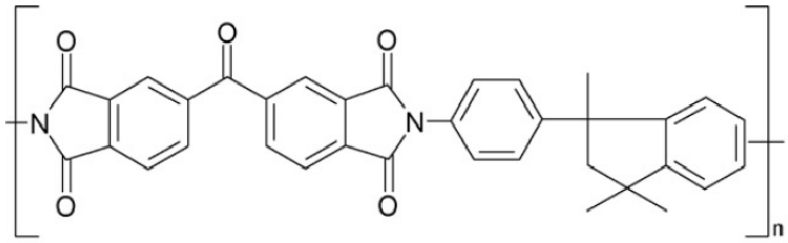

Figure 14: Matrimid structure.

4.-Materials and methods

In this chapter I will give an in-depth analysis and commentary of the materials and methods used during the duration of my master thesis. As we have already stated, our main goal was to develop a polymeric membrane with the goal of separating alcohol-water mixtures for use in bioethanol production industry.

To achieve this goal, we first had to structure our work path.

Firstly, we had to synthetize the different polymers that we were going to use. Then we needed to form the films and TFCMs with the different polymeric solutions previously prepared. After the preparation of the desired films and TFCMs we proceeded with its analysis in Time-Lag and Pressure-Increase respectively.

Here is a list of the different materials that we used during the master thesis:

Polymer films:

- PIM-1
- Matrimid® 5218
- 6FDA-6FpDa

TFCMs:

- PIM-1
- Matrimid/PIM-1
- 6FDA-6FpDA

Penetrants in the Time-Lag:

- Permanent gases
- Water vapour
- Methanol
- Ethanol
- 2-Propanol

Solvents for the polymeric solutions:

- Tetrahydrofuran
- Chloroform

4.1.-Synthesis of diverse polymers

4.1.1.-PIM-1 Synthesis

There are several methods for achieving a successful PIM-1 synthesis, but in this master thesis we will only discuss the two that were used for producing the PIM-1 that we used for our films and TFCMs.

-*High-Temperature Method*: This method is an approach that facilitates the fast production of the polymer, as the name implies, it is characterized by higher temperatures, which cause shorter reaction times when it is compared to the Low-Temperature Method.

First, we must prepare the monomers and solvent that we will use in the synthesis. For the monomers we use a biscatechol derivative with 2 catechol units (we will refer to it as monomer A1), the structure of this monomer is designed to make the formation of dibenzodioxin linkages during the polymerization process, the other monomer is a halide-containing monomer, like bromide or iodide, this is activated by an electron-withdrawing substituent (for example a nitrile group), the presence of the halide is key for the nucleophilic substitution reaction that then leads to the formation of the final polymer.

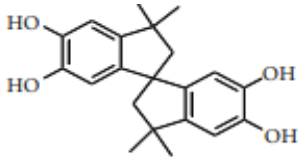

A1

Figure 15: Biscatechol derivative (A1 monomer).

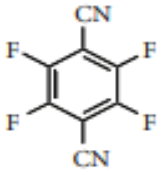

B1

Figure 16: Halide containing monomer (B1).

For the solvent we use dimethyl acetamide (DMAc), this solvent is specifically selected for its ability to dissolve both monomers and facilitate the polymerization process at high temperatures.

Then, we mix both A1 and B1 monomers in equimolar quantities, ensuring a stoichiometric balance for a complete reaction. A base (Potassium carbonate) is also added into the mixture to facilitate the nucleophilic substitution reactions necessary for polymer formation.

The reaction solution has to be subjected to stirring at a high speed, with a temperature of around 155 C. This temperature accelerates the kinetics of the reaction and allows for relatively quick polymerization (only about 8-10 minutes).

The mechanism for this polymerization is via double-aromatic nucleophilic substitution mechanism in which the nucleophilic sites of the monomers react to form the dibenzodioxin linkage that we are looking for, thus forming the microporous polymeric structure that characterizes PIM-1.

After the reaction we cool the mixture at room temperature and then it is precipitated by adding a non-solvent (water in our case). This way, we help isolate PIM-1 from the reaction mixture. At the end we wash the precipitated polymer with the same solvent used during the polymerization (DMAc), water and an alcohol such as methanol.

-*Low-Temperature Method:* This is another well-established method for production of PIM-1, the process is almost exactly the same as for the High-Temperature Method, using both A1 and B1 monomers, but in this case our solvent was dimethyl formamide (DMF), again, it is chosen for the same reasons for using DMAc in the High-Temperature Method (its ability to dissolve the monomers and facilitate the polymeriyation process).

As in the High-Temperature Method, we mix and add a base (K2CO3), but the difference is that in this case the temperature of the mixture moves between 50-60C. This comparatively low temperature is crucial because it allows for controlled polymerization without causing degradation to any of the monomers or the final polymeric structure.

The reaction time is 24-72 hours, an important point is that depending on the duration of the reaction it has been proved that the molecular weight of the final polymer changes. With longer reaction times generally leading to higher molecular weight polymers.

As expected, the polymerization mechanism is the same as in the previously mentioned method. Its cooling, precipitation, filtration and washing is also the same as for the High-Temperature Method

As a short comparison between the two methods, we can say that the High-Temperature Method allows for a quick synthesis of high molecular weight PIM-1, efficient for large scale production, while the Low-Temperature Method allows for greater control over the properties of the polymer and a more uniform molecular weight distribution.[78–80]

4.1.2.-Matrimid synthesis

The synthesis of the Matrimid polymer, a well-known high-performance polyimide, involves a multi-step chemical process that is designed to yield materials with great thermal stability, mechanical strength, and chemical resistance. Matrimid-5218, a well-known commercial polyimide, is usually synthesized through the reaction of benzophenone tetracarboxylic dianhydride (BTDA) with diamines such as diamino-methyl-phenylindane (DAPI). The first step in this synthesis involves the formation of polyamic acid, this acid is then cyclized into the imide form through either thermal or chemical imidization.

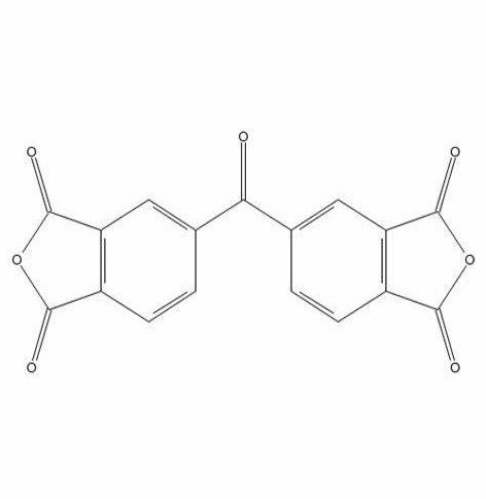

Figure 17: BTDA structure.

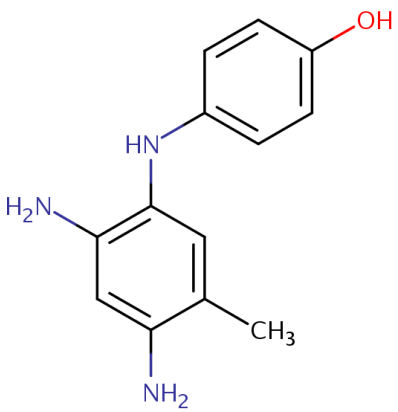

Figurer 18: DAPI structure.

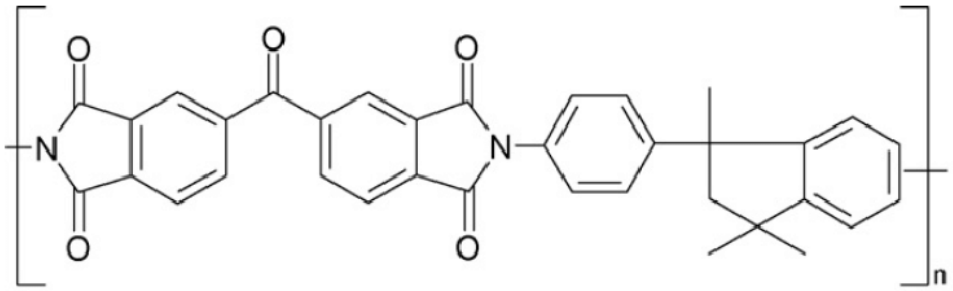

Figure 19: Matrimid polymeric structure.

For example, the direct fluorination of Matrimid-5218 allows for better control over the formation rate of the surface-fluorinated layer of the polymer, and in this way significantly altering its physicochemical properties such as the chemical composition, density, and transparency. This modification can enhance the polymer's resistance to chemical and environmental degradation, thus making it suitable for different advanced applications, such as the case of study for our master thesis.

Another study highlighted the homogeneous blending of Matrimid with Rhodeftal to improve its CO2/N2 separation performance. This approach not only enhanced the polymer's plasticization resistance but also increased its selectivity, demonstrating the versatility of Matrimid in gas separation technology. This gave me the idea to make a Matrimid and PIM-1 blend, to see if their characteristics and properties in relation to water-alcohol separation were improved. We will discuss this in depth in next chapters.

Furthermore, the synthesis of Matrimid can be adapted for creating other great arrays of high-performance polymers. One example would be the successful synthesis Matrimid using 1,3-diamino-5-pentafluorosulfanylbenzene monomer, which resulted in the production of diverse polymers, including polyimides, a polyamide, and a cured epoxy crosslinked polymer.

Its formation mechanism can be separated in a few different steps. First, there the primary amine groups from the DAPI act as nucleophiles and attack the carbonyl group of the anhydride groups in BTDA, this way the anhydride ring is opened and both an amide linkage and a carboxylate anion are formed. Given the high reactivity of this intermediate, it readily undergoes a reaction with another of the anhydride groups, forming polyamic acid.

After this, the polyamic acid is subjected to the heating of the polymer, which causes that the carboxyl groups in the polyamic acid react with the adjacent amide groups, leading to the elimination of water molecules and to the formation of imide rings, in this way, the cyclation process transforms the polyamic acid into polyimide.

The final Matrimid polymer consists of repeating imide units, with the imide rings giving high thermal stability, chemical resistance and mechanical strength to the polymer.

To sum up, the synthesis of Matrimid polymer involves careful selection of the monomers and controlled reaction conditions to achieve desired properties. These modifications and blending techniques expand its application potential in areas requiring robust and durable materials.[81–83]

4.1.3-6FDA-6FpDA synthesis

The synthesis of 6FDA-6FpDA polymer, a kind of polyimide, it typically involves the reaction of 4,4'-(hexafluoroisopropylidene)diphthalic anhydride (6FDA) with 2,2'-bis(trifluoromethyl)benzidine (6FpDA), its two monomers. This process is significant for producing polymers with excellent thermal stability, great mechanical properties, and good chemical resistance, which are highly valued for its various high-performance applications, including the fields of aerospace and electronics, as well as obviously for the matter of our master thesis.

The process begins with the preparation of the diamine, 6FpDA, followed by its polycondensation with 6FDA in a polar and aprotic solvent such as N,N-dimethylacetamide (DMAc) or N-methyl-2-pyrrolidone (NMP). The reaction is normally conducted under inert atmosphere conditions to avoid environmental moisture and water, which can interfere with the anhydride functionalities. The polyamic acid that is formed in this step is then subsequently subjected to a thermal or chemical imidization process, resulting in the formation of the final polyimide structure. This step involves the removal of water or other by-products and the formation of imide rings, which impart the polymer with its characteristic thermal and chemical stability.

According to Zhang et al. (2019), novel synthetic strategies such as caprolactam hydrolysis polymerization combined with transesterification offer flexibility in designing prepolymers for various applications. Additionally, research by Im et al. (2011) highlights the enhanced properties of composite materials incorporating 6FDA-6FpDA polymers, particularly in terms of electrical conductivity and mechanical properties, which are crucial for advanced material application.

In summary, the synthesis of the 6FDA-6FpDA polymer involves a precise control of reaction conditions and processing steps to achieve the high-performance material suitable for demanding applications we desire. The development of novel synthesis techniques continues to expand the potential uses and enhance the properties of these polyimides.

In our case we used both the chemical and thermical imidization methods for our 6FDA-6FpDA synthesis, as we polymers with very similar characteristics, and for our film and TFCM formation we can use them indistinctively.[84–86]

4.2.-Membrane formation

In order to check and characterize the polymers, we first need to form films and put them in the Time-Lag machine with a specific sequence to characterize them, after that, we can create TFCMs of our polymers and also go through their characterization using the Pressure-Increase machine.

4.2.1.-Film formation

The formation of the films for the different polymers that we used does not change a lot between the different polymers, so I will give a general path for the film formation and give the specifications needed for each polymer.

First, we dissolve the synthesized polymer in a proper solvent, for both PIM-1 and Matrimid polymers we used chloroform and THF (tetrahydrofuran). For 6FDA-6FpDA, we only used THF. The solution we prepare should have around 3% polymer in weight. After preparing the solution, we put it for overnight stirring. Then, we use a metallic fiber filter for separating any particles that could remain in the solution, and we put the solution in a film cast (the width is not relevant, as later we will cut the film according to our needs). We then proceed with the slow evaporation of the solvent using N2, usually films are ready after 8-16 hours of slow evaporation. Lastly, we place the films in a vacuum oven with a turbomolecular pump for around 24 hours at 60C. Finally, our film is ready for characterization.[87–90]

4.2.2.-TFCM formation

As for the film formation, TFCM formation follows a similar path for all the TFCMs we formed, so we will use the same explanation procedure as for the film formation, only entering in the specifications for each polymer when we need to.

Following the same procedure as in the film formation process, we prepare a solution in either chloroform or THF for the polymers or polymeric blends we are using, depending on the substrate solubility in THF or chloroform. For TFCMs, as we want a very thin film for the membrane, we just use a 1% weight concentration of the polymer in the solvent.

Then, we stir it overnight and after that, we filter it by the same means as for the films and we use this solution to slowly coat the support layer, we used the same polymer as support layer for all our TFCMs. This polymer was polyacrylonitrile (PAN), which has some interesting characteristics for our purpose, for example it doesn't degrade until it reaches around 300C, its insolubility in water and most organic solvents and also its high tensile strength and modulus makes it a great candidate for its use a TFCM support layer polymer.

After the coating, we let the TFCM rest and dry at room temperature before taking it for characterization.[91–95]

4.3.-Characterization of films and membranes.

Our objective with the characterization of these films and membranes is to check the diffusivity, permeability and solubility properties of our materials for certain gases, mainly alcohols and water. Even though my master thesis is mainly focused in bioethanol production, and we are mostly interested in the relation between ethanol and water mixtures, we decided to also add methanol and iso-propanol as permeants, to imitate to a certain degree the fermentation broth, where you can find a variety of different alcohols.

For both the films and TFCMs, we used similar programming of the gases, so we could have some degree of reproducibility.

The program we used for both running the Time-lag and the Pressure-increase machine was either exactly the following, or a very similar version of it adapted to a specific case (we will discuss this in the following sections of the master thesis).[96–98]

Gas	Permeate volume	Counts of pressure increases	Stop after first data set	Filling up pressure (mbar)
Hydrogen	FALSE	3	TRUE	700
Carbondioxyde	FALSE	3	FALSE	500
Water	TRUE	3	FALSE	500
Hydrogen	FALSE	3	TRUE	700
METHANOL	TRUE	3	FALSE	700
Hydrogen	FALSE	3	TRUE	700
ETHANOL	TRUE	3	FALSE	700
Hydrogen	FALSE	3	TRUE	700
2_Propanol	TRUE	3	FALSE	700
Hydrogen	FALSE	3	TRUE	700

4.3.1.-Time-Lag Method

This method is a well-known and widely used characterizing technique for characterization of the transport properties of gases through polymeric films. It gives us valuable information about the permeability, diffusivity and solubility of diverse gases in the polymer.

The main principle of the Time-lag method is the measurement of the time it takes for a gas to permeate through the polymeric film we introduce into the system. The analysis is based on Fick's laws of diffusion and in this way, we can determine the diffusivity (D),the solubility (S) and the permeability (P) of any gas that we want to study in our polymer of interest.

For the experimental setup, we place our polymeric film in a cell between two compartments, one is a high-pressure upstream side (we get the test gases from here) and the other one is a low-pressure downstream side (which is initially either evacuated or filled with an inert gas).

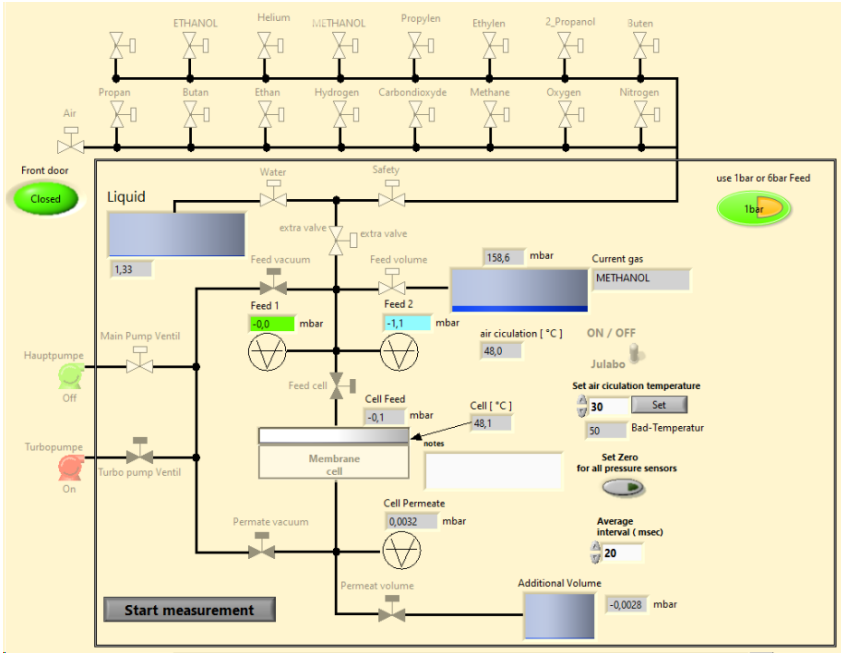

Figure 20: Time-Lag machine control panel.

The main advantage if this method is that it is non-destructive, so we can reuse our already tested films for further analysis, it also provides us with all the parameters mentioned before (diffusivity, solubility and permeability) simultaneously. Finally, it has a relatively simple experimental setup and data analysis, which makes it a great candidate for scientists like me, researching gas transport properties in polymeric films.[99–103]

4.3.2.-Pressure-Increase Method

The Time-lag and Pressure-increase methods are both used to characterize the transport properties of gases through polymeric films and membranes, but they differ in their experimental setup, measurement principles, and data analysis. Here are the main principles of the Pressure Increase Method

Experimental Setup: The Pressure-Increase Method involves a gas-permeation cell that consists of two compartments separated by the polymeric membrane we want to do research about.

The two compartments are the following:

-Feed side (upstream): This compartment is initially pressurized with the gas being tested on the membrane.

-Permeate side (downstream): This compartment is usually under vacuum (our case) or at a much lower pressure.

Gas flow: A single gas (or a mixture of a few gases) is allowed to flow across the membrane, this is achieved by the membrane allowing the gas to permeate thanks to a partial pressure gradient.

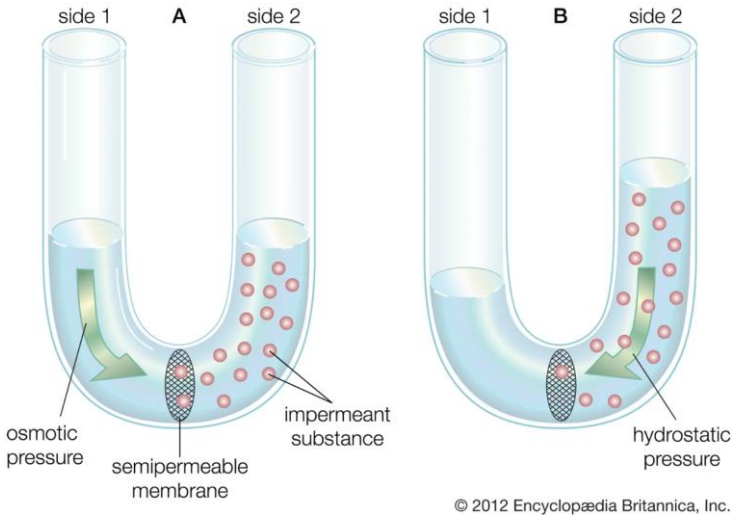

Figure 21: Water diffusion across a semipermeable membrane.

Pressure Monitoring: The permeate side is completely sealed and connected to a highly precise and previously calibrated pressure sensor. As the gas permeates through the membrane, the pressure on the downstream side increases over time. As expected, this pressure rise is continuously recorded so that we can study the transport properties.[104–108]

5.-Results and discussion

This chapter presents and analyzes the experimental results obtained throughout the course of my Master Thesis. Following the systematic characterization of the synthesized polymeric materials and the formation of both films and thin-film composite membranes (TFCMs), the focus for this chapter lies in understanding the separation performance of these membranes in water-alcohol systems, with particular emphasis on their potential application in bioethanol purification processes.

5.1.- Film results

I created a good number of different polymeric films, mainly to test the endurance of the polymer without the support that provides the TFCM.

Our main results for this chapter are the following:

-It is possible to create a stable polymeric film composed of a 50/50 mix of Matrimid and PIM-1, although it doesn't show the separation properties we are interested in.

-6FDA-6FpDA films break easily and are not stable for bioethanol separation in industrial applications.

-PIM-1 films showed the best stability and separation properties, so this is the polymer we decided to continue using for our TFCM analysis.

5.2.- TFCM results

Using the Time-Lag method we characterized different TFCMs.

Most of the TFCMs we designed showed some irregularities and problems while being characterized by this method, so we decided to discard them, nevertheless, the experience we acquired during this trial-and-error process was used for the development of our most interesting membrane.

The results we will discuss in this section are related to one specially promising membrane, a 1% weight PIM-1 dissolved in tetrahydrofuran (THF) with a surface of 0,97cm2 analyzed on 5/08/2024.

We followed the already defined procedure of characterization, this being the use of a sequence of different gases (water, methanol, ethanol and isopropanol) that flow through the membrane at an array of 4 different temperatures, starting from 50 degrees Celsius and ending in 20 degrees Celsius.

After making some calculations using the Antoine´s coefficients of each gas, the feed pressure and the temperature we got the vapour activity for each temperature and we could create different graphs to analyze the important information obtained, specially permeance, vapour activity and time.

5.2.1.-Permeance vs vapor activity graphs

In this chapter I will analyze the 8 graphs in which I compare permeance and vapor activity, to ease the read I divided this chapter into 2 main sections, one in which I will analyze the same gas flow at different temperatures and another in which I will analyze the gas flow of all the different gas flows but all at the same temperature.

5.2.1.1.-Same gases at different temperatures

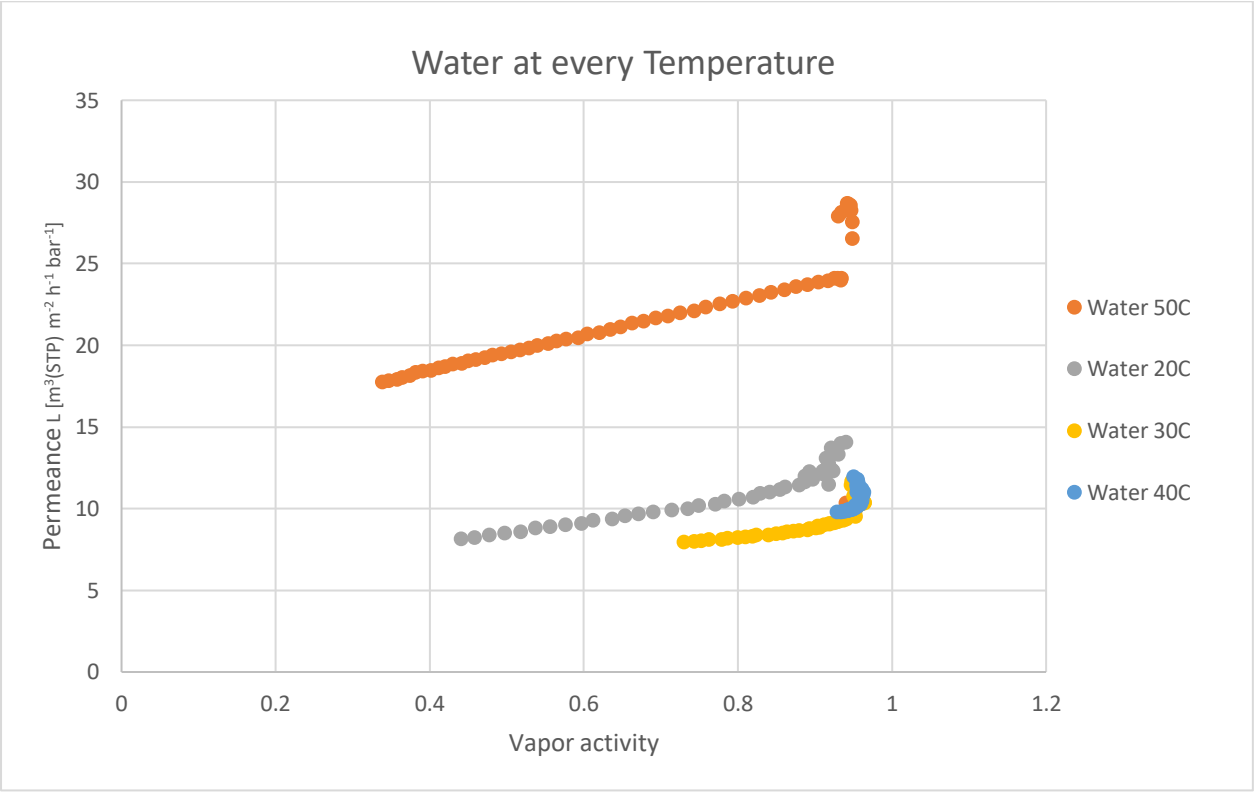

The graph shows the relationship between vapor activity (in the x-axis) and permeance (in the y-axis) of water at different temperatures (20°C, 30°C, 40°C, and 50°C). This is an analysis of the results:

General trend shown:

At all temperatures, we observe a general increase in permeance as vapor activity also increases. This indicates that higher vapor activity may promote higher water permeance through the material or system being studied.

Temperature dependence:

At higher temperatures (as seen for the 50°C line), the permeance values are significantly higher compared to lower temperatures (20°C, 30°C, and 40°C). This suggests that temperature has a strong positive influence on permeance, most likely due to increased molecular activity and diffusion rates at those elevated temperatures.

At 20°C and 30°C, the permeance values are much lower and closer in magnitude, indicating that at lower temperature ranges, the change in permeance with temperature might be less pronounced.

Shape of the Curves:

The curves appear to show a non-linear relationship, particularly at higher temperatures like 50°C. This could indicate us a transition where the permeance increases more rapidly as vapor activity approaches 1. This behavior might reflect the material's interaction with water vapor, such as swelling or aging of the membrane, this aging process can be discussed in more detail when we analyze the Permeance vs Time graphs.

The curves at 20°C and 30°C show a more gradual increase, suggesting that the system is less sensitive to changes in vapor activity at these temperatures.

Outlier Observation:

At 50°C, the orange curve has a steep increase near vapor activity 1. This might represent a threshold effect or material saturation point where water permeance sharply increases.

The clustering of data points at other temperatures around vapor activity 1 suggests that the permeance might plateau or stabilize for lower temperature ranges.

Comparison Between Temperatures:

The permeance at 40°C (blue curve) is intermediate between 30°C and 50°C, following a logical temperature progression. However, there is some overlap between the yellow (30°C) and blue (40°C) points near vapor activity 1, suggesting some potential variability or experimental uncertainty in that region.

Key Insights:

-Higher temperatures enhance water permeance significantly.

-The relationship between vapor activity and permeance becomes more pronounced and non-linear at elevated temperatures.

-At low temperatures, permeance changes more uniformly, indicating a weaker dependence on vapor activity.

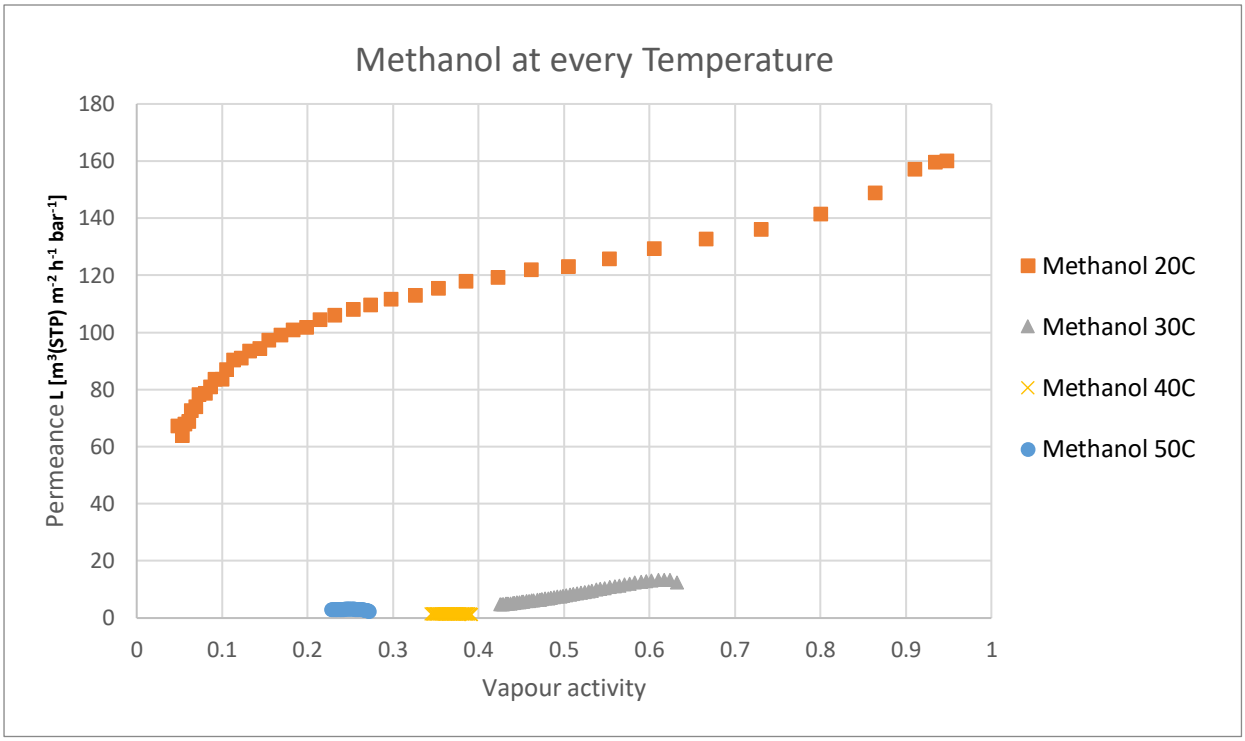

This second graph represents the relationship between vapor activity (in the x-axis) and permeance (in the y-axis) of methanol at various temperatures (20°C, 30°C, 40°C, and 50°C). For this second graph, as well as the remaining, I will use the same analysis procedure I used for the first graph.

General Observations:

The permeance of methanol strongly depends on the temperature and vapor activity.

The permeance values are highest at 20°C (orange squares) compared to the higher temperatures, which is an unusual trend and indicates that methanol's behavior in this membrane differs from that of water shown in the earlier graph.

Temperature Dependence:

20°C: The permeance increases significantly with vapor activity, reaching values as high as 180 at vapor activity ~1. This suggests that at lower temperatures, the material/system has a higher affinity for methanol or higher transport rates.

30°C, 40°C, and 50°C: The permeance values are much lower, showing relatively limited sensitivity to changes in vapor activity compared to the 20°C curve. For instance:

At 30°C (gray triangles), permeance increases gradually and plateaus at a lower level (~20).

At 40°C (yellow crosses) and 50°C (blue dots), permeance values remain even lower, staying well below 20.

Non-linear Behavior:

As seen in the graph, the curve for 20°C is highly non-linear, showing a steep rise at higher vapor activities, likely due to methanol saturation or enhanced interactions with the material at this temperature.

For higher temperatures, the curves are much flatter and suggest that permeance might depend more on intrinsic material limitations than on vapor activity.

Temperature Anomalies:

The 20°C curve being significantly higher than the others indicates that methanol permeance does not follow the typical behavior of increasing permeance with rising temperature. This could be due to different reasons, such as:

Material-specific interactions with methanol at lower temperatures (for example condensation, sorption, or clustering effects).

Some potential experimental factor or material property that restricts permeance at higher temperatures.

Behavior Across Temperatures:

At 30°C, there is a slight increase in permeance as vapor activity rises, but the growth is more gradual compared to 20°C.

At 40°C and 50°C, the permeance remains consistently low, regardless of vapor activity. This could indicate us that the material becomes less permeable to methanol as temperature increases, potentially due to some structural changes in the membrane or decreased methanol affinity.

Key Insights:

-Unexpected Behavior at 20°C: Methanol exhibits the highest permeance at 20°C, contrary to the expectation of increasing permeance with temperature. This may point to methanol-specific interactions at lower temperatures, such as preferential sorption or condensation effects.

-Suppressed Permeance at High Temperatures: The permeance of methanol decreases significantly as temperature rises, with only marginal increases as vapor activity approaches 1.

-Non-linear Increase at 20°C: The steep rise in permeance at high vapor activity for 20°C suggests a threshold or saturation point.

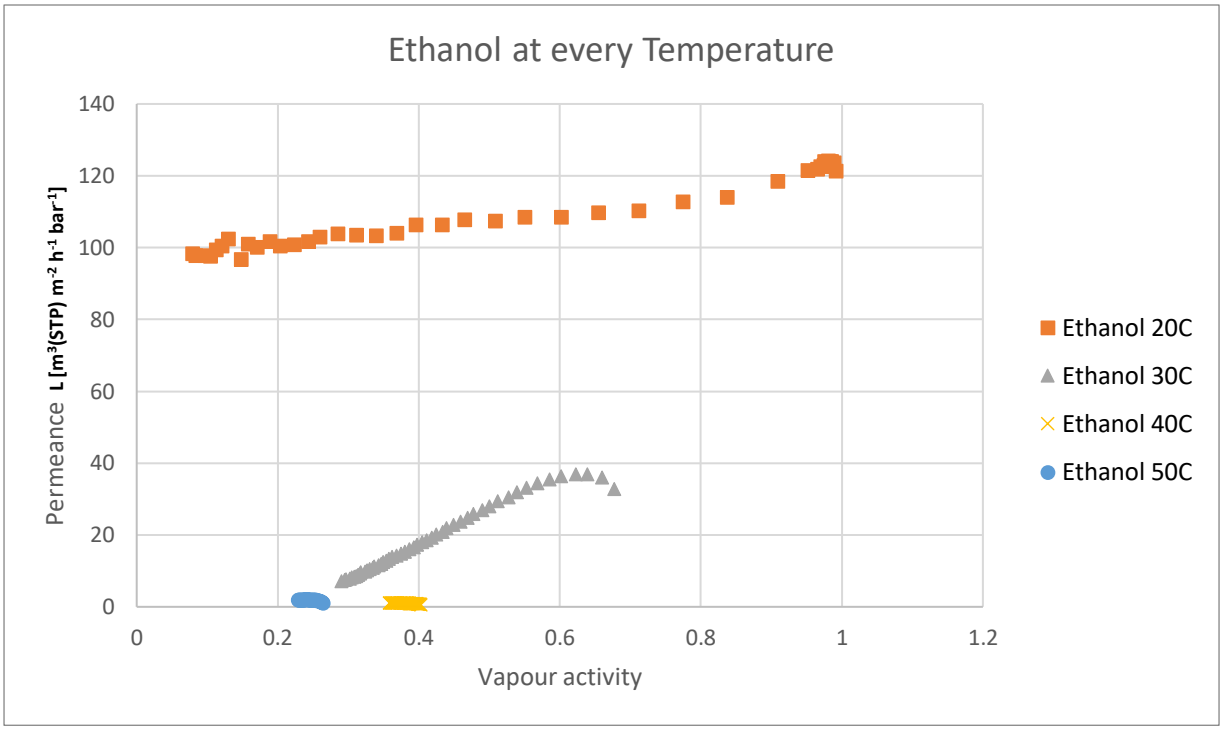

This third graph represents the relationship between vapour activity (in the x-axis) and permeance (in the y-axis) for ethanol at various temperatures (20°C, 30°C, 40°C, and 50°C). Here's an in Depth and detailed analysis:

General Observations:

Similar to the methanol graph, ethanol permeance varies significantly across temperatures, but the highest permeance values are observed at 20°C (orange squares).

The curves at higher temperatures (30°C, 40°C, and 50°C) show much lower permeance values and limited sensitivity to vapor activity.

Temperature Dependence:

20°C (Orange Curve): The permeance is consistently high, increasing slightly as vapor activity rises, peaking near 140 at vapor activity ~1. This indicates a strong interaction between ethanol and the material at low temperatures.

30°C (Gray Curve): The permeance starts to rise with vapor activity but stabilizes around 40. The growth pattern is gradual compared to the steep increases seen at 20°C.

40°C and 50°C (Yellow and Blue Curves): Both show extremely low permeance values (below 10) across the range of vapor activity, suggesting limited ethanol transport through the material at higher temperatures.

Behavior Across Temperatures:

Ethanol exhibits a similar trend to methanol, with permeance being highest at 20°C and drastically reduced at higher temperatures. This could be due to ethanol's interaction with the material, where lower temperatures favor sorption or diffusion.

Unlike methanol, ethanol shows a more gradual increase at 20°C, and the permeance remains stable at high vapor activities.

Unusual High Permeance at 20°C:

The high permeance of ethanol at 20°C suggests a unique interaction between ethanol and the material, potentially driven by factors such as condensation, material swelling, or a high affinity for ethanol at low temperatures.

The steep decline in permeance at higher temperatures might reflect structural changes in the material or reduced ethanol adsorption.

Key Insights:

-Ethanol's behavior is strongly temperature-dependent, with peak permeance observed at 20°C.

-At 30°C, ethanol permeance increases slightly with vapor activity but plateaus quickly, indicating limited permeability at intermediate temperatures.

-At 40°C and 50°C, ethanol permeance is minimal, suggesting that the material becomes significantly less permeable to ethanol as temperature rises.

-The consistent high values at 20°C suggest a strong material-ethanol interaction that diminishes with increasing temperature.

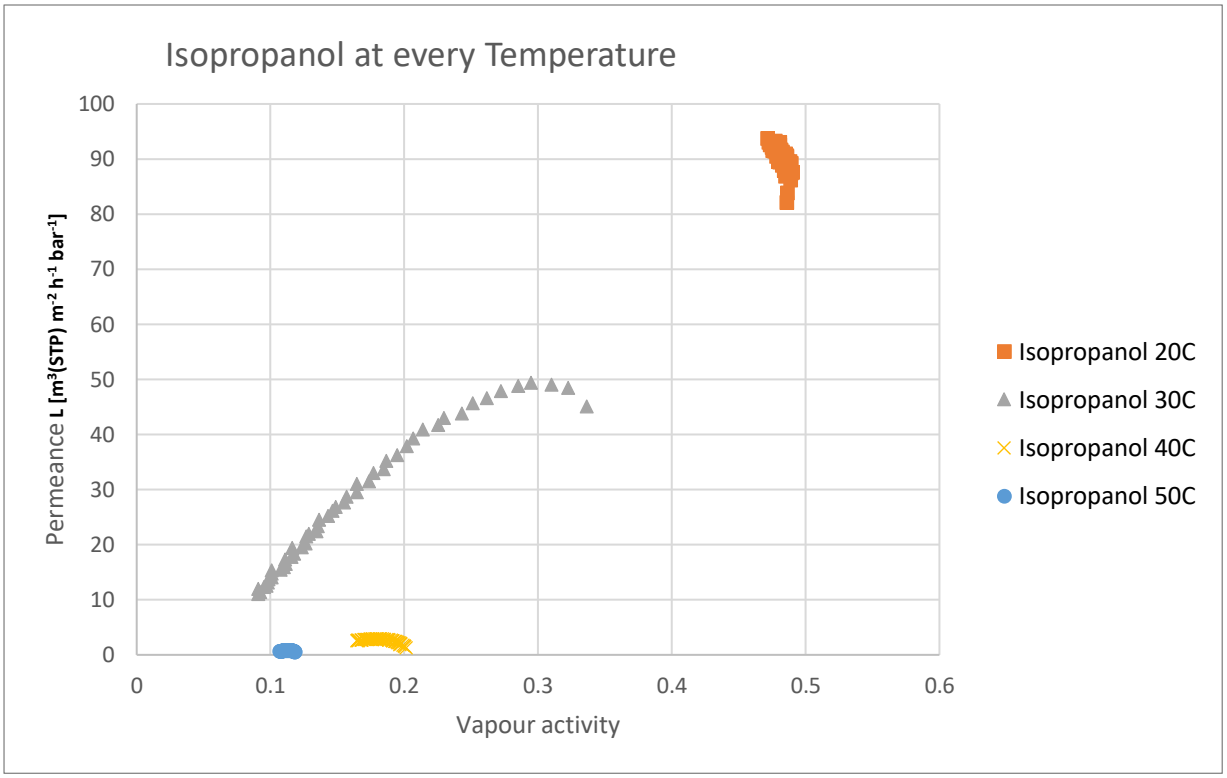

The fourth graph represents the relationship between vapor activity (in the x-axis) and permeance (in the y-axis) for isopropanol at various temperatures (20°C, 30°C, 40°C, and 50°C). Here's the detailed analysis for the graph:

General Observations:

The permeance of isopropanol varies greatly across temperatures, with the highest values observed at 20°C (orange data points), moving between a 80 to around 95 range.

At higher temperatures (30°C, 40°C, and 50°C), the permeance decreases and shows a reduced sensitivity to vapor activity.

The curves for each temperature are clearly separated, suggesting consistent behavior across conditions.

Temperature Dependence:

20°C (Orange Curve): The permeance reaches its highest values, peaking near 95, and increases steeply with vapor activity. This suggests us a strong interaction between isopropanol and the material at low temperatures.

30°C (Gray Curve): The permeance increases significantly with vapor activity, peaking around 50. The curve shows a gradual increase with vapor activity, indicating intermediate interactions compared to 20°C.

40°C (Yellow Curve): The permeance is low, barely exceeding 10, and shows minimal sensitivity to increasing vapor activity. This reflects reduced interaction between isopropanol and the material at this temperature.

50°C (Blue Curve): The permeance values are similarly low, clustering below 10 across the range of vapor activity. This suggests that higher temperatures significantly limit isopropanol transport through the material.

Behavior Across Temperatures:

Isopropanol permeance is strongly temperature-dependent, with the highest values at 20°C and a sharp decline as temperature increases.

The interaction between isopropanol and the material is most favorable at lower temperatures, likely due to enhanced adsorption or diffusion mechanisms.

At 40°C and 50°C, the material appears less permeable, potentially due to reduced adsorption, material structural changes, or changes in vapor pressure.

Unusual High Permeance at 20°C:

The high permeance observed at 20°C might indicate a unique interaction between isopropanol and the material, possibly driven by:

-Enhanced adsorption of isopropanol at low temperatures.

-Swelling of the material, increasing transport pathways.

-Condensation effects under low vapor activity.

The reduction in permeance at higher temperatures might reflect structural changes (e.g., pore collapse) or reduced affinity for isopropanol.

Key Insights:

-Isopropanol permeance is highest at 20°C, with a strong dependence on vapor activity.

-At 30°C, permeance is moderately sensitive to vapor activity but plateaus quickly.

-At 40°C and 50°C, permeance is minimal, suggesting limited isopropanol transport at higher temperatures.

-The consistent high permeance at 20°C highlights favorable isopropanol-material interactions under these conditions.

5.2.1.2.-Comparative Analysis of Gas Permeance and Vapor Activity in TFCM with 1% PIM-1

The four graphs illustrate the permeance of the different gases (water, methanol, ethanol, and isopropanol) as a function of vapor activity across different temperatures (20°C, 30°C, 40°C, and 50°C) when passing through a thin-film composite membrane (TFCM) containing 1% PIM-1. After analyzing these trends, we can extract some meaningful structure-property relationships that help us explain the behavior of the membrane.

5.2.1.2.1.-General Observations Across All Gases

Water: Permeance increases with temperature, with the highest values observed at 50°C. The relationship with vapor activity is nearly linear, indicating strong membrane compatibility with water transport.

Methanol: The highest permeance is observed at 20°C, with a significant drop at higher temperatures. This suggests a favorable interaction between methanol and the membrane at low temperatures.

Ethanol: Exhibits high permeance at 20°C, which declines with temperature, similar to methanol but with a less pronounced drop.

Isopropanol: Shows the lowest permeance across all temperatures, indicating steric hindrance and reduced diffusion capability probably due to its bulkier molecular structure.

5.2.1.2.2.-Comparative Analysis of Each Gas

Water (Graph 1)

Key Trends:

Water permeance increases with temperature, being highest at 50°C.

The permeance-vapor activity relationship is nearly linear.

At 20°C, water permeance is significantly lower than at higher temperatures.

Interpretation:

Water molecules, being small and polar, strongly interact with the membrane.

The increase in permeance with temperature suggests an enhanced diffusivity through the membrane as polymer chain mobility increases.

The linear behavior implies that the transport mechanism is diffusion-driven rather than sorption-limited.

Methanol (Graph 2)

Key Trends:

Methanol shows the highest permeance at 20°C (~160), with a steep decline at higher temperatures.

Permeance at 30°C remains moderate but is significantly lower than at 20°C.

At 40°C and 50°C, methanol permeance is minimal.

Interpretation:

Methanol's high permeance at 20°C suggests strong sorption affinity with the polymer matrix at low temperatures such as 20°C.

The sharp decrease at higher temperatures indicates us that methanol sorption is reduced as the membrane structure tightens or as free volume elements shrink.

The presence of hydroxyl (-OH) groups in methanol may promote hydrogen bonding with the polymer at low temperatures, aiding in the transport through the TFCM.

Ethanol (Graph 3)

Key Trends:

Similar to methanol, ethanol has the highest permeance at 20°C (~120), with a sharp decline at higher temperatures.

Permeance at 30°C is moderate but lower than methanol at the same temperature.

At 40°C and 50°C, ethanol permeance is extremely low.

Interpretation:

The slightly lower permeance compared to methanol at each temperature suggests that ethanol's larger molecular size might create more resistance to diffusion.

Like methanol, ethanol likely benefits from hydrogen bonding with the polymer, though to a lesser extent.

The sharp temperature dependence indicates that ethanol transport is sorption-limited at higher temperatures.

Isopropanol (Graph 4)

Key Trends:

Permeance is significantly lower than for methanol and ethanol at all temperatures.

At 20°C, permeance is relatively high (~90) but still lower than methanol and ethanol.

At 30°C and higher, permeance is minimal.

Interpretation:

The bulkier structure of isopropanol can limit its ability to diffuse through the membrane's free volume.

At higher temperatures, polymer relaxation does not favor isopropanol transport, likely due to steric hindrance.

The weak interaction with the membrane suggests that size exclusion effects dominate over chemical affinity.

5.2.1.2.3.-Structure-Property Relationships

a) Influence of Molecular Size

The molecular size of the permeating species has a significant impact on transport behavior.

Methanol (smallest molecule) > **Ethanol** > **Isopropanol (bulkiest)** in terms of permeance.

Water permeance does not follow this trend because of its strong interactions with the membrane.

b) Hydrogen Bonding and Chemical Affinity

Alcohols interact with the polymer via hydrogen bonding at low temperatures, facilitating their transport.

At higher temperatures, alcohol sorption decreases, reducing permeance.

Water remains highly permeable at all temperatures due to strong hydrogen bonding and its ability to disrupt polymer-polymer interactions.

c) Free Volume and Temperature Dependence

At lower temperatures, the polymer maintains a relatively open structure, allowing smaller molecules like methanol and ethanol to permeate efficiently.

At higher temperatures, polymer chains relax, potentially reducing free volume and restricting alcohol transport.

Water, being a small polar molecule, continues to diffuse efficiently even as temperature increases.

5.2.1.2.4.-Implications for Membrane Performance

-High-Temperature Performance (40°C, 50°C): The membrane is highly selective for water over alcohols, making it suitable for dehydration applications.

-Low-Temperature Performance (20°C, 30°C): High alcohol permeance suggests that the membrane is better suited for alcohol transport at these conditions.

-Size Selectivity: The membrane effectively differentiates between methanol, ethanol, and isopropanol based on molecular size and interaction potential.

5.2.1.2.5.-Conclusion

The analysis of these graphs highlights key structure-property relationships in the TFCM with 1% PIM-1. The membrane shows:

-Strong selectivity for water at high temperatures due to increased diffusivity and interaction strength.

-Higher alcohol transport at low temperatures, particularly for methanol and ethanol, due to favorable hydrogen bonding and lower steric resistance.

-Reduced transport for bulkier molecules like isopropanol, emphasizing the role of size exclusion.

These findings suggest us that the membrane can be optimized for our specific separation application (bioethanol-water separation) by adjusting operating temperatures and polymer composition to balance permeability and selectivity.

5.2.1.3.-Every gas compared at the same temperature:

Now we will make a detailed analysis of the different gases permeance and vapour activity compared at the same temperature.

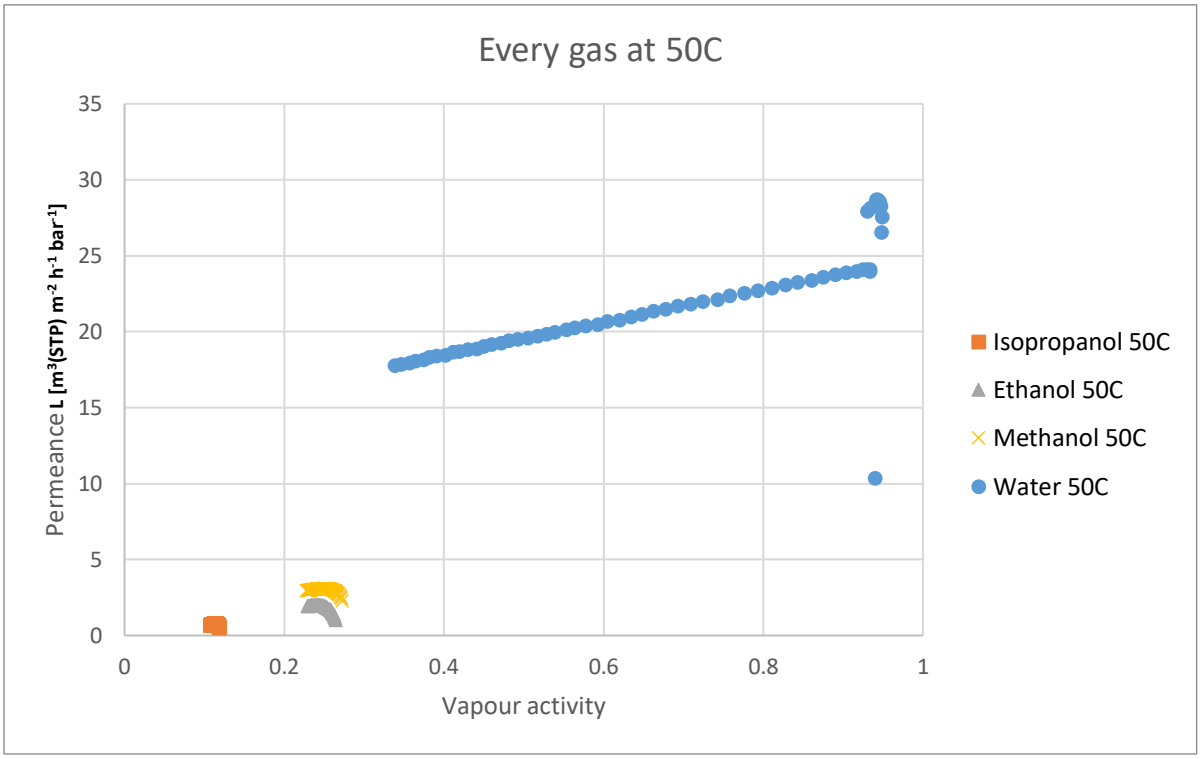

This graph represents the relationship between vapor activity (in the x-axis) and permeance (in the y-axis) for all the different gases that we tested (isopropanol, ethanol, methanol, and water) at 50°C.

General Observations:

The permeance of the gases varies significantly at 50°C.

Water (blue circles) has the highest permeance, increasing steadily with vapor activity, reaching values above 30.

Isopropanol (orange squares) has the lowest permeance, remaining below 5 across the range of vapor activity.

Methanol (yellow crosses) and ethanol (gray triangles) show intermediate permeance values, both peaking slightly below 10.

Gas-Specific Behavior:

Water (Blue Circles):

Permeance increases linearly with vapor activity, indicating strong transport through the membrane at 50°C.

This could reflect a high affinity of the membrane for water, possibly due to hydrogen bonding or other favorable interactions.

Methanol (Yellow Crosses):

Permeance is relatively low, slightly increasing with vapor activity before plateauing near 10.

The lower permeance compared to water may suggest weaker interactions with the membrane or reduced transport efficiency.

Ethanol (Gray Triangles):

Permeance behavior is similar to methanol, but the values are slightly lower, peaking just below 10.

This suggests that ethanol transport is less favorable at 50°C, potentially due to its larger molecular size compared to methanol.

Isopropanol (Orange Squares):

Permeance is minimal, staying below 5 across all vapor activities.

This indicates that the membrane's permeability to isopropanol is significantly limited at higher temperatures, possibly due to its bulkier structure or reduced interaction with the material.

Temperature Impact on Gases:

-At 50°C, the membrane shows a clear preference for water over the alcohols, with water permeance being more than three times higher than that of ethanol or methanol and significantly higher than isopropanol.

-The trend aligns with the idea that water's smaller molecular size and stronger affinity for the membrane material enable easier transport at elevated temperatures.

Key Trends:

-Water Dominance: Water exhibits the most significant increase in permeance with vapor activity, suggesting the membrane's strong selectivity for water at 50°C.

-Limited Transport of Alcohols: Methanol and ethanol show moderate permeance, while isopropanol has negligible transport, reflecting the membrane's limited interaction or permeability for larger alcohol molecules at this temperature.

Key Insights:

-Water Separation Efficiency: The high water permeance at 50°C suggests that the membrane is highly effective at separating water from alcohols under these conditions.

-Isopropanol Exclusion: The significantly lower permeance of isopropanol highlights the membrane's ability to selectively limit the transport of bulkier alcohols.

-Methanol vs. Ethanol: The similarity in methanol and ethanol behavior indicates that molecular size and polarity might have a smaller impact on permeance at 50°C compared to water's dominant properties.

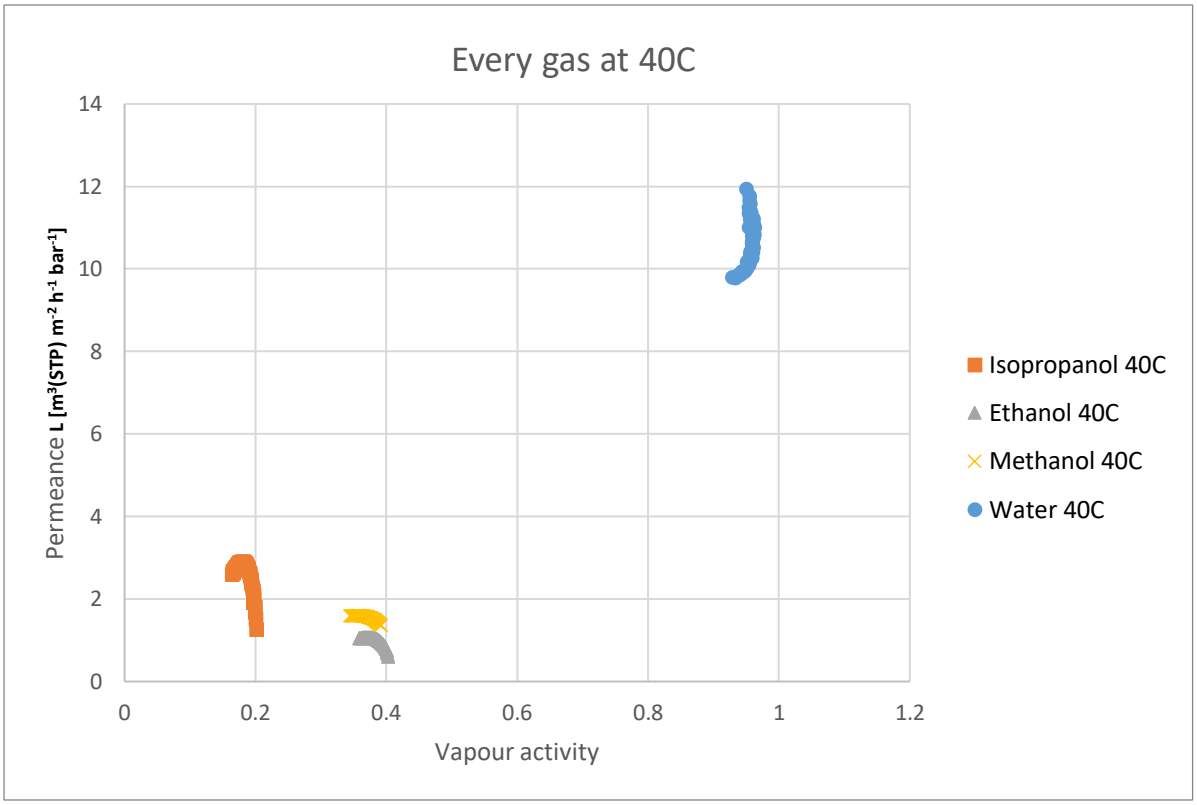

Here is the detailed analysis of the graph titled "Every gas at 40°C," which represents the relationship between vapor activity (in the x-axis) and permeance (in the y-axis) for the different gases (isopropanol, ethanol, methanol, and water) at 40°C.

General Observations:

Water (blue circles) has the highest permeance among the gases, reaching values slightly above 12 and showing a noticeable increase as vapor activity approaches 1.

Isopropanol (orange squares) has the lowest permeance, remaining below 3 for all vapor activities.

Methanol (yellow crosses) and ethanol (gray triangles) display intermediate permeance values, but both stay below 3, similar to isopropanol.

Gas-Specific Behavior:

Water (Blue Circles): Permeance increases significantly as vapor activity rises, peaking above 12 at a vapor activity of approximately 1. The strong permeance trend suggests favorable transport of water through the membrane at 40°C.

Methanol (Yellow Crosses): Permeance remains relatively constant and low, staying just below 2 across the range of vapor activities. This indicates limited transport of methanol, likely due to weaker interactions with the membrane material.

Ethanol (Gray Triangles): Similar to methanol, ethanol permeance remains low, slightly below 2, with minimal sensitivity to vapor activity. The behavior suggests that ethanol transport is restricted at 40°C, possibly due to its larger molecular size or different interaction mechanisms.

Isopropanol (Orange Squares): The permeance is the lowest among the gases, staying below 3 across all vapor activities. This confirms that the membrane shows very limited permeability to isopropanol at 40°C.

Temperature Impact on Gases:

At 40°C, the membrane displays a clear preference for water over the alcohols, similar to the behavior observed at 50°C.

Alcohol permeance (methanol, ethanol, and isopropanol) is low and relatively flat, indicating minimal sensitivity to vapor activity.

Key Trends:

Water Dominance: Water exhibits the highest permeance, increasing as vapor activity rises, which highlights the membrane's selectivity for water over alcohols.

Limited Alcohol Transport: Methanol, ethanol, and isopropanol show minimal permeance and limited variation with vapor activity, suggesting that the membrane becomes less permeable to alcohols at 40°C.

Strong Selectivity at 40°C: The sharp contrast between water and alcohol permeance suggests strong water-alcohol separation potential.

Key Insights:

Water Permeability: The membrane favors water transport at 40°C, with permeance increasing significantly at higher vapor activities.

Minimal Alcohol Permeability: Methanol, ethanol, and isopropanol exhibit low and nearly constant permeance, indicating reduced alcohol transport at this temperature.

Temperature Dependence: Compared to 50°C, permeance values for water remain high, while alcohol permeance shows no significant improvement.

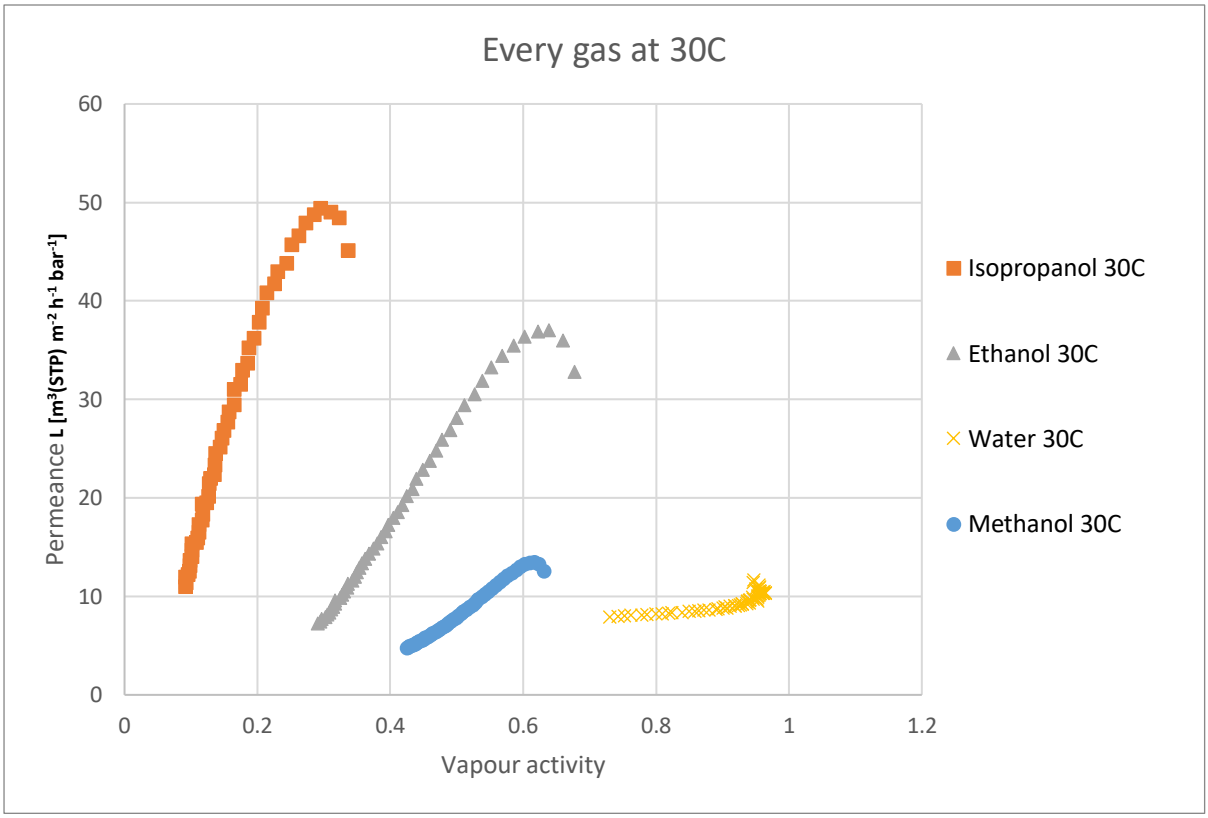

This graph represents the relationship between vapor activity (x-axis) and permeance (y-axis) for various gases (isopropanol, ethanol, water, and methanol) at 30°C.

General Observations:

Isopropanol (orange squares) exhibits the highest permeance at 30°C, peaking above 50, with a steep increase as vapor activity rises.

Ethanol (gray triangles) has the second-highest permeance, with values reaching around 40 and a clear dependence on vapor activity.

Water (yellow crosses) and methanol (blue circles) have significantly lower permeance, staying below 15 across the entire range of vapor activities.

The gases demonstrate a clear distinction in behavior, indicating varying interactions with the membrane at this temperature.

Gas-Specific Behavior:

Isopropanol (Orange Squares): Permeance is the highest among the gases, with a sharp increase as vapor activity rises to approximately 0.3, peaking above 50. This steep growth suggests strong interaction between isopropanol and the membrane at 30°C, possibly due to favorable adsorption or diffusion mechanisms.

Ethanol (Gray Triangles): Permeance rises steadily with vapor activity, reaching values near 40. The behavior indicates moderately strong interaction with the membrane, though slightly less pronounced compared to isopropanol.

Water (Yellow Crosses): Permeance remains low, peaking around 10, with limited sensitivity to vapor activity. This suggests weak transport through the membrane for water at 30°C, in contrast to its dominant behavior at higher temperatures.

Methanol (Blue Circles): Permeance is similar to water, peaking slightly above 10, with a gradual increase as vapor activity rises. The limited permeance indicates reduced affinity or interaction with the membrane at this temperature.

Key Trends:

Isopropanol and Ethanol Dominance: These two alcohols exhibit much higher permeance at 30°C compared to water and methanol, highlighting the membrane's preference for larger alcohol molecules at this temperature.

Vapor Activity Sensitivity: Both isopropanol and ethanol show a strong dependence on vapor activity, with permeance increasing significantly as vapor activity rises.

Limited Transport of Water and Methanol: These gases exhibit relatively flat curves, indicating limited sensitivity to vapor activity and weak transport through the membrane.

Key Insights:

Isopropanol Selectivity: At 30°C, the membrane exhibits the highest selectivity for isopropanol, likely due to strong interactions with the material or enhanced diffusion mechanisms.

Shift in Behavior: The low permeance of water and methanol at 30°C contrasts with their higher permeance at 40°C and 50°C, suggesting temperature-dependent selectivity shifts.

Intermediate Performance for Ethanol: Ethanol shows strong permeance but remains below isopropanol, reflecting differences in molecular size or in the affinity with the membrane.

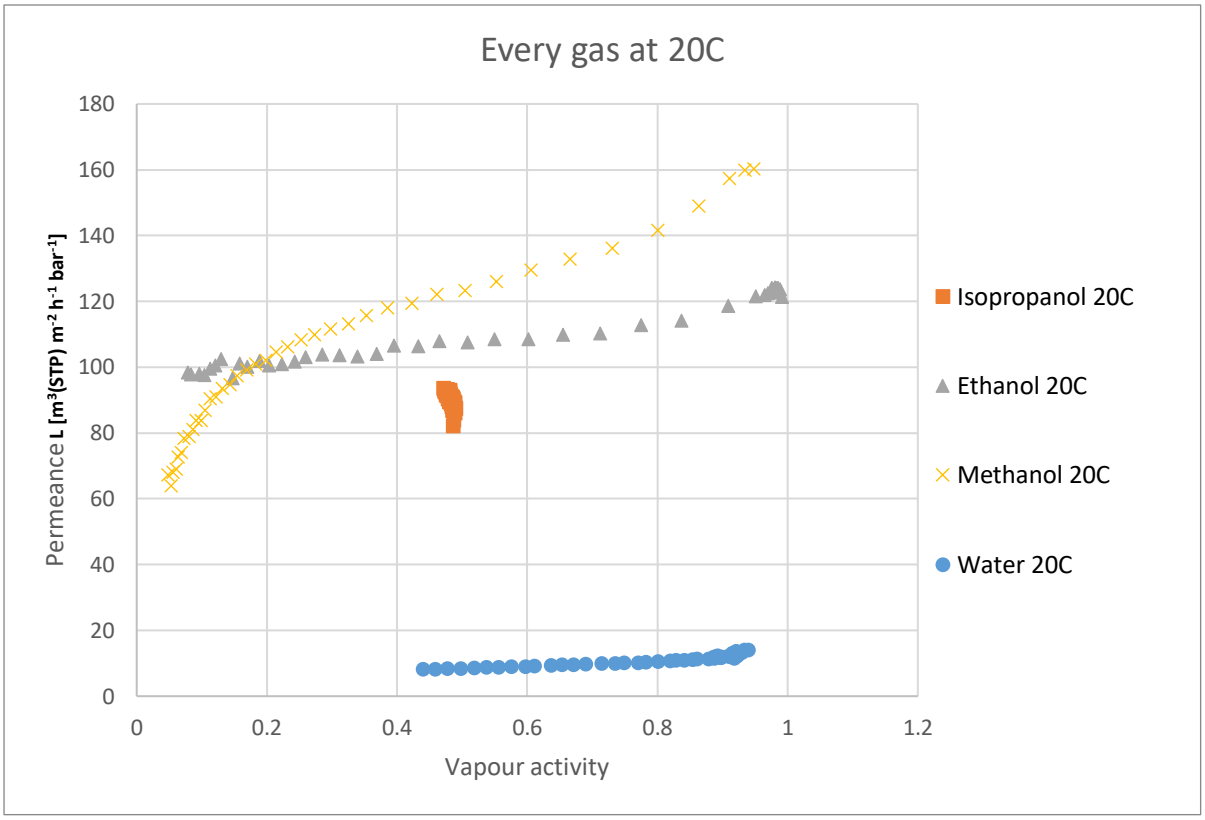

For the analysis of the graph titled "Every gas at 20°C" which represents the relationship between vapor activity (in the x-axis) and permeance (in the y-axis) for our different gases (isopropanol, ethanol, methanol, and water) at 20°C.

General Observations:

-Methanol (yellow crosses) exhibits the highest permeance, peaking near 160 at high vapor activities.

-Ethanol (gray triangles) has the second-highest permeance, reaching values around 120.

-Water (blue circles) and isopropanol (orange squares) show significantly lower permeance, remaining below 40 across all vapor activities.

-The gases display clear differences in permeance behavior, indicating varying interactions with the membrane at this temperature.

Gas-Specific Behavior:

Methanol (Yellow Crosses): Permeance increases steadily with vapor activity, peaking at approximately 160. The sharp increase in permeance suggests a strong affinity of methanol for the membrane material, possibly due to its small molecular size and high diffusivity.

Ethanol (Gray Triangles): Permeance rises gradually with vapor activity, reaching a maximum of around 120. The behavior indicates strong ethanol-membrane interactions, though less pronounced than methanol due to ethanol's slightly larger molecular size.

Water (Blue Circles): Permeance is nearly constant and low, staying below 20 across all vapor activities. This suggests limited transport of water through the membrane at 20°C, likely due to reduced interactions or competition with alcohol molecules.

Isopropanol (Orange Squares): Permeance remains low, peaking around 30 and showing limited sensitivity to vapor activity. The low permeance indicates restricted transport of isopropanol, potentially due to its larger molecular size or weaker interactions with the membrane.

Key Trends:

-Methanol Dominance: Methanol exhibits the highest permeance at 20°C, indicating the membrane's strong affinity for methanol at this temperature.

-Ethanol as Secondary Performer: Ethanol shows similar trends to methanol but with slightly lower permeance values.

-Water and Isopropanol Limitations: Both gases exhibit minimal permeance, suggesting that the membrane strongly favors alcohol transport at low temperatures.

Key Insights:

Alcohol Selectivity: At 20°C, the membrane favors methanol and ethanol over water and isopropanol, likely due to the smaller molecular sizes of methanol and ethanol and their stronger interactions with the membrane.

Water Permeability Shift: The low permeance of water at 20°C contrasts with its dominant behavior at higher temperatures, highlighting temperature-dependent selectivity.

Isopropanol Limitations: Isopropanol consistently shows low permeance, suggesting that the membrane is less suited for its separation under these conditions.

5.2.1.4.-Comparative analysis of the 4 graphs

The four graphs represent the permeance of different gases (water, methanol, ethanol, and isopropanol) across a thin-film composite membrane (TFCM) with 1% PIM-1 as a function of vapor activity at 20°C, 30°C, 40°C, and 50°C. Since the main goal of this thesis is to separate bioethanol-water mixtures, this analysis will focus on membrane selectivity for water over ethanol and its implications for bioethanol purification.

5.2.1.4.1.-General Observations

-Water permeance is dominant at high temperatures (40°C and 50°C).

-Ethanol, methanol, and isopropanol show significantly lower permeance at elevated temperatures.

-At low temperatures (20°C, 30°C), alcohols exhibit higher permeance, particularly methanol and ethanol.

-Isopropanol consistently shows the lowest permeance across all temperatures.

-Water permeance increases almost linearly with vapor activity, whereas alcohols exhibit a more complex trend.

5.2.1.4.2.-Comparative Analysis by Gas Type

Water (Graph 1)

Key Trends:

-Water permeance is highest at 50°C (~25-30), decreasing at lower temperatures.

-At 20°C, water permeance is relatively low (~10) but still shows an increasing trend with vapor activity.

-The permeance-vapor activity relationship is nearly linear, suggesting that water transport is diffusion-driven.

Implications for Bioethanol Separation:

-High water permeance at 40°C and 50°C suggests that the membrane is more effective at separating water from ethanol at elevated temperatures.

-At lower temperatures (20°C and 30°C), ethanol permeance approaches water permeance, which may reduce selectivity for bioethanol dehydration.

Methanol (Graph 2)

Key Trends:

-Methanol shows very high permeance at 20°C (~160), which decreases dramatically at 30°C and nearly disappears at 40°C and 50°C.

-The permeance trend is non-linear with vapor activity, showing a rapid increase at low activity before stabilizing.

Implications for Bioethanol Separation:

-The high methanol permeance at 20°C suggests strong affinity with the membrane, likely due to its small molecular size and ability to hydrogen bond.

-The sharp decline at higher temperatures means that at 40°C and 50°C, methanol removal will be ineffective, making the membrane unsuitable for methanol recovery at high temperatures.

-This behavior indicates that sorption effects dominate at low temperatures, while diffusion limitations take over at higher temperatures.

Ethanol (Graph 3)

Key Trends:

-Ethanol permeance is highest at 20°C (~120), slightly lower than methanol, and decreases significantly at higher temperatures.

-At 30°C, ethanol permeance remains moderate (~40), but at 40°C and 50°C, it drops to near-zero values.

Implications for Bioethanol Separation:

-Ethanol's high permeance at 20°C suggests that at low temperatures, the membrane does not effectively separate ethanol from water.

-At 40°C and 50°C, ethanol permeance is negligible compared to water, making these temperatures ideal for selective water removal from bioethanol.

-The temperature-dependent behavior suggests that ethanol interacts with the polymer via sorption mechanisms at low temperatures, while reduced polymer free volume at higher temperatures restricts ethanol transport.

Isopropanol (Graph 4)

Key Trends:

-Permeance is significantly lower than for methanol and ethanol across all temperatures.

-At 20°C, isopropanol has moderate permeance (~90), but this drops drastically at higher temperatures.

-The vapor activity-permeance relationship is relatively weak, indicating diffusion limitations.

Implications for Bioethanol Separation:

-Isopropanol's bulky molecular structure hinders its diffusion through the membrane, confirming that size exclusion plays a significant role in separation.

-This suggests that the membrane is more effective at rejecting larger molecules (such as isopropanol) while allowing water to pass at higher temperatures.

5.2.1.4.3.-Key Structure-Property Relationships

a) *Effect of Molecular Size on Permeance*

Gas	Kinetic Diameter (nm)	Permeance (20°C)	Permeance (50°C)
Water	~0.265	Moderate	High
Methanol	~0.36	Very High	Low
Ethanol	~0.44	High	Low
Isopropanol	~0.50	Moderate	Very Low

-Water's small size allows it to diffuse efficiently through the membrane.

-Larger alcohols (ethanol, isopropanol) exhibit lower permeance due to steric hindrance.

-Methanol, despite being larger than water, has high permeance at 20°C, likely due to hydrogen bonding and strong sorption effects.

-At higher temperatures, polymer chain mobility decreases, reducing alcohol permeance while maintaining high water permeance.

b) *Free Volume and Polymer Mobility*

- At lower temperatures, the polymer matrix has more available free volume, allowing easier alcohol diffusion.
- At higher temperatures, the membrane structure tightens, restricting alcohol transport but still permitting water passage.
- Water's ability to disrupt polymer-polymer interactions may enhance its transport even as polymer chains contract at high temperatures.

c) *Hydrogen Bonding and Sorption Effects*

- Alcohols interact with the polymer matrix through hydrogen bonding, which facilitates sorption at lower temperatures.
- At higher temperatures, reduced hydrogen bonding lowers alcohol permeance, favoring water selectivity.
- The membrane's affinity for alcohols at 20°C suggests it behaves as a sorption-driven system at low temperatures and a diffusion-limited system at high temperatures.

5.2.1.4.4.-Implications for Bioethanol Dehydration

Best Operating Conditions for Bioethanol-Water Separation

Temperature	Water Permeance	Ethanol Permeance	Selectivity (Water/Ethanol)	Suitability for Dehydration
20°C	Low	High	Poor	Not recommended
30°C	Moderate	Moderate	Low	Not ideal
40°C	High	Low	Good	Effective
50°C	Very High	Very Low	Excellent	Optimal

-Operating at 40°C–50°C is the best strategy for bioethanol dehydration using this membrane.

-At these temperatures, ethanol permeance is minimal, while water permeance is maximized, ensuring effective water removal.

-At lower temperatures (20°C, 30°C), ethanol transport is too high, making the membrane ineffective for bioethanol dehydration.

5.2.1.4.5.-Final Conclusions

The membrane exhibits strong temperature-dependent selectivity, favoring water permeation over alcohols at higher temperatures.

- Methanol and ethanol have high permeance at 20°C but become nearly impermeable at 50°C, highlighting the role of hydrogen bonding and polymer relaxation in transport behavior.
- Isopropanol's limited permeance across all temperatures suggests that size exclusion effects also influence separation.
- The membrane is highly effective for bioethanol dehydration at 40°C and 50°C, where water permeance is high and ethanol permeance is low.
- Lower temperatures (20°C, 30°C) are unsuitable for bioethanol dehydration due to excessive ethanol transport.

Recommendation for Industrial Application:

- Operate the membrane at 50°C to achieve the best bioethanol-water separation efficiency.
- Consider membrane modifications to further enhance ethanol rejection and water permeability for improved separation performance.

5.2.2.-Permeance vs time graphs (results and discussion)

To understand how the TFCM´s permeance evolves through time, in this chapter we have created different graphs following the same structure as for the permeance vs vapor activity. Following what we did in the previous chapter, I will divide it into 2 sections, one in which I will analyze the graphs with the same gas flow and its different temperatures and the other one, in which I will analyze the different gases at the same temperature.

5.2.2.1.-Same gas at different temperatures

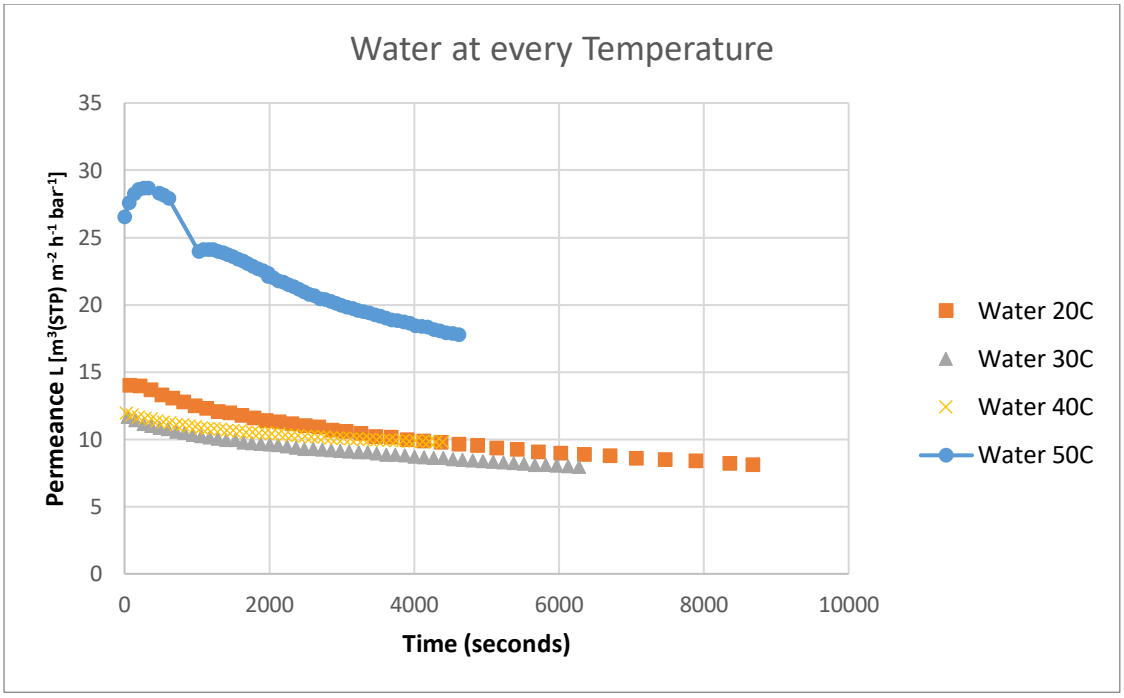

This graph represents the relationship between time (in the x-axis) and permeance (in the y-axis) for water at the different temperatures we previously stablished (20°C, 30°C, 40°C, and 50°C).

General Observations:

The permeance of water decreases over time for all temperatures.

At higher temperatures (50°C), the initial permeance is the highest, peaking around 30, but it declines sharply with time.

At lower temperatures (20°C, 30°C, and 40°C), the permeance starts lower and decreases more gradually over time.

All curves tend to stabilize at lower permeance values as time progresses.

Temperature-Specific Behavior:

Water at 50°C (Blue Line): Starts with the highest permeance, around 30, but decreases rapidly within the first 2000 seconds. After the initial decline, the permeance stabilizes near 20, suggesting that the membrane undergoes rapid changes (e.g., saturation or structural adjustments) before reaching equilibrium.

Water at 40°C (Yellow Crosses): Begins with an intermediate permeance around 15, which decreases steadily over time. The decline is less sharp compared to 50°C, and the permeance stabilizes near 10 after around 4000 seconds.

Water at 30°C (Gray Triangles): Starts with a lower permeance (just below 15) and decreases gradually, showing a consistent decline over the entire time range. Stabilizes near 10, similar to 40°C, but takes longer to reach this equilibrium point.

Water at 20°C (Orange Squares): Starts with the lowest permeance, around 10, and decreases very gradually over time. The decline is minimal, and the permeance remains just below 10 throughout the time range, indicating that the membrane is less affected by time-related changes at lower temperatures.

Key Trends:

Initial Permeance vs. Temperature: Higher temperatures correspond to higher initial permeance values, suggesting increased water transport through the membrane at elevated temperatures.

Permeance Decline Over Time: The rate of decline is steeper at higher temperatures (50°C), likely due to faster saturation, fouling, or material relaxation. At lower temperatures (20°C), the decline is minimal, indicating more stable long-term performance.

Equilibrium Permeance: All curves tend to stabilize at similar permeance values (around 10), regardless of the initial permeance or temperature.

Key Insights:

Temperature Impact: The membrane's initial water permeance is strongly temperature-dependent, with higher temperatures leading to significantly higher initial values. This is likely due to increased water diffusivity and interaction with the membrane material at elevated temperatures.

Long-Term Stability: Over time, the permeance values converge, suggesting that the membrane stabilizes after initial changes (e.g., saturation or structural adjustment), regardless of temperature.

Optimal Performance: At lower temperatures (e.g., 20°C), the permeance is stable and changes minimally over time, potentially indicating better long-term stability for industrial applications requiring consistent performance.

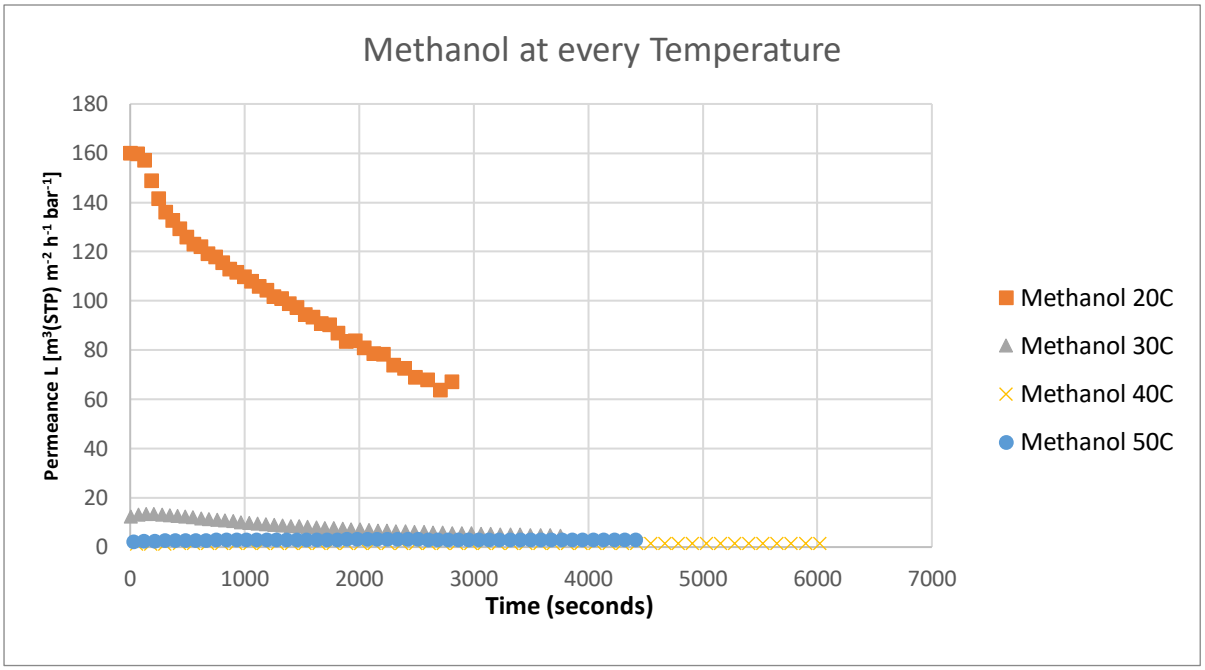

Analysis of the graph titled "Methanol at Every Temperature," which represents the relationship between time (in the x-axis) and permeance (in the y-axis) for methanol at our different temperatures (20°C, 30°C, 40°C, and 50°C).

General Observations:

Methanol at 20°C (Orange Squares): Exhibits the highest initial permeance, starting near 160, but decreases rapidly over time. By around 3000 seconds, the permeance has declined to approximately 80, showing a significant reduction in transport efficiency.

Methanol at 30°C (Gray Triangles): Displays much lower permeance compared to 20°C, starting below 20 and decreasing slowly over time. Stabilizes around 10 after approximately 2000 seconds.

Methanol at 40°C (Yellow Crosses): Shows minimal permeance, starting below 10 and maintaining a nearly flat curve. There is little to no decline over time, suggesting limited methanol transport through the membrane at this temperature.

Methanol at 50°C (Blue Circles): Similar to 40°C, the permeance is very low (close to zero) across the entire time range. This indicates negligible methanol transport at 50°C.

Temperature-Specific Behavior:

Methanol at 20°C: The high initial permeance suggests strong interactions between methanol and the membrane material at lower temperatures. The sharp decline over time could be due to saturation of the membrane or structural changes affecting transport pathways.

Methanol at 30°C: Permeance is much lower than at 20°C, with a gradual decline indicating weaker interactions or a slower saturation process.

Methanol at 40°C and 50°C: Permeance values are extremely low, indicating that higher temperatures significantly limit methanol transport. This could be due to changes in the membrane's structure or reduced affinity for methanol at elevated temperatures.

Key Trends:

Temperature Impact on Permeance: Methanol permeance is strongly temperature-dependent, with the highest values at 20°C and minimal transport at 40°C and 50°C.

Permeance Decline Over Time: The decline is most pronounced at 20°C, suggesting that methanol transport is highly dynamic and sensitive to time at lower temperatures. At higher temperatures (40°C and 50°C), the minimal transport remains stable over time.

Key Insights:

Optimal Temperature for Methanol Transport: At 20°C, the membrane exhibits the highest methanol permeance, indicating strong compatibility with methanol at low temperatures.

Reduced Permeance at Higher Temperatures: The significant drop in permeance at 30°C and above suggests that the membrane's selectivity or permeability for methanol decreases sharply as temperature increases.

Long-Term Stability: The permeance decline over time is most significant at 20°C, likely due to saturation effects. At higher temperatures, the stable but low permeance suggests limited interaction with methanol.

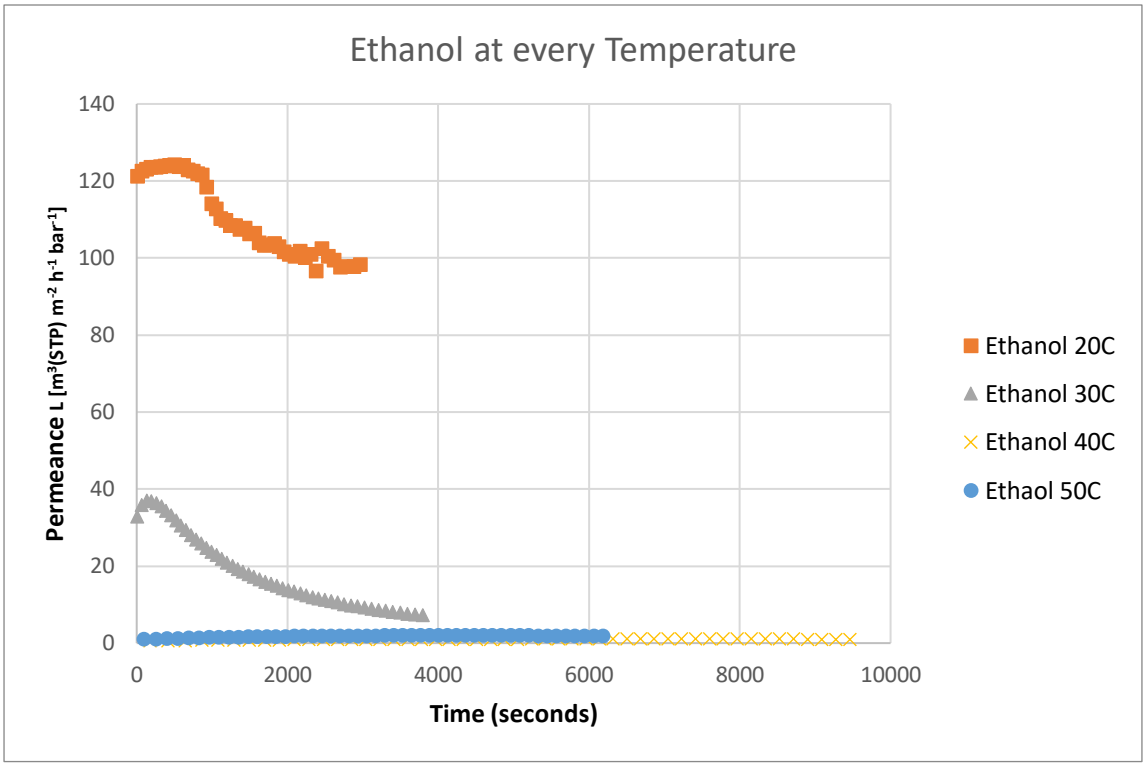

Here is the detailed analysis of the graph titled "Ethanol at Every Temperature," which represents the relationship between time (in the x-axis) and permeance (in the y-axis) for ethanol at various temperatures (20°C, 30°C, 40°C, and 50°C).

General Observations:

Ethanol at 20°C (Orange Squares): Exhibits the highest permeance, starting above 120, and gradually decreases over time. By 4000 seconds, the permeance stabilizes around 100, showing a slower decline compared to methanol at the same temperature.

Ethanol at 30°C (Gray Triangles): Starts with moderate permeance, around 40, and decreases steadily over time. Permeance stabilizes near 10 after approximately 3000 seconds, indicating reduced ethanol transport at this temperature.

Ethanol at 40°C (Yellow Crosses): Shows minimal permeance, starting near 5 and remaining relatively constant over the entire time range. The flat curve suggests limited ethanol transport at this temperature.

Ethanol at 50°C (Blue Circles): Similar to 40°C, the permeance is very low (close to zero) and stable throughout the time range, indicating negligible ethanol transport at this temperature.

Temperature-Specific Behavior:

Ethanol at 20°C: The high initial permeance suggests strong interactions between ethanol and the membrane material at low temperatures. The slow decline over time indicates relatively stable transport compared to other temperatures, likely due to favorable conditions for diffusion and adsorption.

Ethanol at 30°C: Moderate initial permeance indicates weaker ethanol-membrane interactions compared to 20°C. The steady decline and stabilization around 10 suggest saturation or structural adjustments in the membrane.

Ethanol at 40°C and 50°C: Permeance values are extremely low, indicating that higher temperatures significantly hinder ethanol transport. This could result from reduced affinity between ethanol and the membrane or changes in the material's structure.

Key Trends:

Temperature Impact on Permeance: Ethanol permeance is strongly temperature-dependent, with the highest values at 20°C and minimal transport at 40°C and 50°C.

Permeance Decline Over Time: The decline is most pronounced at 20°C and 30°C, suggesting that ethanol transport is dynamic and influenced by time at these temperatures. At higher temperatures, the minimal transport remains stable over time.

Key Insights:

Optimal Temperature for Ethanol Transport: At 20°C, the membrane exhibits the highest ethanol permeance, indicating strong compatibility with ethanol at low temperatures.

Reduced Permeance at Higher Temperatures: The significant drop in permeance at 30°C and above suggests that the membrane's selectivity or permeability for ethanol decreases sharply as temperature increases.

Long-Term Stability: At 20°C, the permeance stabilizes at a high value (around 100), while at 30°C and higher temperatures, permeance stabilizes at significantly lower values.

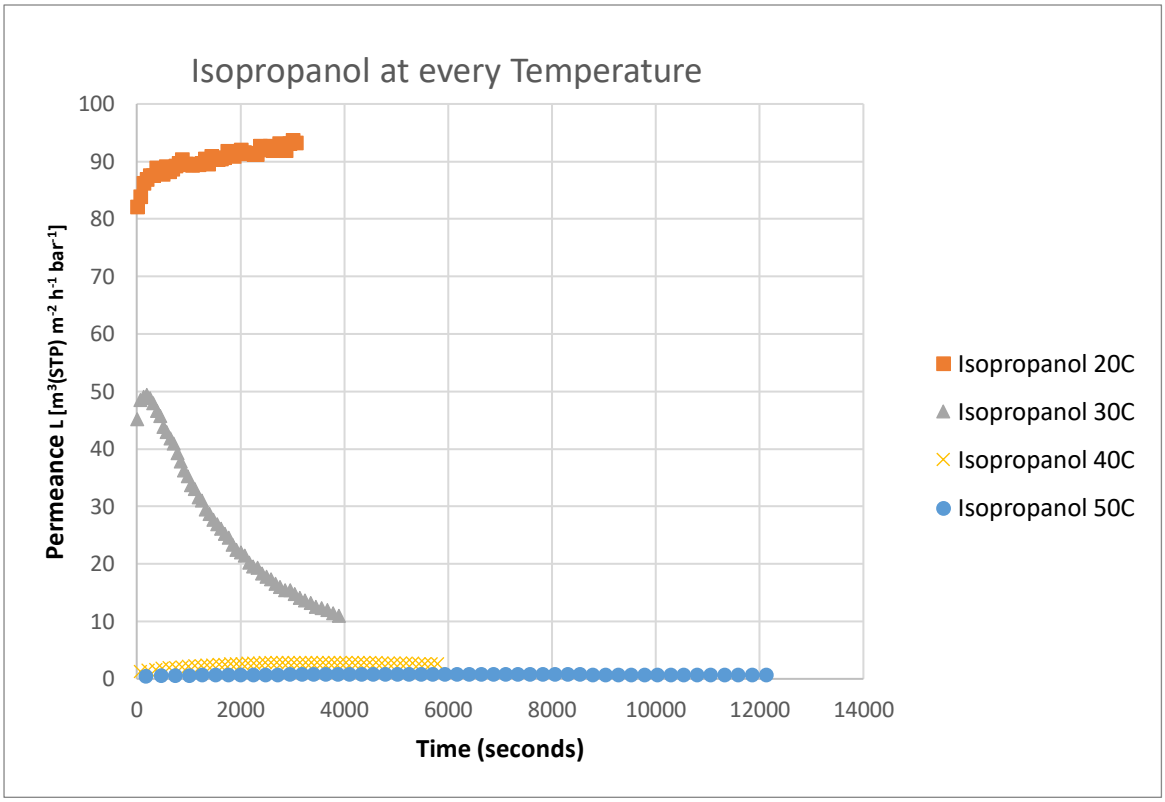

Here is the detailed analysis of the graph titled "Isopropanol at Every Temperature," which represents the relationship between time (in the x-axis) and permeance (in the y-axis) for isopropanol at various temperatures (20°C, 30°C, 40°C, and 50°C).

General Observations:

Isopropanol at 20°C (Orange Squares): Exhibits the highest permeance, starting around 90, with a gradual stabilization over time. The curve remains relatively flat, showing minimal decline, suggesting consistent transport through the membrane at this temperature.

Isopropanol at 30°C (Gray Triangles): Begins with a moderate permeance, around 50, and declines steadily over time. By 4000 seconds, permeance stabilizes near 10, indicating a significant reduction in isopropanol transport.

Isopropanol at 40°C (Yellow Crosses): Shows minimal permeance, starting below 10 and remaining relatively flat over the time range. The low and stable values indicate very limited isopropanol transport at this temperature.

Isopropanol at 50°C (Blue Circles): Similar to 40°C, permeance values are extremely low (close to zero) throughout the time range. This suggests negligible interaction between isopropanol and the membrane at higher temperatures.

Temperature-Specific Behavior:

Isopropanol at 20°C: High permeance indicates a strong interaction between isopropanol and the membrane material at lower temperatures. The flat curve suggests minimal saturation effects or material changes over time.

Isopropanol at 30°C: The decline in permeance over time suggests that isopropanol transport decreases due to saturation or structural adjustments in the membrane.

Isopropanol at 40°C and 50°C: The consistently low permeance at these temperatures indicates that the membrane is significantly less permeable to isopropanol as temperature increases. This could be due to reduced affinity for isopropanol or changes in membrane structure at elevated temperatures.

Key Trends:

Temperature Impact on Permeance: Isopropanol permeance is strongly temperature-dependent, with the highest values at 20°C and minimal transport at 40°C and 50°C.

Permeance Decline Over Time: The decline is most significant at 30°C, indicating dynamic transport behavior at this intermediate temperature. At 20°C, the permeance stabilizes quickly, suggesting more stable long-term performance.

Key Insights:

Optimal Temperature for Isopropanol Transport: The membrane exhibits the highest isopropanol permeance at 20°C, indicating strong compatibility with isopropanol at low temperatures.

Reduced Permeance at Higher Temperatures: The permeance drop at 30°C and near-zero values at 40°C and 50°C suggest that the membrane is far less suited for isopropanol transport at elevated temperatures.

Stability Over Time: At 20°C, permeance remains stable over time, while at 30°C, there is a gradual decline before stabilization, possibly due to saturation effects.

5.2.2.2.-Comparative Analysis of Gas Permeance Over Time in our TFCM

The provided graphs illustrate us the time-dependent permeance of water, methanol, ethanol, and isopropanol at different temperatures (20°C, 30°C, 40°C, and 50°C) through the thin-film composite membrane (TFCM) with 1% PIM-1. Since the primary objective of this thesis is to separate bioethanol from water, the focus will obviously be on assessing the long-term stability of membrane performance, selectivity trends, and their implications for bioethanol dehydration.

5.2.2.2.1.-General Observations

-Water exhibits the highest permeance at higher temperatures (40°C and 50°C) and remains relatively stable over time.

-Methanol and ethanol show high permeance at 20°C but experience significant time-dependent declines.

-Isopropanol displays moderate permeance at 20°C and 30°C but drops drastically at higher temperatures.

-At 40°C and 50°C, alcohol permeance is nearly negligible, reinforcing the membrane's ability to separate water from alcohols at elevated temperatures.

5.2.2.2.2.-Comparative Analysis by Gas Type

Water (Graph 1)

Key Trends: Water permeance remains consistently high at 50°C, with only a slight decline over time. At lower temperatures (20°C, 30°C), water permeance decreases gradually, with more significant time-dependent reduction at 20°C. The rate of decline over time is relatively minor compared to alcohols, indicating stable water transport.

Implications for Bioethanol Separation: Water permeance stability at higher temperatures (40°C and 50°C) confirms the membrane's suitability for bioethanol dehydration. The slower decline in water permeance over time suggests long-term effectiveness for water removal in continuous separation processes.

Methanol (Graph 2)

Key Trends: Methanol exhibits the highest initial permeance at 20°C (~160), but this value declines steeply over time, stabilizing around 60–80. At 30°C, methanol permeance starts lower (~20) and decreases gradually. At 40°C and 50°C, methanol permeance is nearly zero, indicating an inability to permeate effectively at higher temperatures.

Implications for Bioethanol Separation: The sharp decline in methanol permeance over time suggests initial sorption-dominated transport, followed by polymer saturation or relaxation effects. The inability of methanol to permeate at 40°C and 50°C supports selective water transport over methanol, which is desirable for ethanol-water separation.

Ethanol (Graph 3)

Key Trends: Ethanol shows high permeance at 20°C (~120), but it declines significantly over time. At 30°C, the permeance is lower (~40) and continues decreasing with time. At 40°C and 50°C, ethanol permeance approaches zero, similar to methanol.

Implications for Bioethanol Separation: The rapid decline in ethanol permeance suggests strong polymer-alcohol interactions at low temperatures, which may lead to temporary sorption before equilibrium is reached. At higher temperatures, the membrane effectively blocks ethanol transport, making it highly selective for water at 40°C and 50°C. This confirms that bioethanol dehydration using this membrane is most effective at 40°C–50°C.

Isopropanol (Graph 4)

Key Trends: At 20°C, isopropanol has moderate permeance (~90), but it declines significantly over time. At 30°C, the permeance starts at ~40 and drops to near zero over time. At 40°C and 50°C, isopropanol permeance is almost undetectable.

Implications for Bioethanol Separation: Isopropanol's bulkier structure leads to steric hindrance, making diffusion more difficult. The rapid decline in permeance over time suggests poor long-term transport, reinforcing the membrane's selectivity for smaller molecules like water. At 40°C and 50°C, the near-zero permeance further validates the membrane's effectiveness in separating water from alcohols.

5.2.2.2.3.-Key Structure-Property Relationships

a) Molecular Size and Diffusivity

Gas	Kinetic Diameter (nm)	Initial Permeance (20°C)	Final Permeance (After Time)
Water	~0.265	Moderate (~15)	Stable (~10-12)
Methanol	~0.36	Very High (~160)	Declines (~60-80)
Ethanol	~0.44	High (~120)	Declines (~40-50)
Isopropanol	~0.50	Moderate (~90)	Near zero

- Water's small size allows for stable permeance over time, reinforcing membrane selectivity.

- Methanol and ethanol exhibit high initial permeance but decline significantly, indicating sorption-based interactions at low temperatures.
- Isopropanol, due to its bulkiness, faces steric hindrance and limited diffusion.

b) Free Volume and Polymer Relaxation

- At lower temperatures (20°C, 30°C), the polymer has more free volume, allowing alcohols to permeate temporarily.
- At higher temperatures (40°C, 50°C), the polymer contracts, restricting alcohol diffusion while still allowing water transport.
- Water's strong hydrogen bonding ability helps maintain transport even as polymer structure tightens.

c) Sorption vs. Diffusion Control

- Methanol and ethanol show sorption-dominated transport at 20°C, leading to initial high permeance followed by polymer relaxation effects.
- At 40°C and 50°C, alcohol permeance drops to near-zero, suggesting that the separation mechanism shifts to diffusion control.
- Water transport remains high across all temperatures, confirming the membrane's strong water affinity.

5.2.2.2.4.-Implications for Bioethanol Dehydration

Best Operating Conditions for Long-Term Stability

Temperature	Water Permeance Stability	Ethanol Permeance Stability	Selectivity (Water/Ethanol)	Suitability for Dehydration
20°C	Moderate Decline	Sharp Decline	Poor	Not recommended
30°C	Moderate Decline	Gradual Decline	Low	Not ideal
40°C	Stable	Near zero	High	Effective
50°C	Very Stable	Near zero	Excellent	Optimal

- 40°C and 50°C provide the best selectivity for bioethanol-water separation due to stable water permeance and near-zero ethanol transport.
- At 20°C and 30°C, ethanol permeance is still significant, reducing separation efficiency.
- Long-term performance is most stable at 50°C, making it the preferred operating condition.

5.2.2.2.5.-Final Conclusions

- Water permeance remains stable over time, reinforcing membrane efficiency for dehydration applications.
- Methanol and ethanol show high initial permeance but decline significantly, confirming that low-temperature operation is not ideal for bioethanol separation.
- Isopropanol exhibits the lowest permeance, further validating the role of size exclusion in membrane selectivity.
- The membrane is most effective for bioethanol dehydration at 40°C and 50°C, where water transport remains high, and ethanol transport is nearly eliminated.
- Long-term stability is a key advantage at higher temperatures, making this membrane a strong candidate for industrial bioethanol-water separation applications.

5.2.2.3.-Every gas compared at the same temperature

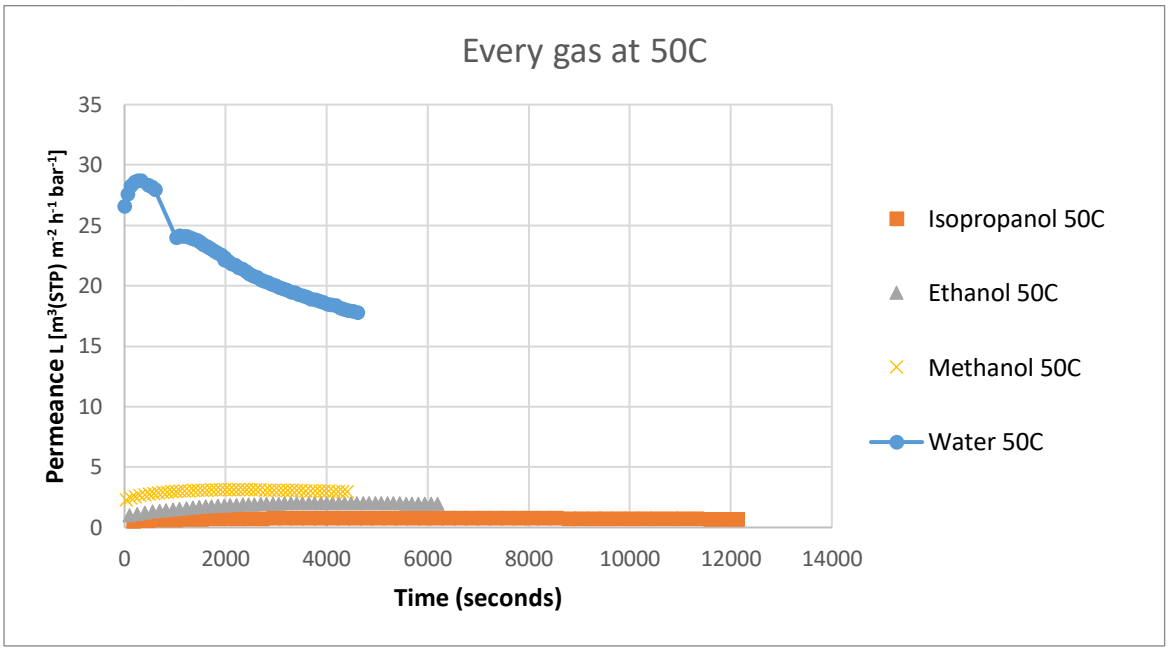

This is the detailed analysis of the graph titled "Every gas at 50°C," which represents the relationship between time (in the x-axis) and permeance (in the y-axis) for our four gases (isopropanol, ethanol, methanol, and water) at 50°C.

General Observations:

Water (Blue Line): Exhibits the highest permeance, starting around 30 and declining steadily over time. Stabilizes near 20 after approximately 2000 seconds, maintaining the highest permeance among all gases.

Methanol (Yellow Crosses): Displays very low permeance, starting below 5 and remaining relatively flat over the time range. This suggests minimal methanol transport through the membrane at 50°C.

Ethanol (Gray Triangles): Similar to methanol, ethanol permeance is minimal, remaining consistently below 5 throughout the time range. There is little to no change over time, reflecting limited interaction with the membrane.

Isopropanol (Orange Squares): Shows the lowest permeance among the four gases, remaining close to zero for the entire time range. Indicates negligible transport of isopropanol through the membrane at 50°C.

Gas-Specific Behavior:

Water: The steep initial decline suggests that the membrane undergoes rapid saturation or adjustment to water transport at 50°C. The stabilization near 20 permeance indicates consistent long-term transport performance.

Methanol and Ethanol: Both alcohols show extremely low permeance, indicating that the membrane is highly selective against them at this temperature. The stable flat curves suggest minimal interaction or negligible diffusion through the membrane.

Isopropanol: The nearly zero permeance highlights the membrane's significant resistance to isopropanol transport at 50°C.This may be due to isopropanol's larger molecular size or reduced affinity for the membrane at higher temperatures.

Key Trends:

Water Dominance: Water exhibits the highest permeance at 50°C, suggesting the membrane's strong selectivity for water over alcohols at elevated temperatures.

Minimal Alcohol Transport: Methanol, ethanol, and isopropanol show consistently low permeance, indicating that higher temperatures severely limit their transport through the membrane.

Time Dependence: Water permeance decreases with time, stabilizing after the initial decline. In contrast, the permeance of alcohols remains almost constant throughout the time range.

Key Insights:

Selective Water Transport: The high water permeance compared to alcohols at 50°C indicates that the membrane is well-suited for separating water from alcohol mixtures at elevated temperatures.

Temperature-Driven Selectivity: The negligible transport of methanol, ethanol, and isopropanol at 50°C highlights a shift in membrane behavior, possibly favoring water due to differences in molecular interactions or diffusivity.

Stable Long-Term Performance: Water transport stabilizes over time, suggesting that the membrane's performance is consistent once initial saturation effects are accounted for.

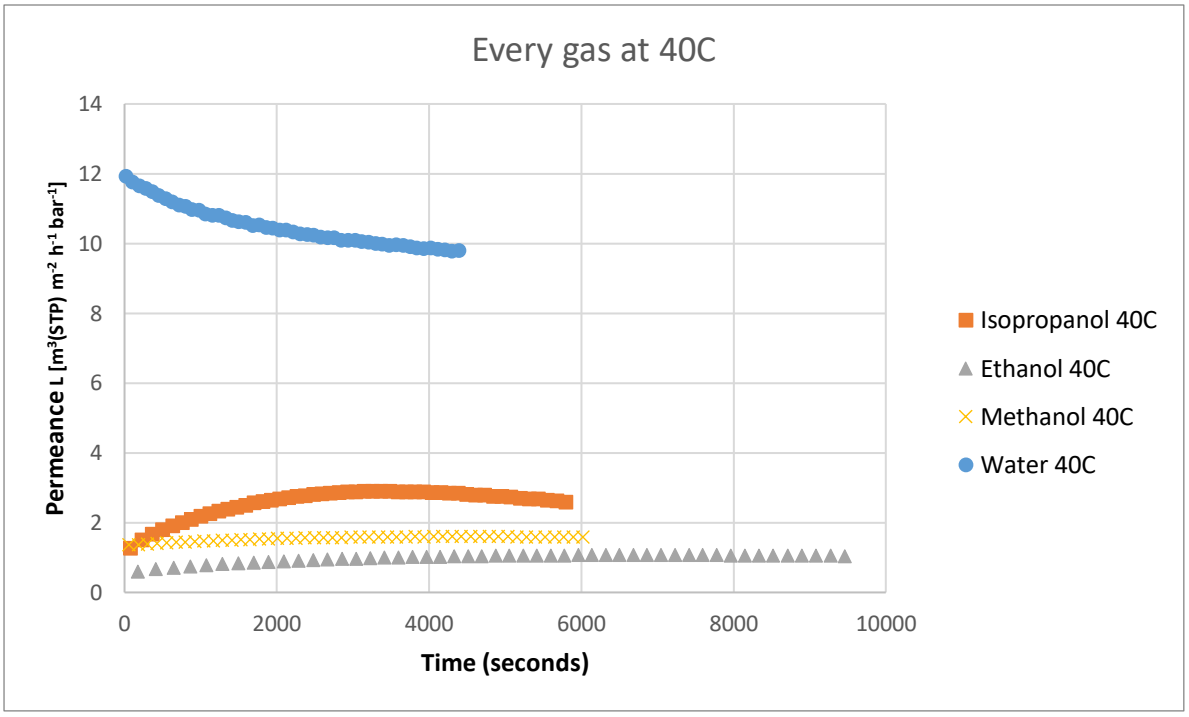

Here we have the detailed analysis of the graph titled "Every gas at 40°C," which represents the relationship between time (in the x-axis) and permeance (in the y-axis) for four gases (isopropanol, ethanol, methanol, and water) at 40°C.

General Observations:

Water (Blue Line): Exhibits the highest permeance among the gases, starting around 12 and gradually declining over time. Stabilizes near 10 after approximately 2000 seconds, indicating consistent transport performance at this temperature.

Isopropanol (Orange Squares): Displays moderate permeance, starting below 3 and increasing slightly before stabilizing around 2.5 over time. This indicates limited but consistent isopropanol transport at 40°C.

Methanol (Yellow Crosses): Shows very low permeance, starting just above 1 and remaining relatively flat throughout the time range. The minimal permeance reflects weak interaction with the membrane.

Ethanol (Gray Triangles): Similar to methanol, ethanol permeance is very low, remaining consistently below 1.5 across the entire time range. This indicates negligible ethanol transport through the membrane at 40°C.

Gas-Specific Behavior:

Water: The gradual decline in permeance over time suggests slight saturation effects but overall stability. The higher permeance compared to other gases indicates a strong affinity for water at this temperature.

Isopropanol: The initial increase and stabilization suggest that the membrane allows limited but measurable transport of isopropanol. The higher permeance compared to methanol and ethanol reflects slightly stronger interactions with the membrane.

Methanol and Ethanol: Both alcohols show minimal permeance and flat curves, indicating weak transport through the membrane. The consistently low values highlight the membrane's reduced permeability to these smaller alcohols at 40°C.

Key Trends:

Water Dominance: Water exhibits the highest permeance at 40°C, suggesting that the membrane is selective for water over alcohols at this temperature.

Limited Alcohol Transport: Methanol, ethanol, and isopropanol all show significantly lower permeance compared to water, indicating that higher temperatures reduce alcohol transport efficiency.

Time Dependence: Water permeance decreases gradually over time, stabilizing after the initial decline, while alcohol permeance remains stable and low throughout the time range.

Key Insights:

Selective Water Transport: The higher water permeance compared to alcohols suggests that the membrane is well-suited for separating water from alcohols at 40°C.

Temperature-Driven Selectivity: The low permeance of methanol, ethanol, and isopropanol highlights the membrane's reduced affinity for these alcohols at elevated temperatures.

Stability Over Time: Water permeance stabilizes after an initial decline, reflecting consistent long-term transport performance.

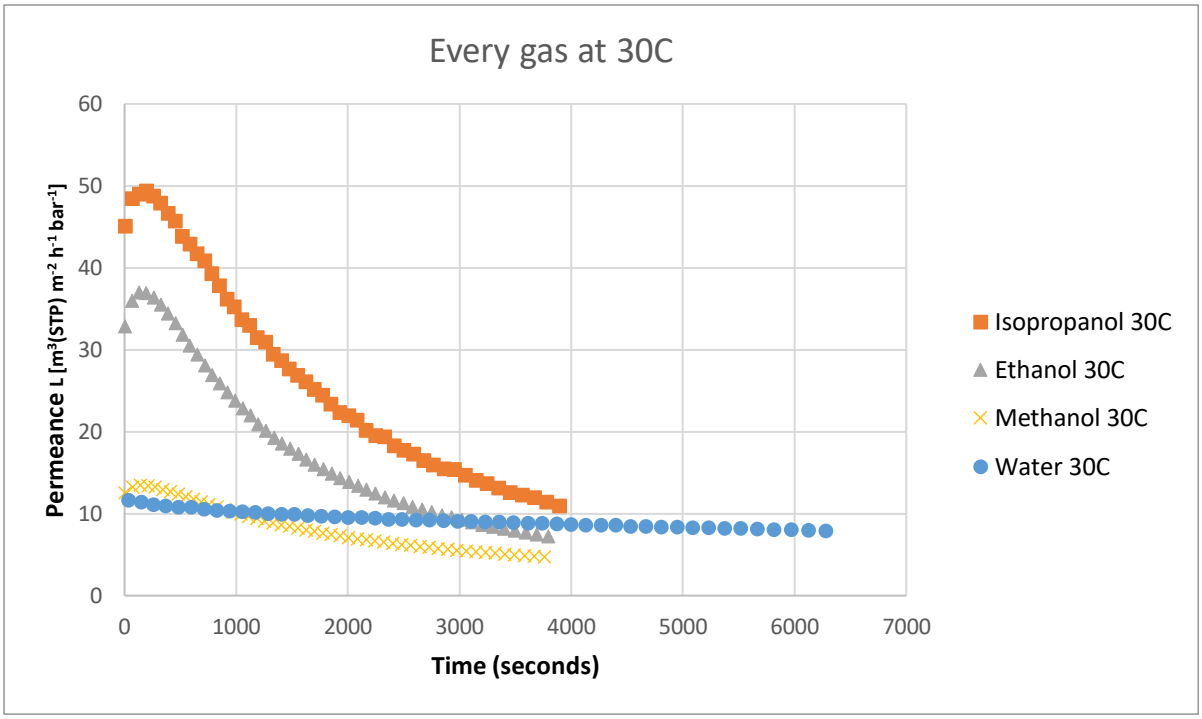

Here is the detailed analysis of the graph titled "Every gas at 30°C," which represents the relationship between time (x-axis) and permeance (y-axis) for four gases (isopropanol, ethanol, methanol, and water) at 30°C.

General Observations:

Isopropanol (Orange Squares): Exhibits the highest initial permeance, starting around 50, but decreases sharply over time. Stabilizes near 10 after approximately 3000 seconds, indicating significant permeance decline.

Ethanol (Gray Triangles): Starts with a moderate permeance of around 40, declining steadily over time. Stabilizes near 10 after approximately 2000 seconds, following a similar pattern to isopropanol but with a steeper initial decline.

Methanol (Yellow Crosses): Displays lower initial permeance, starting below 15, and decreases gradually over time. Stabilizes near 10, reflecting limited transport compared to isopropanol and ethanol.

Water (Blue Circles): Exhibits the lowest initial permeance among the gases, starting around 10, and remains stable with only a slight decline over time. The consistent flat curve indicates steady transport performance at 30°C.

Gas-Specific Behavior:

Isopropanol: The sharp decline in permeance suggests that the membrane initially facilitates high isopropanol transport, likely due to strong interactions or higher diffusivity. The stabilization near 10 permeance indicates eventual saturation or structural adjustments in the membrane.

Ethanol: Similar to isopropanol, ethanol permeance declines over time but starts lower and stabilizes earlier. This behavior reflects slightly weaker interactions with the membrane compared to isopropanol.

Methanol: The lower initial permeance and gradual decline indicate limited methanol transport at 30°C, likely due to weaker diffusion or lower affinity with the membrane.

Water: The stable and low permeance highlights the membrane's reduced preference for water transport at 30°C compared to the alcohols. The slight decline over time suggests minimal saturation effects or structural changes.

Key Trends:

Alcohol Dominance: Isopropanol and ethanol exhibit significantly higher initial permeance compared to methanol and water, indicating stronger compatibility with the membrane.

Permeance Decline Over Time: All gases show a decline in permeance over time, with isopropanol and ethanol exhibiting the steepest drops. Water permeance remains the most stable, with minimal changes throughout the time range.

Stabilization: By 3000–4000 seconds, all gases stabilize near 10 permeance, indicating consistent long-term transport performance regardless of the initial permeance.

Key Insights:

Selective Alcohol Transport: The higher initial permeance of isopropanol and ethanol suggests that the membrane favors these alcohols over water and methanol at 30°C.

Time-Dependent Behavior: The sharp decline in alcohol permeance over time indicates dynamic interactions between the membrane and the alcohols, potentially linked to saturation or structural relaxation.

Stable Water Performance: The consistent water permeance suggests that the membrane's transport properties for water are less influenced by time or initial conditions at 30°C.

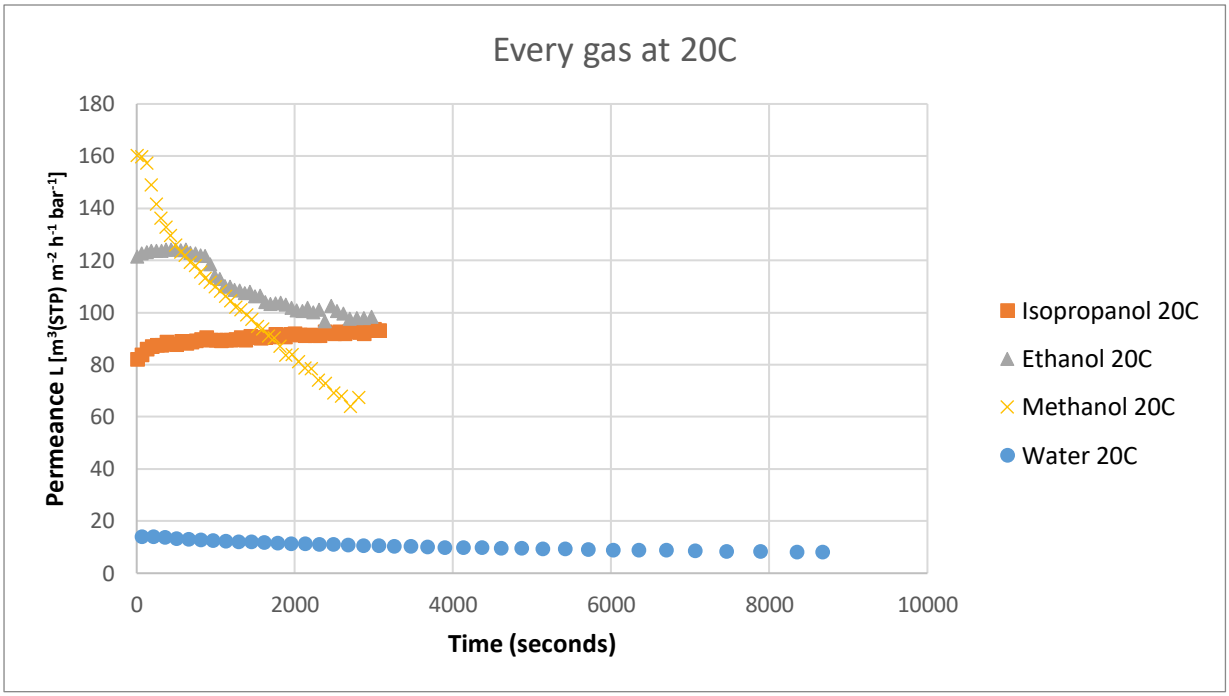

This is the detailed analysis of the graph titled "Every gas at 20°C," which represents the relationship between time (in the x-axis) and permeance (in the y-axis) for four gases (isopropanol, ethanol, methanol, and water) at 20°C.

General Observations:

Methanol (Yellow Crosses): Exhibits the highest initial permeance, starting around 160, but experiences a steep decline over time. Stabilizes near 80 after approximately 2000 seconds.

Ethanol (Gray Triangles): Starts with the second-highest permeance, around 120, and also declines over time. Stabilizes near 100 after 2000 seconds, showing less decline compared to methanol.

Isopropanol (Orange Squares): Starts with moderate permeance, around 90, and declines gradually over time. Stabilizes near 80, reflecting similar long-term performance to methanol.

Water (Blue Circles): Shows the lowest permeance, starting around 20, and remains stable over time with no significant decline. The consistent flat curve indicates steady water transport performance.

Gas-Specific Behavior:

Methanol: The steep decline suggests dynamic interactions between methanol and the membrane, potentially due to saturation or structural changes. The stabilization near 80 permeance indicates consistent long-term transport.

Ethanol: Exhibits a slower decline compared to methanol, stabilizing at a higher permeance of 100. The behavior highlights strong compatibility between ethanol and the membrane at 20°C.

Isopropanol: The gradual decline and stabilization near 80 permeance reflect reduced interaction compared to ethanol but comparable performance to methanol.

Water: The flat, stable curve indicates steady and low water permeance, suggesting limited interaction with the membrane at 20°C.

Key Trends:

Alcohol Dominance: Methanol, ethanol, and isopropanol exhibit significantly higher permeance compared to water, highlighting the membrane's preference for alcohols at 20°C.

Time Dependence: Alcohol permeance declines over time, stabilizing after 2000 units. Methanol shows the steepest decline, followed by ethanol, with isopropanol exhibiting the slowest decrease.

Stable Water Permeance: Water permeance remains consistently low and stable, indicating limited sensitivity to time or initial conditions.

Key Insights:

Selective Alcohol Transport: The membrane shows strong selectivity for alcohols over water at 20°C, with ethanol achieving the highest long-term permeance.

Time-Dependent Behavior: The sharp decline in methanol and ethanol permeance suggests initial saturation effects or dynamic interactions with the membrane material.

Stable Water Performance: Water permeance remains unaffected by time, reflecting consistent and low transport through the membrane.

5.2.2.4.-Comparative Analysis of Gas Permeance Over Time for the last 4 graphs

The provided graphs depict time-dependent permeance of water, methanol, ethanol, and isopropanol at different temperatures (20°C, 30°C, 40°C, and 50°C) through a thin-film composite membrane (TFCM) with 1% PIM-1. Since the main goal of this study is to separate bioethanol-water mixtures, this comparison will focus on:

-Permeance stability over time – critical for industrial membrane applications.

-Temperature-dependent selectivity trends – assessing how the membrane performs at different temperatures.

-Implications for bioethanol dehydration – evaluating how well the membrane separates water from ethanol.

5.2.2.4.1.-General Observations

Water permeance is consistently high across all temperatures, particularly at 50°C, showing minor decline over time.

Methanol and ethanol exhibit high initial permeance at 20°C, but their values decline significantly over time.

At higher temperatures (40°C and 50°C), alcohol permeance approaches near-zero, confirming strong water selectivity.

Isopropanol consistently has the lowest permeance, indicating steric hindrance due to its bulky molecular structure.

At lower temperatures (20°C, 30°C), alcohols initially permeate well but decline over time, indicating polymer relaxation or saturation effects.

5.2.2.4.2.-Comparative Analysis by Gas Type

Water (Graph 1)

Key Trends: Water permeance is highest at 50°C (~25-30) and remains relatively stable over time. At 40°C, water permeance is lower (~12), but it maintains a steady trend. At 20°C and 30°C, water permeance starts lower (~10-12) and declines slightly over time.

Implications for Bioethanol Separation: The stability of water permeance at high temperatures (40°C and 50°C) confirms strong suitability for dehydration applications. The gradual decline at lower temperatures suggests potential membrane saturation effects. For bioethanol purification, operating at 50°C maximizes water removal efficiency.

Methanol (Graph 2)

Key Trends: Methanol exhibits very high initial permeance at 20°C (~160), but this value declines steeply over time, stabilizing at ~60-80.At 30°C, methanol permeance starts lower (~20) and gradually decreases. At 40°C and 50°C, methanol permeance is almost zero.

Implications for Bioethanol Separation: The sharp decline in methanol permeance over time suggests initial sorption effects followed by polymer relaxation. The near-zero permeance at 40°C and 50°C supports selective water transport over methanol. Membrane operation at high temperatures effectively prevents methanol permeation, making it unsuitable for methanol dehydration but ideal for water removal from ethanol-methanol mixtures.

Ethanol (Graph 3)

Key Trends: Ethanol permeance starts high at 20°C (~120), but it declines significantly over time. At 30°C, permeance is lower (~40) and continues to decrease. At 40°C and 50°C, ethanol permeance is nearly zero, similar to methanol.

Implications for Bioethanol Separation: The sharp decrease over time indicates polymer-alcohol interactions, likely hydrogen bonding, causing temporary sorption. At 40°C and 50°C, the membrane completely rejects ethanol, making it ideal for bioethanol dehydration. Operating the membrane at high temperatures ensures selective water removal, leaving ethanol behind.

Isopropanol (Graph 4)

Key Trends: At 20°C, isopropanol has moderate permeance (~90), but it declines significantly over time. At 30°C, initial permeance is lower (~40), and it also declines steadily. At 40°C and 50°C, isopropanol permeance is negligible.

Implications for Bioethanol Separation: Isopropanol's bulky structure limits its diffusion, supporting the role of steric hindrance in separation. Its low permeance suggests that the membrane is highly selective against larger alcohols, favoring water transport instead. For

bioethanol-water separation, the membrane will effectively prevent isopropanol loss, which is beneficial in mixed-alcohol separations.

5.2.2.4.3.-Key Structure-Property Relationships

a) Molecular Size and Transport Efficiency

Gas	Kinetic Diameter (nm)	Initial Permeance (20°C)	Final Permeance (After Time)
Water	~0.265	Moderate (~15)	Stable (~10-12)
Methanol	~0.36	Very High (~160)	Declines (~60-80)
Ethanol	~0.44	High (~120)	Declines (~40-50)
Isopropanol	~0.50	Moderate (~90)	Near zero

- Water's small molecular size allows for stable permeance, making the membrane ideal for dehydration.
- Methanol and ethanol exhibit high initial permeance but decline significantly, suggesting a transition from sorption to diffusion control.
- Isopropanol's low permeance is due to steric hindrance, supporting size-exclusion effects.

b) Free Volume and Polymer Relaxation

- At lower temperatures (20°C, 30°C), the polymer has more free volume, allowing alcohols to permeate initially.
- At higher temperatures (40°C, 50°C), the polymer compacts, restricting alcohol transport while still allowing water.
- Water's ability to hydrogen bond with the polymer keeps its permeance relatively stable, even as the membrane tightens.

c) Sorption vs. Diffusion Control

- Methanol and ethanol undergo sorption-driven transport at 20°C, leading to initial high permeance before polymer saturation occurs.
- At higher temperatures, alcohol permeance drops to near-zero, suggesting a shift from sorption to diffusion-controlled transport.

- Water remains highly permeable across all temperatures, confirming the membrane's water affinity.

5.2.2.4.4.-Implications for Bioethanol Dehydration

Best Operating Conditions for Long-Term Stability

Temperature	Water Permeance Stability	Ethanol Permeance Stability	Selectivity (Water/Ethanol)	Suitability for Dehydration
20°C	Moderate Decline	Sharp Decline	Poor	Not recommended
30°C	Moderate Decline	Gradual Decline	Low	Not ideal
40°C	Stable	Near zero	High	Effective
50°C	Very Stable	Near zero	Excellent	Optimal

- 40°C and 50°C provide the best conditions for bioethanol dehydration, as water permeance remains high while ethanol permeance approaches zero.
- At 20°C and 30°C, ethanol permeance is too high, reducing separation efficiency.
- 50°C is the most stable for long-term performance, making it the recommended operational temperature.

5.2.2.4.5.-Final Conclusions

- Water permeance remains stable, making the membrane ideal for dehydration applications.
- Methanol and ethanol show high initial permeance but decline significantly over time, confirming that low-temperature operation is unsuitable for bioethanol separation.
- Isopropanol has the lowest permeance due to steric hindrance, reinforcing size exclusion as a key mechanism.
- The membrane performs best at 40°C and 50°C, where water transport remains high, and ethanol transport is nearly eliminated.
- Long-term stability at high temperatures makes this membrane a strong candidate for industrial bioethanol-water separation applications.

Recommendation for Industrial Application

- Operate the membrane at 50°C for optimal water-ethanol separation.
- Monitor long-term performance to assess potential fouling effects.
- Optimize membrane formulation to enhance water permeance while maintaining ethanol rejection.

6.-Conclusion

6.1.-Summary of our findings

This study systematically evaluated the permeance behavior of water, methanol, ethanol, and isopropanol across a thin-film composite membrane (TFCM) containing 1% PIM-1 at different temperatures (20°C, 30°C, 40°C, and 50°C). The primary goal was to assess the membrane's efficiency in separating bioethanol-water mixtures by analyzing the temperature dependence of permeance, time-dependent stability, and structure-property relationships. The results revealed key trends regarding gas selectivity, polymer-molecule interactions, and membrane performance.

6.1.1 Temperature-Dependent Permeance Trends

- Water Permeance
    - Highest at 50°C (~25-30 GPU) and remains relatively stable over time.
    - Moderate at 40°C (~12 GPU), with a steady trend.
    - Lower at 20°C and 30°C (~10-12 GPU), with minor decline over time.
    - The linear increase with vapor activity confirms diffusion-controlled transport.
- Methanol Permeance
    - Extremely high at 20°C (~160 GPU), declining steeply over time to ~60-80 GPU.
    - Lower at 30°C (~20 GPU), with gradual decline.
    - Negligible at 40°C and 50°C (~0-5 GPU), confirming strong water selectivity at high temperatures.
- Ethanol Permeance
    - High at 20°C (~120 GPU), with rapid decline over time.
    - Lower at 30°C (~40 GPU), decreasing gradually.
    - Near zero at 40°C and 50°C, demonstrating effective ethanol rejection for bioethanol dehydration.
- Isopropanol Permeance
    - Moderate at 20°C (~90 GPU), but declines over time.
    - Lower at 30°C (~40 GPU), with gradual decay.
    - Negligible at 40°C and 50°C (~0-5 GPU), reinforcing size-exclusion mechanisms.

6.1.2 Time-Dependent Stability and Long-Term Performance

- Water permeance remains high and stable, particularly at 40°C and 50°C.
- Methanol and ethanol show steep initial permeance followed by a decline, indicating sorption-dominated transport at low temperatures.
- Isopropanol shows consistent low permeance, highlighting steric hindrance effects.
- The membrane demonstrates long-term effectiveness for bioethanol dehydration at 40°C and 50°C, where ethanol transport is minimal and water permeance is optimized.

6.2. Structure-Property Relationships

6.2.1 Molecular Size and Transport Efficiency

Gas	Kinetic Diameter (nm)	Initial Permeance (20°C)	Final Permeance (After Time)
Water	~0.265	Moderate (~15 GPU)	Stable (~10-12 GPU)
Methanol	~0.36	Very High (~160 GPU)	Declines (~60-80 GPU)
Ethanol	~0.44	High (~120 GPU)	Declines (~40-50 GPU)
Isopropanol	~0.50	Moderate (~90 GPU)	Near zero (~0-5 GPU)

- Water's small molecular size allows for stable permeance, making the membrane ideal for dehydration applications.
- Methanol and ethanol exhibit high initial permeance but decline significantly over time, indicating a transition from sorption to diffusion control.
- Isopropanol's low permeance is attributed to steric hindrance, supporting size-exclusion effects.

6.2.2 Role of Polymer Relaxation and Free Volume

- At lower temperatures (20°C, 30°C), the polymer has more free volume, allowing alcohols to permeate initially.
- At higher temperatures (40°C, 50°C), the polymer structure compacts, restricting alcohol transport while still allowing water to pass.
- Water's strong hydrogen bonding ability maintains its permeance, even as polymer chains tighten.

6.2.3 Sorption vs. Diffusion-Controlled Transport

- Methanol and ethanol exhibit sorption-driven transport at 20°C, leading to initial high permeance followed by polymer saturation.
- At higher temperatures, alcohol permeance drops to near-zero, confirming a shift from sorption-limited to diffusion-controlled transport.
- Water remains highly permeable across all temperatures, reinforcing water selectivity.

6.3. Implications for Bioethanol Dehydration

6.3.1 Best Operating Conditions for Long-Term Stability

Temperature	Water Permeance Stability	Ethanol Permeance Stability	Selectivity (Water/Ethanol)	Suitability for Dehydration
20°C	Moderate Decline	Sharp Decline	Poor	Not recommended
30°C	Moderate Decline	Gradual Decline	Low	Not ideal
40°C	Stable	Near zero	High	Effective
50°C	Very Stable	Near zero	Excellent	Optimal

- 40°C and 50°C provide the best conditions for bioethanol dehydration, where water transport remains high, and ethanol transport is near zero.
- At 20°C and 30°C, ethanol permeance remains significant, reducing selectivity.
- 50°C provides the most stable long-term performance, making it the recommended operational temperature.

6.4. Final Conclusions and Future Recommendations

- Water permeance remains stable across time and temperature, reinforcing the membrane's effectiveness for bioethanol dehydration.
- Methanol and ethanol show high initial permeance at low temperatures but decline significantly, confirming that low-temperature operation is unsuitable for bioethanol separation.
- Isopropanol has the lowest permeance due to steric hindrance, reinforcing the role of size exclusion.
- The membrane performs best at 40°C and 50°C, where water permeance is maximized, and ethanol is effectively rejected.
- Long-term stability at high temperatures makes this membrane a strong candidate for industrial bioethanol-water separation applications.

Future Work Recommendations:

- Optimize membrane formulations to enhance water permeance while maintaining ethanol rejection.
- Evaluate real bioethanol feed mixtures to assess performance under industrial conditions.
- Investigate membrane fouling resistance and develop strategies to improve long-term durability.
- Explore alternative polymer modifications to further improve separation efficiency.

By leveraging the insights from this study, future research can further refine membrane-based separation technologies, enabling more efficient and sustainable bioethanol dehydration.

7.- Outlook and Future Directions

The findings presented in this thesis provide us with a strong foundation for understanding the performance of thin-film composite membranes (TFCMs) with 1% PIM-1 in the separation of bioethanol-water mixtures. The results obtained highlighted the temperature-dependent selectivity of the membrane, demonstrating its real potential for energy-efficient bioethanol purification. However, several key areas require further investigation to improve performance, optimize scalability, and enable industrial implementation. This last chapter outlines the key future research directions and technological advancements needed to bring this membrane technology closer to real-world applications.

7.1. Enhancing Membrane Performance

While in this study we demonstrate high water selectivity at 40°C and 50°C, further improvements can be made in terms of permeability, selectivity, and stability.

Optimization of PIM-1 Content in the Selective Layer

- The 1% PIM-1 loading showed promising results, but different polymer concentrations could enhance selectivity further.
- Future Work: Investigate the effects of higher or lower PIM-1 loadings in the selective layer on both water permeability and ethanol rejection.

Incorporation of Mixed-Matrix Membranes (MMMs)

- Combining PIM-1 with porous fillers, such as zeolites or MOFs, could enhance membrane separation by improving free volume and water affinity.
- Future Work: Explore hybrid TFCMs incorporating advanced nanofillers to further tune permeability and selectivity.

Enhancing Membrane Stability and Longevity

- Long-term performance remains a key challenge, particularly in the presence of complex fermentation broths that may cause fouling.
- Future Work: Investigate antifouling coatings or crosslinking modifications to improve stability during prolonged operation.

7.2. Application in Real Fermentation Broths

This study primarily focused on binary water-alcohol mixtures (methanol, ethanol, isopropanol). However, real bioethanol production streams contain impurities, dissolved solids, and other organic components.

Testing with Real Bioethanol Feeds

- The presence of acids, sugars, and fermentation byproducts could impact membrane performance.
- Future Work: Conduct pilot-scale trials using real bioethanol fermentation broths to assess membrane selectivity under industrial conditions.

Evaluating the Effect of Mixed Alcohol Systems

- Industrial bioethanol may contain methanol, butanol, and fusel alcohols, which could affect separation performance.
- Future Work: Perform experiments on multi-alcohol systems to determine the membrane's behavior in more complex separation scenarios.

7.3. Scale-Up and Industrial Feasibility

For membrane-based bioethanol dehydration to become a viable alternative to distillation, several scalability challenges must be addressed.

Energy and Cost Analysis of TFCM Separation vs. Distillation

- While membranes offer a lower-energy alternative, their true cost-effectiveness compared to conventional methods remains unclear.
- Future Work: Conduct techno-economic analysis comparing:
    - Energy consumption of membrane separation vs. azeotropic distillation.
    - Operational costs of TFCM membranes at scale.

Development of Continuous Membrane Processes

- Most industrial separation processes are continuous, while laboratory studies are often conducted in batch mode.
- Future Work: Design and test continuous membrane modules, such as spiral-wound or hollow fiber configurations, for real-world implementation.

Integration with Hybrid Separation Technologies

- Instead of replacing distillation, membranes could be integrated as pre-concentration steps to reduce energy use.

- Future Work: Explore hybrid approaches, where membranes are combined with adsorption, pervaporation, or vacuum-assisted separation.

7.4. Expanding Beyond Bioethanol

The high water selectivity observed in this study suggests that TFCMs with PIM-1 could be useful beyond bioethanol dehydration.

Application in Other Alcohol-Water Separations

- The membrane's ability to separate water from methanol, ethanol, and isopropanol indicates broader applications.
- Future Work: Investigate its use in pharmaceutical, cosmetic, or fine chemical industries where alcohol purification is essential.

Potential Use in Organic Solvent Nanofiltration (OSN)

- The presence of microporous structures in PIM-1 could enable its use in organic solvent separation for high-value chemical production.
- Future Work: Explore TFCMs for organic solvent nanofiltration, particularly in green chemistry and pharmaceutical manufacturing.

7.5. Final Remarks

This study has demonstrated the high potential of TFCMs with 1% PIM-1 for bioethanol-water separation, particularly at 40-50°C, where water permeance is maximized while ethanol permeance is nearly eliminated. However, key challenges remain, including membrane scalability, stability in complex feeds, and integration into industrial processes.

Future research should focus on:

1. Optimizing membrane composition (e.g., mixed-matrix membranes, crosslinking strategies).
2. Testing with real bioethanol feeds and multi-alcohol systems.
3. Scaling up membrane modules for continuous industrial operation.
4. Evaluating energy savings and cost benefits in comparison to traditional distillation.
5. Exploring broader applications in solvent separation technologies.

Addressing these challenges will be critical for advancing membrane-based bioethanol dehydration as a commercially viable, energy-efficient alternative to distillation.

8.-References and bibliography

(1) Tsoskounoglou, M.; Ayerides, G.; Tritopoulou, E. The End of Cheap Oil: Current Status and Prospects. *Energy Policy* **2008**, *36* (10), 3797–3806. https://doi.org/10.1016/J.ENPOL.2008.05.011.

(2) Ahmed, N. M. The International Relations of Crisis and the Crisis of International Relations: From the Securitisation of Scarcity to the Militarisation of Society. *Global Change, Peace & Security* **2011**, *23* (3), 335–355. https://doi.org/10.1080/14781158.2011.601854.

(3) Lenshie, N. E.; Ojeh, V. N.; Oruonye, E. D.; Ezeibe, C.; Ajaero, C.; Nzeadibe, T. C.; Celestine, U. U.; Osadebe, N. Geopolitics of Climate Change-Induced Conflict and Population Displacement in West Africa. *Local Environ* **2022**, *27* (3), 287–308. https://doi.org/10.1080/13549839.2022.2040461.

(4) Smith, P. J. The Geopolitics of Climate Change: Power Transitions, Conflict and the Future of Military Activities. *Conflict, Security and Development* **2011**, *11* (3), 309–334. https://doi.org/10.1080/14678802.2011.593810.

(5) Streck, C.; Terhalle, M. The Changing Geopolitics of Climate Change. *Climate Policy* **2013**, *13* (5), 533–537. https://doi.org/10.1080/14693062.2013.823809.

(6) Wang, W.; Liu, Y. Geopolitics of Global Climate Change and Energy Security. *Chinese Journal of Population Resources and Environment* **2015**, *13* (2), 119–126. https://doi.org/10.1080/10042857.2015.1017907.

(7) Bai, F. W.; Anderson, W. A.; Moo-Young, M. Ethanol Fermentation Technologies from Sugar and Starch Feedstocks. *Biotechnol Adv* **2008**, *26* (1), 89–105. https://doi.org/10.1016/J.BIOTECHADV.2007.09.002.

(8) Beliya, E.; Tiwari, S.; Jadhav, S.; Tiwari, K. De-Oiled Rice Bran as a Source of Bioethanol. *http://dx.doi.org/10.1260/0144-5987.31.5.771* **2013**, *31* (5), 771–782. https://doi.org/10.1260/0144-5987.31.5.771.

(9) Festel, G. W. Biofuels - Economic Aspects. *Chem Eng Technol* **2008**, *31* (5), 715–720. https://doi.org/10.1002/CEAT.200700335.

(10) Chum, H. L.; Overend, R. P. Biomass and Renewable Fuels. *Fuel Processing Technology* **2001**, *71* (1–3), 187–195. https://doi.org/10.1016/S0378-3820(01)00146-1.

(11) Fuels from Biomass. *Green Energy and Technology* **2010**, *26*, 33–73. https://doi.org/10.18280/TI-IJES.630112.

(12) Dave, N.; Selvaraj, R.; Varadavenkatesan, T.; Vinayagam, R. A Critical Review on Production of Bioethanol from Macroalgal Biomass. *Algal Res* **2019**, *42*, 101606. https://doi.org/10.1016/J.ALGAL.2019.101606.

(13) Demirbaş, A. Bioethanol from Cellulosic Materials: A Renewable Motor Fuel from Biomass. *Energy Sources* **2005**, *27* (4), 327–337. https://doi.org/10.1080/00908310390266643.

(14) Demirbas, A. Producing and Using Bioethanol as an Automotive Fuel. *Energy Sources, Part B: Economics, Planning and Policy* **2007**, *2* (4), 391–401. https://doi.org/10.1080/15567240600705466.

(15) Cheikh, F. Z. Ben; Douadi, A.; Boussebaa, W. Emerging Techniques in Agricultural Waste Valorization in Bioethanol Production. *Asian Journal of Research in Chemistry* **2021**, *14* (5), 375–379. https://doi.org/10.52711/0974-4150.2021.00064.

(16) Ramakrishna, S.; Ma, Z.; Matsuura, T. Membrane and Membrane Separation Process. *Polymer Membranes in Biotechnology* **2011**, 1–37. https://doi.org/10.1142/9781848163812_0001.

(17) Ramakrishna, S.; Ma, Z.; Matsuura, T. Polymer Membranes in Biotechnology: Preparation, Functionalization and Application. *Polymer Membranes in Biotechnology: Preparation, Functionalization and Application* **2011**, 1–287. https://doi.org/10.1142/P636/SUPPL_FILE/P636_CHAP01.PDF.

(18) Ramakrishna, S.; Ma, Z.; Matsuura, T. Membrane Preparation. *Polymer Membranes in Biotechnology* **2011**, 39–70. https://doi.org/10.1142/9781848163812_0002.

(19) Glüsen, A.; Stolten, D. Membranen Für Polymerelektrolyt-Brennstoffzellen. *Chemie Ingenieur Technik* **2003**, *75* (11), 1591–1597. https://doi.org/10.1002/CITE.200306146.

(20) Fane, A. G.; Wang, R.; Hu, M. X. Synthetic Membranes for Water Purification: Status and Future. *Angewandte Chemie - International Edition* **2015**, *54* (11), 3368–3386. https://doi.org/10.1002/ANIE.201409783.

(21) Zhang, H.; Zhu, S.; Yang, J.; Ma, A. Advancing Strategies of Biofouling Control in Water-Treated Polymeric Membranes. *Polymers 2022, Vol. 14, Page 1167* **2022**, *14* (6), 1167. https://doi.org/10.3390/POLYM14061167.

(22) Morales-Jiménez, M.; Palacio, D. A.; Palencia, M.; Meléndrez, M. F.; Rivas, B. L. Bio-Based Polymeric Membranes: Development and Environmental Applications. *Membranes 2023, Vol. 13, Page 625* **2023**, *13* (7), 625. https://doi.org/10.3390/MEMBRANES13070625.

(23) Cui, Z. F.; Jiang, Y.; Field, R. W. Fundamentals of Pressure-Driven Membrane Separation Processes. *Membrane Technology: A Practical Guide to Membrane Technology and Applications in Food and Bioprocessing* **2010**, 1–18. https://doi.org/10.1016/B978-1-85617-632-3.00001-X.

(24) Le, N. L.; Nunes, S. P. Materials and Membrane Technologies for Water and Energy Sustainability. *Sustainable Materials and Technologies* **2016**, *7*, 1–28. https://doi.org/10.1016/j.susmat.2016.02.001.

(25) Jambo, S. A.; Abdulla, R.; Mohd Azhar, S. H.; Marbawi, H.; Gansau, J. A.; Ravindra, P. A Review on Third Generation Bioethanol Feedstock. *Renewable and Sustainable Energy Reviews* **2016**, *65*, 756–769. https://doi.org/10.1016/j.rser.2016.07.064.

(26) Wei, P.; Cheng, L. H.; Zhang, L.; Xu, X. H.; Chen, H. L.; Gao, C. J. A Review of Membrane Technology for Bioethanol Production. *Renewable and Sustainable Energy Reviews* **2014**, *30*, 388–400. https://doi.org/10.1016/J.RSER.2013.10.017.

(27) Khan, N.; Sudhakar, K.; Mamat, R. Role of Biofuels in Energy Transition, Green Economy and Carbon Neutrality. *Sustainability (Switzerland)* **2021**, *13* (22). https://doi.org/10.3390/SU132212374.

(28) Stuart, T.; Sorenson, O. The Geography of Opportunity: Spatial Heterogeneity in Founding Rates and the Performance of Biotechnology Firms. *Res Policy* **2003**, *32* (2), 229–253. https://doi.org/10.1016/S0048-7333(02)00098-7.

(29) Kirch, P. V. Archaeology and Global Change: The Holocene Record. *Annu Rev Environ Resour* **2005**, *30*, 409–440. https://doi.org/10.1146/ANNUREV.ENERGY.29.102403.140700.

(30) Mascu*, S.; Simionescu, V. Eco-Bio-Economic Development And Emissions Reductions By Changing Technology. **2019**, 1612–1620. https://doi.org/10.15405/EPSBS.2019.08.03.197/IMAGE/2.

(31) *Economic Aspects of Greenhouse Gas Emissions Reduction by Utilisation of Wind and Solar Energies to Produce Electricity and hydrogen | IEEE Conference Publication | IEEE Xplore*. https://ieeexplore.ieee.org/document/4057292 (accessed 2025-01-15).

(32) Mascu*, S.; Simionescu, V. Eco-Bio-Economic Development And Emissions Reductions By Changing Technology. **2019**, 1612–1620. https://doi.org/10.15405/EPSBS.2019.08.03.197/IMAGE/1.

(33) Ostrom, E. Sustainable Social-Ecological Systems: An Impossibility? *SSRN Electronic Journal* **2007**. https://doi.org/10.2139/SSRN.997834.

(34) Kung, S. S.; Zhang, L.; Gong, X.; Kung, C. C. A Sector-Wide Economic and Environmental Analysis on Bioenergy Production and Emission Consequences. *Energy Exploration and Exploitation* **2019**, *37* (4), 1408–1425. https://doi.org/10.1177/0144598719854807/ASSET/IMAGES/LARGE/10.1177_0144598719854807-FIG3.JPEG.

(35) Mathur, S.; Waswani, H.; Singh, D.; Ranjan, R. Alternative Fuels for Agriculture Sustainability: Carbon Footprint and Economic Feasibility. *AgriEngineering 2022, Vol. 4, Pages 993-1015* **2022**, *4* (4), 993–1015. https://doi.org/10.3390/AGRIENGINEERING4040063.

(36) Suárez, J.; Martín, G.; Cepero, L.; Blanco, D.; Savran, V.; Sotolongo, J. A.; López, A.; Donis, F.; González, O.; Peña, A.; Hernández Mesa, M.; Hernández, M. Producción Integrada de Alimentos y Bioenergía: La Experiencia Cubana. *Agroecología, ISSN 1887-1941, ISSN-e 1989-4686, Vol. 12, Nº. 1, 2017, págs. 47-55* **2017**, *12* (1), 47–55.

(37) Bušić, A.; Mardetko, N.; Kundas, S.; Morzak, G.; Belskaya, H.; Šantek, M. I.; Komes, D.; Novak, S.; Šantek, B. Bioethanol Production from Renewable Raw Materials and Its Separation and Purification: A Review. *Food Technol Biotechnol* **2018**, *56* (3), 289. https://doi.org/10.17113/FTB.56.03.18.5546.

(38) Cherubini, F.; Strømman, A. H. Principles of Biorefining. *Biofuels: Alternative Feedstocks and Conversion Processes* **2011**, 3–24. https://doi.org/10.1016/B978-0-12-385099-7.00001-2.

(39) de Wit, M. P. Bioenergy Development Pathways for Europe: Potentials, Costs and Environmental Impacts. **2011**.

(40) *View of Economic and social impacts of the biodiesel industry: Assessment and policy implications in Spain*. https://sjar.revistas.csic.es/index.php/sjar/article/view/16580/4918 (accessed 2025-01-21).

(41) *View of Economic and social impacts of the biodiesel industry: Assessment and policy implications in Spain*. https://sjar.revistas.csic.es/index.php/sjar/article/view/16580/4918 (accessed 2025-01-21).

(42) Young, C. E. F.; Steffen, P. G. Biocombustibles Como Estrategia de Desarrollo: ¿rumbo Hacia La Sustentabilidad o Hacia Una Nueva Periferia? *Polis (Santiago)* **2008**, *7* (21). https://doi.org/10.4067/S0718-65682008000200009.

(43) Khattak, W. A.; Khan, T.; Ha, J. H.; Ul-Islam, M.; Kang, M. K.; Park, J. K. Enhanced Production of Bioethanol from Waste of Beer Fermentation Broth at High Temperature through Consecutive Batch Strategy by Simultaneous Saccharification and Fermentation. *Enzyme Microb Technol* **2013**, *53* (5), 322–330. https://doi.org/10.1016/J.ENZMICTEC.2013.07.004.

(44) Nair, L. G.; Agrawal, K.; Verma, P. An Overview of Sustainable Approaches for Bioenergy Production from Agro-Industrial Wastes. *Energy Nexus* **2022**, *6*. https://doi.org/10.1016/j.nexus.2022.100086.

(45) Ridara, R.; Muhammad, M.; Setiawan, A.; Riskina, S.; Nurjannah, S. Characterization of Bioethanol from Tuber of Porang Waste Fermented with Saccharomyces Cerevisiae Enzyme: Effect of Fermentation Time and Yeast Ratio. *Jurnal Teknik Kimia dan Lingkungan* **2023**, *7* (2), 48–57. https://doi.org/10.33795/JTKL.V7I2.3199.

(46) AbdElhafez, S. E.; Taha, T.; Mansy, A. E.; El-Desouky, E.; Abu-Saied, M. A.; Eltaher, K.; Hamdy, A.; El Fawal, G.; Gamal, A.; Hashim, A. M.; Elgharbawy, A. S.; El-Latif, M. M. A.; Hamad, H.; Ali, R. M. Experimental Optimization with the Emphasis on Techno-Economic Analysis of Production and Purification of High Value-Added Bioethanol from Sustainable Corn Stover. *Energies (Basel)* **2022**, *15* (17), 6131. https://doi.org/10.3390/EN15176131/S1.

(47) Shaghaghi-Moghaddam, R.; Jafarizadeh-Malmiri, H.; Mehdikhani, P.; Alijanianzadeh, R.; Jalalian, S. Optimization of Submerged Fermentation Conditions to Overproduce Bioethanol Using Two Industrial and Traditional Saccharomyces Cerevisiae Strains. *Green Processing and Synthesis* **2019**, *8* (1), 157–162. https://doi.org/10.1515/GPS-2018-0044/MACHINEREADABLECITATION/RIS.

(48) Adiya, Z. I. S. G.; Adamu, S. S.; Ibrahim, M. A.; Okoh, E. V. C.; Ibrahim, D. Comparative Study of Bioethanol Produced from Different Agro-Industrial Biomass Residues. *Earthline Journal of Chemical Sciences* **2022**, *7* (2), 143–152. https://doi.org/10.34198/EJCS.7222.143152.

(49) Cheikh, F. Z. Ben; Douadi, A.; Boussebaa, W. Emerging Techniques in Agricultural Waste Valorization in Bioethanol Production. *Asian Journal of Research in Chemistry* **2021**, *14* (5), 375–379. https://doi.org/10.52711/0974-4150.2021.00064.

(50) Akinyele, B. J.; Olaniyi, O. O.; Arotupin, D. J. Bioconversion of Selected Agricultural Wastes and Associated Enzymes by Volvariella Volvacea: An Edible Mushroom. *Res J Microbiol* **2011**, *6* (1), 63–70. https://doi.org/10.3923/JM.2011.63.70.

(51) Yang, Z.; Zhou, Y.; Feng, Z.; Rui, X.; Zhang, T.; Zhang, Z. A Review on Reverse Osmosis and Nanofiltration Membranes for Water Purification. *Polymers (Basel)* **2019**, *11* (8), 1252. https://doi.org/10.3390/POLYM11081252.

(52) Bušić, A.; Mardetko, N.; Kundas, S.; Morzak, G.; Belskaya, H.; Šantek, M. I.; Komes, D.; Novak, S.; Šantek, B. Bioethanol Production from Renewable Raw Materials and Its Separation and Purification: A Review. *Food Technol Biotechnol* **2018**, *56* (3), 289. https://doi.org/10.17113/FTB.56.03.18.5546.

(53) Khalid, A.; Aslam, M.; Qyyum, M. A.; Faisal, A.; Khan, A. L.; Ahmed, F.; Lee, M.; Kim, J.; Jang, N.; Chang, I. S.; Bazmi, A. A.; Yasin, M. Membrane Separation Processes for Dehydration of

Bioethanol from Fermentation Broths: Recent Developments, Challenges, and Prospects. *Renewable and Sustainable Energy Reviews* **2019**, *105*, 427–443. https://doi.org/10.1016/J.RSER.2019.02.002.

(54) Errico, M.; Rong, B. G. Synthesis of New Separation Processes for Bioethanol Production by Extractive Distillation. *Sep Purif Technol* **2012**, *96*, 58–67. https://doi.org/10.1016/J.SEPPUR.2012.05.022.

(55) Giesa, R.; Schmidt, H.-W. High-Temperature Stable Polymers. *Encyclopedia of Materials: Science and Technology* **2001**, 3803–3806. https://doi.org/10.1016/B0-08-043152-6/00677-X.

(56) Xie, L.; Abliz, D.; Li, D. Thin Film Coating for Polymeric Micro Parts. *Comprehensive Materials Processing: Thirteen Volume Set* **2014**, *7*, V7-157-V7-170. https://doi.org/10.1016/B978-0-08-096532-1.00713-5.

(57) Lau, W. J.; Gray, S.; Matsuura, T.; Emadzadeh, D.; Paul Chen, J.; Ismail, A. F. A Review on Polyamide Thin Film Nanocomposite (TFN) Membranes: History, Applications, Challenges and Approaches. *Water Res* **2015**, *80*, 306–324. https://doi.org/10.1016/J.WATRES.2015.04.037.

(58) Fan, S. T.; Wang, J. X.; Liao, L. G.; Feng, J. F.; Li, B. J.; Zhang, S. Enhanced Selectivity in Thin Film Composite Membrane for CO2 Capture through Improvement to Support Layer. *Chemical Engineering Journal* **2023**, *468*, 143645. https://doi.org/10.1016/J.CEJ.2023.143645.

(59) Cadotte, J. E. EVOLUTION OF COMPOSITE REVERSE OSMOSIS MEMBRANES. *ACS Symposium Series* **1985**, 273–294. https://doi.org/10.1021/BK-1985-0269.CH012.

(60) Baker, R. W. Membrane Technology and Applications. *Membrane Technology and Applications* **2012**. https://doi.org/10.1002/9781118359686.

(61) Ismail, A. F.; Rahman, M. A.; Othman, M. H. D.; Matsuura, T. Membrane Separation Principles and Applications: From Material Selection to Mechanisms and Industrial Uses. *Membrane Separation Principles and Applications: From Material Selection to Mechanisms and Industrial Uses* **2018**, 1–481. https://doi.org/10.1016/C2016-0-04031-7.

(62) Mohammad, A. W.; Teow, Y. H.; Chong, W. C.; Ho, K. C. Hybrid Processes: Membrane Bioreactor. *Membrane Separation Principles and Applications: From Material Selection to Mechanisms and Industrial Uses* **2018**, 401–470. https://doi.org/10.1016/B978-0-12-812815-2.00013-2.

(63) Mulder, M. Basic Principles of Membrane Technology. **1996**. https://doi.org/10.1007/978-94-009-1766-8.

(64) Ezugbe, E. O.; Rathilal, S. Membrane Technologies in Wastewater Treatment: A Review. *Membranes 2020, Vol. 10, Page 89* **2020**, *10* (5), 89. https://doi.org/10.3390/MEMBRANES10050089.

(65) Geise, G. M.; Lee, H. S.; Miller, D. J.; Freeman, B. D.; McGrath, J. E.; Paul, D. R. Water Purification by Membranes: The Role of Polymer Science. *J Polym Sci B Polym Phys* **2010**, *48* (15), 1685–1718. https://doi.org/10.1002/POLB.22037.

(66) Zhang, Y.; Wan, Y.; Guo, M.; Pan, G.; Shi, H.; Yao, X.; Liu, Y. Surface Modification on Thin-Film Composite Reverse Osmosis Membrane by Cation Complexation for Antifouling. *Journal of Polymer Research* **2019**, *26* (3), 1–12. https://doi.org/10.1007/S10965-019-1701-0/METRICS.

(67) Freeman, B. D. Basis of Permeability/Selectivity Tradeoff Relations in Polymeric Gas Separation Membranes. *Macromolecules* **1999**, *32* (2), 375–380. https://doi.org/10.1021/MA9814548.

(68) *Sci-Hub | Polymers of intrinsic microporosity (PIMs): robust, solution-processable, organic nanoporous materials. Chemical Communications, (2), 230 | 10.1039/B311764B*. https://sci-hub.st/10.1039/B311764B (accessed 2025-02-10).

(69) Li, P.; Chung, T. S.; Paul, D. R. Temperature Dependence of Gas Sorption and Permeation in PIM-1. *J Memb Sci* **2014**, *450*, 380–388. https://doi.org/10.1016/J.MEMSCI.2013.09.030.

(70) Rezakazemi, M.; Sadrzadeh, M.; Matsuura, T. Thermally Stable Polymers for Advanced High-Performance Gas Separation Membranes. *Prog Energy Combust Sci* **2018**, *66*, 1–41. https://doi.org/10.1016/j.pecs.2017.11.002.

(71) *Sci-Hub | Permeation and separation properties of polyimide membranes to olefins and paraffins. Journal of Membrane Science, 121(2), 197–207 | 10.1016/S0376-7388(96)00182-2*. https://sci-hub.st/10.1016/S0376-7388(96)00182-2 (accessed 2025-02-10).

(72) *Sci-Hub | The synthesis of polymers of intrinsic microporosity (PIMs). Science China Chemistry, 60(8), 1023–1032 | 10.1007/s11426-017-9058-x*. https://sci-hub.st/10.1007/s11426-017-9058-x (accessed 2025-02-10).

(73) Alexander Stern, S. Polymers for Gas Separations: The next Decade. *J Memb Sci* **1994**, *94* (1), 1–65. https://doi.org/10.1016/0376-7388(94)00141-3.

(74) Tripathi, B. P.; Shahi, V. K. Organic–Inorganic Nanocomposite Polymer Electrolyte Membranes for Fuel Cell Applications. *Prog Polym Sci* **2011**, *36* (7), 945–979. https://doi.org/10.1016/J.PROGPOLYMSCI.2010.12.005.

(75) Qiu, W.; Xu, L.; Chen, C. C.; Paul, D. R.; Koros, W. J. Gas Separation Performance of 6FDA-Based Polyimides with Different Chemical Structures. *Polymer (Guildf)* **2013**, *54* (22), 6226–6235. https://doi.org/10.1016/J.POLYMER.2013.09.007.

(76) Wang, D. M.; Lai, J. Y. Recent Advances in Preparation and Morphology Control of Polymeric Membranes Formed by Nonsolvent Induced Phase Separation. *Curr Opin Chem Eng* **2013**, *2* (2), 229–237. https://doi.org/10.1016/J.COCHE.2013.04.003.

(77) ÎÂmpol'skiĭ, I. P. .; Pinnau, I. .; Freeman, B. D. . Materials Science of Membranes for Gas and Vapor Separation. **2006**.

(78) Foster, A. B.; Tamaddondar, M.; Luque-Alled, J. M.; Harrison, W. J.; Li, Z.; Gorgojo, P.; Budd, P. M. Understanding the Topology of the Polymer of Intrinsic Microporosity PIM-1: Cyclics, Tadpoles, and Network Structures and Their Impact on Membrane Performance. *Macromolecules* **2020**, *53* (2), 569–583. https://doi.org/10.1021/ACS.MACROMOL.9B02185/ASSET/IMAGES/LARGE/MA9B02185_0005.JPEG.

(79) Tian, M.; Rochat, S.; Fawcett, H.; Burrows, A. D.; Bowen, C. R.; Mays, T. J. Chemical Modification of the Polymer of Intrinsic Microporosity PIM-1 for Enhanced Hydrogen Storage. *Adsorption* **2020**, *26* (7), 1083–1091. https://doi.org/10.1007/S10450-020-00239-Y/FIGURES/6.

(80) Foster, A. B.; Tamaddondar, M.; Luque-Alled, J. M.; Harrison, W. J.; Li, Z.; Gorgojo, P.; Budd, P. M. Understanding the Topology of the Polymer of Intrinsic Microporosity PIM-1: Cyclics, Tadpoles, and Network Structures and Their Impact on Membrane Performance. *Macromolecules* **2020**, *53* (2), 569–583. https://doi.org/10.1021/ACS.MACROMOL.9B02185/ASSET/IMAGES/LARGE/MA9B02185_0005.JPEG.

(81) Kharitonov, A. P.; Moskvin, Y. L.; Syrtsova, D. A.; Starov, V. M.; Teplyakov, V. V. Direct Fluorination of the Polyimide Matrimid® 5218: The Formation Kinetics and Physicochemical Properties of the Fluorinated Layers. *J Appl Polym Sci* **2004**, *92* (1), 6–17. https://doi.org/10.1002/APP.13565.

(82) Jagur-Grodzinski, J. Modification of Polymers under Heterogeneous Conditions. *Prog Polym Sci* **1992**, *17* (3), 361–415. https://doi.org/10.1016/0079-6700(92)90020-Y.

(83) Chang, Y. S.; Kumari, P.; Munro, C. J.; Szekely, G.; Vega, L. F.; Nunes, S.; Dumée, L. F. Plasticization Mitigation Strategies for Gas and Liquid Filtration Membranes - A Review. *J Memb Sci* **2023**, *666*. https://doi.org/10.1016/j.memsci.2022.121125.

(84) Im, H.; Yun, S.; Kim, J. Electro Conductivities of Well-Dispersed PMMA-g-MWNTs/6FDA-Based Polyimide Composites: Effect of Chemical Structure. *Polym Compos* **2011**, *32* (3), 368–377. https://doi.org/10.1002/PC.21049.

(85) Huggins, M. L. Principles of Polymer Chemistry. *J Am Chem Soc* **1954**, *76* (10), 2854–2854. https://doi.org/10.1021/JA01639A090.

(86) Zhang, S.; Zhang, J.; Tang, L.; Huang, J.; Fang, Y.; Ji, P.; Wang, C.; Wang, H. A Novel Synthetic Strategy for Preparing Polyamide 6 (PA6)-Based Polymer with Transesterification. *Polymers 2019, Vol. 11, Page 978* **2019**, *11* (6), 978. https://doi.org/10.3390/POLYM11060978.

(87) Arshad, N.; Batool, S. R.; Razzaq, S.; Arshad, M.; Rasheed, A.; Ashraf, M.; Nawab, Y.; Nazeer, M. A. Recent Advancements in Polyurethane-Based Membranes for Gas Separation. *Environ Res* **2024**, *252*, 118953. https://doi.org/10.1016/J.ENVRES.2024.118953.

(88) Tirelli, N.; Lutolf, M. P.; Napoli, A.; Hubbell, J. A. Poly(Ethylene Glycol) Block Copolymers. *Reviews in Molecular Biotechnology* **2002**, *90* (1), 3–15. https://doi.org/10.1016/S1389-0352(01)00057-5.

(89) Ismail, A. F.; Lorna, W. Penetrant-Induced Plasticization Phenomenon in Glassy Polymers for Gas Separation Membrane. *Sep Purif Technol* **2002**, *27* (3), 173–194. https://doi.org/10.1016/S1383-5866(01)00211-8.

(90) Carta, M.; Malpass-Evans, R.; Croad, M.; Rogan, Y.; Jansen, J. C.; Bernardo, P.; Bazzarelli, F.; McKeown, N. B. An Efficient Polymer Molecular Sieve for Membrane Gas Separations. *Science (1979)* **2013**, *339* (6117), 303–307. https://doi.org/10.1126/SCIENCE.1228032/SUPPL_FILE/CARTA-SOM.PDF.

(91) Zhu, T.; Xia, Q.; Zuo, J.; Liu, S.; Yu, X.; Wang, Y. Recent Advances of Thin Film Composite Membranes for Pervaporation Applications: A Comprehensive Review. *Advanced Membranes* **2021**, *1*, 100008. https://doi.org/10.1016/J.ADVMEM.2021.100008.

(92) Geise, G. M.; Park, H. B.; Sagle, A. C.; Freeman, B. D.; McGrath, J. E. Water Permeability and Water/Salt Selectivity Tradeoff in Polymers for Desalination. *J Memb Sci* **2011**, *369* (1–2), 130–138. https://doi.org/10.1016/J.MEMSCI.2010.11.054.

(93) Wang, Y.; Ma, X.; Ghanem, B. S.; Alghunaimi, F.; Pinnau, I.; Han, Y. Polymers of Intrinsic Microporosity for Energy-Intensive Membrane-Based Gas Separations. *Mater Today Nano* **2018**, *3*, 69–95. https://doi.org/10.1016/J.MTNANO.2018.11.003.

(94) Goh, P. S.; Ismail, A. F.; Ng, B. C. Carbon Nanotubes for Desalination: Performance Evaluation and Current Hurdles. *Desalination* **2013**, *308*, 2–14. https://doi.org/10.1016/J.DESAL.2012.07.040.

(95) Al-Hobaib, A. S.; Al-Sheetan, K. M.; Shaik, M. R.; Al-Suhybani, M. S. Modification of Thin-Film Polyamide Membrane with Multi-Walled Carbon Nanotubes by Interfacial Polymerization. *Appl Water Sci* **2017**, *7* (8), 4341–4350. https://doi.org/10.1007/S13201-017-0578-5/TABLES/1.

(96) Piermarini, G. J.; Block, S.; Barnett, J. D. Hydrostatic Limits in Liquids and Solids to 100 Kbar. *J Appl Phys* **1973**, *44* (12), 5377–5382. https://doi.org/10.1063/1.1662159.

(97) Martin, T. M.; Solvason, C. C.; Roberts, C. B. Demixing Pressure Measurements of Aerosol-OT in Ethane + Alcohol Solvent Mixtures. *J Chem Eng Data* **2001**, *46* (3), 769–772. https://doi.org/10.1021/JE000281Q.

(98) Tinjacá, D. A.; Martínez, F.; Almanza, O. A.; Jouyban, A.; Acree, W. E. Solubility, Dissolution Thermodynamics and Preferential Solvation of Meloxicam in (Methanol + Water) Mixtures. *J Solution Chem* **2021**, *50* (5), 667–689. https://doi.org/10.1007/S10953-021-01084-5/METRICS.

(99) Raheem, H.; Craster, B.; Seshia, A. A Comparison of Calculation Methods for the Diffusion Coefficient as a Potential Tool for Identifying Material Alteration with Time. *Polym Test* **2024**, *132*. https://doi.org/10.1016/J.POLYMERTESTING.2024.108356.

(100) Monteleone, M.; Esposito, E.; Fuoco, A.; Lanč, M.; Pilnáček, K.; Friess, K.; Bezzu, C. G.; Carta, M.; McKeown, N. B.; Jansen, J. C. A Novel Time Lag Method for the Analysis of Mixed Gas Diffusion in Polymeric Membranes by On-Line Mass Spectrometry: Pressure Dependence of Transport Parameters. *Membranes (Basel)* **2018**, *8* (3), 73. https://doi.org/10.3390/MEMBRANES8030073.

(101) Fraga, S. C.; Monteleone, M.; Lanč, M.; Esposito, E.; Fuoco, A.; Giorno, L.; Pilnáček, K.; Friess, K.; Carta, M.; McKeown, N. B.; Izák, P.; Petrusová, Z.; Crespo, J. G.; Brazinha, C.; Jansen, J. C. A Novel Time Lag Method for the Analysis of Mixed Gas Diffusion in Polymeric Membranes by On-Line Mass Spectrometry: Method Development and Validation. *J Memb Sci* **2018**, *561*, 39–58. https://doi.org/10.1016/j.memsci.2018.04.029.

(102) Fuoco, A.; Monteleone, M.; Esposito, E.; Bruno, R.; Ferrando-Soria, J.; Pardo, E.; Armentano, D.; Jansen, J. C. Gas Transport in Mixed Matrix Membranes: Two Methods for Time Lag Determination. *Computation* **2020**, *8* (2), 28. https://doi.org/10.3390/COMPUTATION8020028.

(103) Al-Ismaily, M.; Wijmans, J. G.; Kruczek, B. A Shortcut Method for Faster Determination of Permeability Coefficient from Time Lag Experiments. *J Memb Sci* **2012**, *423–424*, 165–174. https://doi.org/10.1016/j.memsci.2012.08.009.

(104) Jan Roman, P.; Detlev, F.; Thomas, K.; Klaus-Viktor, P. Gas Permeation Measurement under Defined Humidity via Constant Volume/Variable Pressure Method. *J Memb Sci* **2012**, *389*, 343–348. https://doi.org/10.1016/j.memsci.2011.10.046.

(105) Vadlamudi, V.; Ram, M.; Elenchezhian, P.; Raheem, H.; Craster, B.; Seshia, A. Analysis of Permeation and Diffusion Coefficients to Infer Aging Attributes in Polymers Subjected to Supercritical CO2 and H2 Gas at High Pressures. *Polymers (Basel)* **2022**, *14* (18), 3741–3741. https://doi.org/10.3390/POLYM14183741.

(106) Fujiwara, H.; Ono, H.; Onoue, K.; Nishimura, S. High-Pressure Gaseous Hydrogen Permeation Test Method -Property of Polymeric Materials for High-Pressure Hydrogen Devices (1)-. *Int J Hydrogen Energy* **2020**, *45* (53), 29082–29094. https://doi.org/10.1016/j.ijhydene.2020.07.215.

(107) Innocentini, M. D. de M.; Formigoni, C. E. Rapid Pressure-Decay Technique for Determining the O2 and CO2 Permeability Coefficients of Polymeric Films Considering the Gas Compressibility Effect. *Chem Eng Commun* **2023**, *210* (12), 1–8. https://doi.org/10.1080/00986445.2023.2189108.

(108) Dargahi, A.; Duncan, M.; Runka, J.; Hammami, A.; Naguib, H. E. Supercritical CO2 Permeation in Polymeric Films: Design, Characterization, and Modeling. *Mater Des* **2023**, *227*, 111715. https://doi.org/10.1016/J.MATDES.2023.111715.